THE DEVELOPMENT OF AMINE-BASED EXTRACTANTS FOR SEPARATION OF BASE METALS IN A SULFATE MEDIUM

A THESIS SUBMITTED IN FULFILMENT OF THE

REQUIREMENTS FOR THE DEGREE OF

DOCTOR OF PHILOSOPHY

IN THE FACULTY OF SCIENCE

OF

RHODES UNIVERSITY

by

NOMAMPONDO PENELOPE MAGWA

FEBRUARY 2014

TABLE OF CONTENT

ABSTRACT

Tridentate benzimidazole-based ligands, *bis*((*1H*-benzimidazol-2-yl)methyl)sulfide (BNSN) and *bis*((1*H*-benzimidazol-2-yl)methyl)amine (BNNN), along with dinonylnaphthalene sulfonic acid (DNNSA) as a synergist, were investigated as potential selective extractants for Ni^{2+} from base metals in a solvent extraction system using 2-octanol/Shellsol 2325 (8:2) as diluent and modifier. However, extraction studies show a lack of pH-metric separation of the later 3d metal ions with *bis*((1-octylbenzimidazol-2-yl)methyl)sulfide (BONSN) and *bis*((1-decylbenzimidazol-2-yl)methyl)amine (BDNNN) as extractants, but extractions occurred in the low pH range with an opportunity for back extraction. This investigation suggested that tridentate ligands (at least those of the nature investigated here) are not feasible extractants for separation of base metal ions due to their lack of stereochemical "tailor-making."

The coordination chemistry of the later 3d metal ions with *bis*((1*H*-benzimidazol-2-yl)methyl)sulfide (BNSN) and *bis*((1*H*-benzimidazol-2-yl)methyl)amine (BNNN) were investigated. All the complexes had general formula $[M(L)_2]X\cdot yH_2O$, where M = Co(II), Ni(II), Cu(II), and Zn(II), L = BNSN or BNNN, X = SO_4^{2-} or RSO_3^-, and y = 2–5. The infrared and conductivity measurements show that sulfate and sulfonate are counter anions in the isolation of the dicationic complexes. X-ray crystal structures of $[Co(BNSN)_2](RSO_3)_2\cdot 4H_2O$ and $[Ni(BNSN)_2](RSO_3)_2\cdot 2H_2O$ revealed a distorted octahedral geometry for the complexes which was in support of the spectroscopic data.

Since tridentate benzimidazole-based ligand were not suitable extractants for the nickel(II) extraction, the study was extended to a bidentate benzimidazole-based extractant, (1*H*-benzimidazol-2-yl)-*N*-methylmethanamine (BIMA) along with dinonylnaphthalene sulfonic

acid (DNNSA). (1-Octylbenzimidazol-2-yl)-*N*-methylmethanamine (OBIMA) was investigated as a possible selective extractant of Ni^{2+} from base metals in a solvent extraction system using 2-octanol/Shellsol 2325 (8:2) used as a diluent and modifier. The separation of Ni^{2+} from the borderline hard/soft acids and hard acids; Co^{2+}, Cu^{2+}, Zn^{2+}, Fe^{2+}, Fe^{3+}, Mn^{2+}, Mg^{2+} and Ca^{2+} at a pH range of 0.5-3.5 with OBIMA and DNNSA was achieved to the tune of a $\Delta pH_{½} \approx 1.6$ with respect to cobalt from a sulfate medium. The extraction system further showed a lack of extraction of the A-type metals ions in the pH range of interest. The absence of DNNSA results in a very low extraction efficiency of the base metals.

The fundamental chemistry of the solvent extraction systems was investigated through solid state and solution studies of the complexation of the ligands with the base metals. It is apparent, therefore, that separations achieved (or not achieved) are driven by stereochemical factors and Hofmeister bias. Therefore, OBIMA is seemingly a nickel(II)-selective extractant.

ACKNOWLEDGEMENTS

First of all I would like to give all the Glory to Jesus Christ my Lord and Saviour. Without Him I can do nothing. He, through the Holy Spirit, is my primary source of favour, strength, endurance, knowledge and wisdom.

I would like to thank my parents, Swelekile and Mkasoka Magwa, even though you no longer live your love and teachings will always be part of me. Without the foundation you instilled in me I never would have had the opportunity to reach my goals.

Foremost, I would like to express my sincere gratitude to my advisor, Prof. Zenixole Tshentu, for the continuous support of my PhD research studies, for his patience, motivation, enthusiasm, and immense knowledge. His mentorship was paramount in providing a well-rounded experience consistent with my long-term career goals. He encouraged me to not only grow as an experimentalist and a chemist but also as an instructor and an independent thinker. I could not have imagined having a better advisor and mentor for my PhD study.

I would like to gratefully and sincerely thank my co-supervisor Prof. Gareth Watkins for his guidance, understanding and patience, during my graduate studies at Rhodes University. He was the first person to trigger my love for Inorganic Chemistry. His enthusiasm and immense knowledge in the field of Inorganic Chemistry had planted a seed that directed my future.

Also, thanks the entire Department of Chemistry at Rhodes University for giving me the opportunity to study towards a Doctor of Philosophy (Science) degree in Chemistry. Prof N. Torto, the former Head of Department is acknowledged for encouragement.

My sincere gratitude goes to all the support staff of the Chemistry Department, in particular Mr Francis Chindeka (DST/Mintek-NIC, Rhodes University Chemistry Department) for the microanalysis results and for all his help fixing anything electronic and doing it with a smile and laughter and also like to thank A. Adriaan, V. Dondashe, R. Douglas, H. Mcuba, J. Fourie for their help

Dr E. Hosten from the NMMU Chemistry Department is appreciated for his assistance with the solid state UV/Vis studies and and for collecting the crystal data and solving the crystal structures. The five crystal structures were solved by Dr Hosten but four crystals were grown by myself and the $[Cu(PIMH)_2(H_2O)]SO_4 \cdot H_2O$ crystals were grown by Prof Tshentu.

I must also thank all my colleagues in the Inorganic-Analytical chemistry Group (F2, F3 and F5) for the support and fun times. First and foremost, my thanks to Mr Adeleye Ishola Okewole my labmate in Lab F2, and Lukholo Funde (NMMU) for his tremendous assistance in the stability constants determination. Mrs C. K. Idahosa, Isaac Zvikomborero Gundhla, Ryan Wamsley, Vital Ugirinema, Sunday Ogunlaja, Omolola Fayemi, Avela Majavu, Phumelele Kleyi, and Abdullahi Sobola you all made my study exciting.

Thanks to Vuyiseka Makabe, my sister and friend your unfailing support and love pulled me through.

Special thanks go to Apostle B.E. Geelbooi of Gospel Ambassadors Ministries, South Africa for being my encouragers when I needed to vent.

I would like to thank National Research Foundation for their financial support and for funding this research work.

Finally, I would like to gratefully acknowledge my family. Thanks to my three sisters, Phakama, Phumza and Thumeka after my mother's passing you guys did not hesitate to take the motherly role in my life for that I would be always in debt to you. Bongeka Magwa your help and support have contributed to this success. To my nephew Andisiwe Magwa every time we talked about school you humbled me. Sivuyile, Phateka, Fezeka, Nomthetho, Mvuyisi, and Buyekezwa thank you for your support and encouragement.

I thank my incredible fiancé, Thompho Jason Rashamuse (Susu wamga), who was forced to listen to many of my complaints and frustrations from the lab. Thank you, for your love, respect, support and encouragement. It strengthened me during the long hours that I had to work on this project.

LIST OF FIGURES

LIST OF TABLES

LIST OF SCHEMES

LIST OF ABBREVIATIONS

AC - Alternating Current

Amplats - Anglo American Platinum Corporation Ltd

BC - Before Christ

BET- Brunauer- Emmet-Teller

CFSE - Crystal Field Stabilization Energy

D - Distribution Ratio

DC - Direct Current

DEPHA - Di-2-Ethyl Hexyl Phosphoric Acid

DIMOX-1-Decylimidazole-2-aldoxime

DMF-Dimethylformamide

DMG - Dimethylglyoxime

DNNSA - Dinonyl Naphthalene Sulfonic Acid

DpH - Decomplexation pH

DPIM -1-Decyl-2-(2′-pyridyl)imidazole

FTIR - Fourier Transform Infrared

GC - Gas Chromatography

HL - Chelating Agent

HPIM -1-Hetyl-2-(2′-pyridyl)imidazole

HSAB- Hard and Soft Acid and Base

ICP-MS- Inductively Coupled plasma-Mass spectrometry

ICP-OES - Inductively Coupled plasma-Optical Omission Spectroscopy

IX - Ion Exchange

K_{DHL}- Distribution coefficients of the extractant (reagent)

K_a - Ionization constant

K_{ex} -Extractive equilibrium constant

K_f - Formation constant

K_{sp}- Solubility product

L - Ligand

logβ - Stability constant

MIMOX -1-Methylimidazole-2-aldoxime

ML - Metal Ligand chelate

N-donor - Nitrogen-donor

NMR - Nuclear Magnetic Resonance

O-donor - Oxygen-donor

Oh- Octahedral

OIMOX-1-Octylimidazole-2-aldoxime

OPIM -1-Octyl-2-(2′-pyridyl)imidazole

PGM- Platinum Group Metals

PIMH - 2,2′-Pyridylimidazole

p*K*a - Acid dissociation constant

PLS - Pregnant Liquor Solution

SEM - Scanning Electron Microscopy

SPE - Solid Phase Extraction

SSX - Synergistic Solvent Extraction

SX - Solvent Extraction

Td– Tetrahedral

tms - Transition metal series

XPS - X-ray Photoelectron Spectroscopy

UV-Vis – Ultraviolet-visible spectrophotometry

β - Separation factor

CHAPTER 1

1. INTRODUCTION

1.1. Overview

The upsurge in mineral markets has continued to motivate for the development of processes that seek to improve the dissolution of ores and separation methods for the recovery of high purity value added metals. South Africa depends on mineral resources more than any other trading country, and their contribution to the GDP accounts for 16% of the total.[1] The country's prolific mineral reserves include precious metals and minerals, energy minerals, non-ferrous metals and minerals, ferrous minerals, and industrial minerals. In South Africa, base metals are recovered as by-products from the production of platinum group metals. Base metals together with precious metals occur in economic concentrations in three layered reefs, and these are Merensky Reef, UG2 chromitite layer and Platreef.[1] Beneficiation of metals from their ores is achieved through metallurgical processes. The application of metallurgical process dates back to 4000 BC,[2] in which metals were isolated as alloys such as brass or bronze by crude and time consuming methods of purification. However, incremental improvement and development resulted in techniques that provide the high degree of purity of metals such as pyrometallurgy and hydrometallurgy.

Pyrometallurgical techniques involve the processes that use thermal treatment on minerals, metallurgical ores and concentrates to bring change on the physical and chemical properties of the materials to enable recovery of valuable metals. Pyrometallurgy is grouped into different categories and these include calcining, roasting, smelting and refining. Due to the high cost of

the high temperature processing and the emission of metal-containing particulates, noxious gases, greenhouse gases and toxic metals the method is slowly being replaced by hydrometallurgy. Hydrometallurgy deals with the processes that apply much lower temperatures for the dissolution of metals from their ore (leaching), followed by the use of reagents for the selective extraction (solvent extraction or ion exchange) or precipitation of metals from aqueous solutions. Traditionally, hydrometallurgical methods are known to be inexpensive and to have fewer environmental problems,[2] and these include the loss of solvent to the environment and the formation of potential new pollutants during the introduction of reagents. The major break-through in the application of hydrometallurgy is traced back to 1887 with the leaching of gold using cyanide and the Bayer process for the refining of alumina. Both processes marked the birth of the modern field of hydrometallurgy.[3]

It must be noted that technological developments for the hydrometallurgical processes over the past century have been driven by factors such as the demand for higher purity metals and achieving inexpensive routes.[3,4,5] In order to overcome the challenges and to bring an improvement in the traditional routes, intensive research should be directed towards the development of meaningful knowledge. This requires the investigation of the chemistry involved in the separation process particularly the coordination chemistry.

As far as base metal ions are concerned there are still some problems which require major attention concerning their separation.[6] For instance, the presence of iron in base metal ores which is readily oxidized to Fe(III) poses a great challenge since it is preferentially extracted over other divalent ions by the majority of existing extractants since it is a strong Lewis acid.

Separating agents that would be feasible for base metals separation in a strongly acidic medium must therefore be able to reject impurities such as Fe(III) in addition to being specific to the metal ion of interest. The fundamental understanding of coordination chemistry is very important in coming up with successful strategies for the separation of base metals.

1.2. The chemistry of base metals and their extraction

Base metals are metals that oxidize or corrode easily. They react with hydrochloric acid to form hydrogen.[7] These metal ions are naturally found in earth's crust and their market value is less than that of precious metals. Some examples of base metals include nickel, cobalt, copper, iron, lead, zinc, cadmium and manganese. Base metals can be classified as early, mid or late 3d metals since most are found in the 3d row of transition metals.

1.2.1. Copper

Copper is one metal that has a greater impact on the history of civilization and is the first metal to be put to practical use.[8,9,10] It is still the world's third most used metal and is the most important metal in the generation and distribution of electricity. The metal copper is one of the first metals to be discovered, probably during the seventh millennium BC in the Near East. In nature copper normally occurs chemically combined with other elements, in a form of minerals. The most common minerals exploited for the recovery of copper are chalcopyrite, malachite and cuprite.[11] The principal deposits of copper include porphyry, sedimentary, massive sulfide, magmatic and vein.

For copper recovery, both hydrometallurgy and pyrometallurgy methods are used to extract copper from its ores. In hydrometallurgy method, copper in an oxide form is separated by

leaching, followed by selective extraction; while the sulfide ores are turned to a pure metal by heat (smelting). In both processes the fundamental chemistry of copper is very important. The element copper occurs in different oxidation states, these include copper(0) in the metallic state, copper(I) in cuprous compounds, copper(II) in cupric compounds, and copper(III)/(IV). Copper(II) ion is a borderline Lewis acid, forms stable coordination compounds and is more prolific in formation of good crystals. The well-known stereochemistries for copper complexes are four-coordinate square planar, tetrahedral geometries, five-coordinate trigonal bipyramidal geometry and six-coordinate octahedral geometry. The six-coordinate compounds are not very common.[12] The relative stabilization of these various geometries can result in stereochemical "tailor-making" as a way of exploiting separation of metals through coordination preferences.

The best donor atoms that stabilize copper(II) are nitrogen and oxygen. The copper-specific extractants which have contributed significantly to the production of copper are hydroxyoximes and they have been commercialized by General Mills Inc., an example being LIX 64.[13,14,15] The hydroxyoxime (**Figure 1.1**) extractants are used to extract copper from other base metals in acidic sulfate liquors. The nature of the interaction between the copper metal ion and the hydroxyoxime is known as chelation.[16] The complexation of copper by the hydroxyoximes is shown in **Scheme 1.1**. During the extraction of copper with hydroxyoximes, two protons are lost from each ligand per copper ion, and this therefore implies that pH becomes an important parameter in controlling the reaction equilibrium.[13,17,18,19] Recently, Tasker and co-workers have extended the chemistry of hydroxyoxime ligands as copper(II) extractants by incorporating the hydrogen bond buttressing effect which results in greater stabilization of copper(II) leading to better separation.[20]

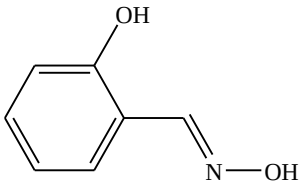

Figure 1.1: The basic structure of salicylaldoxime

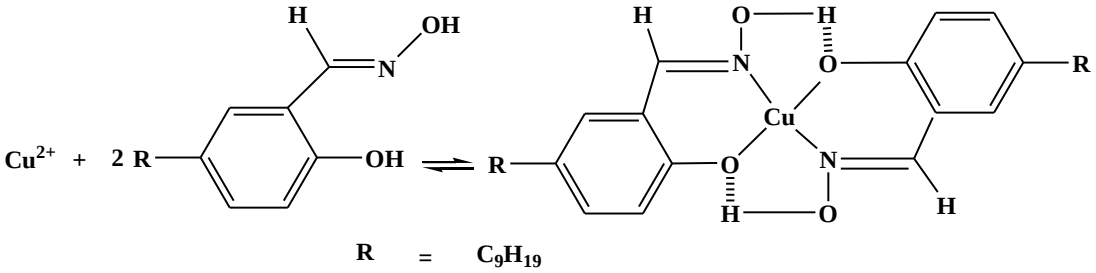

Scheme 1.1: The complexation reaction of copper and oxime

The first commercial reagents used for the extraction of copper were aliphatic α-hydroxyoxime-based ligands (LIX 63) back in 1962 (see **Figure 1.2** for the chemical structures). The aliphatic-oxime based ligands are very selective for copper(II), and its extraction occurs at pH values of 5 to 8 from ammonia solution. LIX 63 (1) reagent was considered a good extractant for copper from ammonia solution, but its application commercially was hindered by the stripping problems and also because of the development of a more versatile and less expensive LIX 64N. LIX 64N, a β-hydroxybenzophenone oxime (2**)** was the first reagent to be used on a full scale plan in 1968.

The introduction of aromatic ring into the oxime structure provided an electron-withdrawing effect resulting into the greater acidity of the changeable protons, and this allowed the copper(II) extraction to occur at lower pH values.

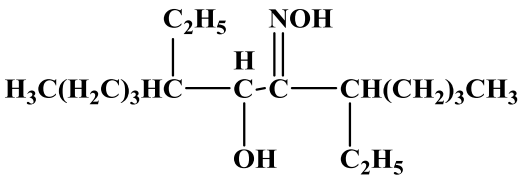

1

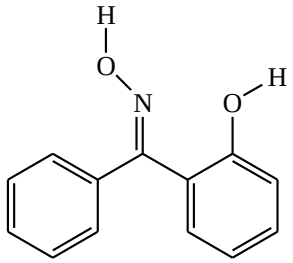

2

Figure 1.2: Chemical structures of LIX 63 (**1)** and LIX 64N (**2)**

1.2.2. Nickel

The element nickel occurs in nature mainly in combination with other elements such as arsenic, antimony and sulfur. Nickel is the 24th most abundant element in earth's crust.[21] Nickel falls into two principal type ores; sulfides and laterites.[22] Nickel is mostly recovered from sulfide ores. The occurrence of nickel was first discovered by miners in the seventeenth century in Erzgebirge (Germany). They came across a red-colored ore thought to be copper, but now known to have niccolite (NiAs). Nickel sulfides are commonly found in the form of pyrrhotite [$(NiFe)_7S_8$] and pentlandite [$(NiFe)_9S_8$]. Nickel laterite ores are low grade deposits and are also an important source of nickel. The first application of nickel was in Greek coins by Alexander the Great around 327 BC. The coins were found to have a composition of 80:20 copper:nickel, and a current widespread application of nickel is the use of ferronickel in stainless steel products.

In Africa nickel production still remained above 80 900 t with South Africa contributing 50% and Zimbabwe and Botswana the rest, and the production is mainly from sulfide ores. Africa produces 70t of refined nickel, which represents only around 5% of global supply. Nickel is produced primarily from South Africa, Zimbabwe and Botswana. Nickel production in South

Africa (SA) is mainly as by-product of platinum group metals (PGM's). The largest producer of nickel in SA is Anglo American Platinum Corporation (Amplats),[23,24] accounting for over half of the total production. Half of Amplats' nickel production comes from the Rustenburg mines. The PGM mines are on both the Merensky reef and UG2, but the higher content of nickel is on Merensky.[25] The extraction route for nickel can be pyrometallurgy and/or hydrometallurgy process.[26,27] Pyrometallurgy is mostly used to process ores that are not amenable to leaching such as saprolite ore (laterite). The well-known pyrometallurgical route is to smelt the ore (ferronickel) by the rotary kiln or electric furnace (RKEF) route. For the hydrometallurgical process there are essentially two broad routes; the Caron process and high pressure acid leach (HPAL) process.[28] There are few companies that adopted the Caron process such as BHP Billiton's QNI refinery in Queensland and Tocantins in Brazil. The process involves the drying and roasting of the ore, followed by ammonia leach and refining. The process is not economical due to the drying and roasting stages. The recovery of nickel and cobalt are higher in the Caron process. It operates at high temperature and pressures with highly corrosive fluids. The companies that use APL process include Moa, Freeport Sulfur Company, Port Nickel and General Nickel Co. in Cuba. The acid pressure leach process involves the use of hydrogen sulfide to treat nickel ores to produce a high grade sulfide containing at least 50% nickel. This mixed sulfide is then pressure leached to give a high purity concentrated nickel-cobalt solution, suitable for solvent extraction to separate the valuable metals.

This process is best used for processing of limonite ores, the presence of aluminium and magnesium in high content is known to result in high acid consumption. The ore is leached in an autoclave with sulfuric acid at 240-270^{o}C dissolving most of the ore into solution and to produce

a high purity concentrated nickel-cobalt solution, suitable for solvent extraction to separate the valuable metals. The high temperature ensures fast reaction times of 60-90 minutes, and also results in the precipitation of much of the dissolved iron as hematite or jarosite and aluminium as alunite.

While many metal ions have been described for their selective extraction behavior by the industrially-important extractants, it seems not much has been achieved for the selective extraction of nickel(II) ion. The first reagents to be considered of potential commercial interest is α-hydroxyoxime/carboxylic acid mixtures in the1960s and 1970s due to the fact that separation factors of up to 50 were observed for nickel over cobalt in a sulfate medium and the reagents were able to extract nickel(II) in preference to ferric ion.[29] However, the kinetics of nickel extraction were very slow, taking 3 hours to reach equilibrium at ambient temperature. The studies conducted by Flett[30] in 1974 indicated that the slow kinetics were due to the interfacial effect in the system.

The application of oxygen donor ligands, such as organophosphorus extractants (Cyanex reagents) or oxime-type extractants (LIX reagents), is well known commercially but their application in nickel extraction is known to have disadvantages due to the extraction of Fe(III). The selective extraction of nickel(II) ion can be driven by considering the stereochemical factors. Nickel(II) forms a large number of complexes encompassing coordination numbers four, five and six.[31] Nickel(II) is known to form the most stable spin free octahedral (O_h) complexes of all base metal ions.[32] While four coordinate complexes are unstable and uncommon,[33] the square-planar and tetrahedral are found, and five coordinate complexes such as square-pyramid and

trigonal-bipyramid are rare. As mentioned above that oxygen donor ligands have been exploited for the extraction of nickel, but the limitation of these systems is their high affinity for Fe(III) and the formation of extractible complexes at high pH.

1.2.3. Cobalt

Cobalt constitutes about 0.001% of the earth's crust, and it is widely distributed. The primary ores capable of being commercially exploited are arsenides, sulfides and oxides. These ores tend to contain both cobalt and nickel minerals because both metals have similar physical and chemical properties. Hence there is continuous research on the separation of nickel and cobalt. The cobalt metal was first separated and recognized as an element by a Swedish chemist Brandt in 1735.[34] The metal resembles iron and nickel in appearance and is used in variety of steels designed to have specific magnetic properties. The production of cobalt in South Africa is mostly obtained as by-product in the processing of PGMs as well as co-product in the single nickel operation.[35] The first commercial operation for cobalt recovery using solvent extraction in South Africa was conducted by Anglo Platinum Rustenburg base metal refining in 1979.[35] The recovery of cobalt in this plant was obtained via cobalt precipitation which was produced from the main nickel electrolyte with nickel hydroxide. The dissolution of the cobalt cake resulted in a solution (2:1 to 4:1 Co:Ni) which was treated by solvent extraction with D_2EPHA at 50^oC to achieve a cobalt recovery of > 95% at cobalt to nickel ratio of > 500:1.[35]

Cobalt(II) forms a range of stable coordination compounds with different ligands, and is known to adopt a wide variety of geometries. The ligands that form stable complexes with cobalt are oxygen and nitrogen donor ligands and the well-known geometries for cobalt(II) ion are

tetrahedral, square-planar, square-bipyramidal, trigonal-bipyramidal and octahedral. Co(II) and Ni(II) have similarities, and both metal ions are known to exist as hexahydrated ions $[M(H_2O)_6]^{2+}$ with an octahedral geometry in aqueous solutions, but the displacement reaction process of water molecules occurs much faster in cobalt than in nickel. Cobalt(II) is known to form a tetrahedral geometry much more readily than Ni(II) while Ni(II) forms an octahedral geometry much more readily than Co(II) in a concentrated electrolytic solution.

1.2.4. Zinc

Zinc is widely distributed over the earth's surface and is the 25th element in order of abundance.[36,37] The early reports show that the native zinc was found in Australia.[38] This element is found concentrated into sulfide, carbonate, silicate and phosphate rocks, but the chief commercial sources are sulfide and carbonate. The first application is dated back to 1450 AD by Chinese where the element was used to make coin. The major primary zinc production is done *via* hydrometallurgical route (solvent extraction) and the major extraction of zinc was conducted in India.

The extraction of zinc through hydrometallurgical route (electrowinning of zinc) is still a challenge due to the presence of traces of organics in the electrolyte solution. These may deposit on the cathode which leads to a lower current efficiencies and for the successful separation of zinc through electrowinning a high purity of electrolyte is required.[39] To overcome the major problems associated with the extraction of zinc, a process known as Zincex process is employed for the recovery of zinc, through which the necessary electrolyte purity is achieved by two cycle design of the solvent extraction circuit. The first anionic cycle involves the use of amine

extractant which extracts zinc together with some iron from the chloride leach liquor which originate from the chloride leaching of pyrites cinder. The stripped liquor from the anionic cycle is thereafter transferred into the cationic cycle where di-2-ethyl phosphoric acid (D_2EPHA) is used to re-extract zinc from the stripped liquor chloride solution.[40]

1.2.5. Iron

Iron is the fourth most abundant element in the earth's crust. It is believed that the earth's core consist of iron. It is well known that most minerals consists of iron. The most important sources of iron are the oxides and carbonates. The principal sources of iron are magnetite (Fe_3O_4) which constitutes the richest ore of iron, hematite (Fe_3O_3) which contains about 70% of iron, limonite ($2Fe_2O_3 \cdot 3H_2O$) and siderite ($FeCO_3$). The iron in the form of ferric ion is considered to be a major impurity in other metal ion ores and its removal is considered one of the challenges that need to be dealt with in order to achieve successful separation techniques in base metal separations.

The chemistry of iron(III) or its position as hard acid classification is the main driver for its interfering behavior in the extraction of base metals using current extractants that contain oxygen donor atoms.[41] The ferrous ion is a borderline element and has low affinity for oxygen donor ligands, therefore its presence is regarded as less challenging compared to the ferric ion. The removal of ferric ion is attained by selective precipitation prior to the separation of the targeted elements either by solvent extraction or ion exchange.[42]

1.2.6. The rest of other base metals

The other elements under the base metal classification are present in low concentrations in the pregnant liquor solution. They are also considered as impurities. These include manganese, cadmium, aluminum and the alkaline earth elements such as magnesium and calcium. The presence of these ions does not pose much of a challenge for the separation of base metals as compared with the ferrous ion.

1.3. Traditional methods for separation of base metals

There are several methods that are used for the recovery and purification of base metals and they range from froth flotation, precipitation, distillation, evaporation to fractional crystallization. For the separation of base metals on a large scale, pyrometallurgy and hydrometallurgy are the most applied techniques.

1.3.1. Hydrometallurgy

Hydrometallurgical route of metal ion separation has been commercially applied for the recovery of base metals especially in the separation of cobalt and nickel. Several techniques have been used such as sulfide precipitation,[43] precipitation by exploiting the oxidation/reduction chemistry, ion exchange (is a process of exchange of one ion for another ion on the solid phase), and solvent extraction (applies a two-phase solution chemistry to recover metal ions). It must be noted that the processes are still in use today, but they have challenges. Solvent extraction is widely applied and has high impact in separation of metals than the other processes due the high degree of separation it provides as well as high yield. It provides cheaper operational costs and is a very flexible process that can easily adapt to suit the system under consideration. The latest

advance in hydrometallurgy is the use of a synergistic solvent extraction system (SSX). The synergistic solvent extraction system is a technology that uses the synergistic combination of two or more extractants in the extraction of metal ions, which enhances efficiency as compared to the individual extractant.[44,45]

1.3.2. Precipitation

The precipitation process as the tool for the separation of cobalt and nickel is still popular and is carried out by a number of processes. These include sulfide and selective oxidation/reduction precipitation.[46] The sulfide precipitation method exploits the low solubility of cobalt sulfide as compared to nickel sulfide. The drawback of this method is the contamination of the cobalt due to the low cobalt to nickel ratio in the industrial feed solutions. The more advanced technique in the application of precipitation method is the selective oxidation/reduction. This method involves the selective reduction of nickel from a mixed sulfate solution by hydrogen under pressure or the oxidation of cobalt from mixed sulfides at ambient temperature under pressure in the presence of ammonia to form cobalt(III) state while nickel remains in the solution as nickel(II). Then the nickel element is recovered as nickel(II) ammonium sulfate.[47]

1.3.3. Ion exchange

The ion exchange method involves the exchange of ions on a solid phase with conservation of charge. The technique has also been employed in the separation of base metals with both anion and cation exchanger, but the application of this method is limited in industry due to its slow kinetics. However, the separation of cobalt and nickel is accomplished from chloride medium with anion exchanger. The factor which is exploited in this process is the tendency for cobalt to

form anionic chlorido complexes such as $[CoCl_3]^-$ and $[CoCl_4]^{2-}$ which nickel does not, and this allows for the separation between the two metals. Since these chlorido complexes are quite weak, a relatively high concentrations of chloride ions are required in order to form $[CoCl_4]^{2-}$ species which are tetrahedral. But in highly concentrated chloride solutions metal ions such as Fe^{3+}, Cu^{2+} and Zn^{2+} also form stable tetrachlorido complexes which hinders/interferes with the extraction of cobalt,[48] hence these anion exchange resins have limited commercial application. The cation exchange resin functionalized with sulfonate groups (sulfonated copolymers of styrene) are used for the removal of nickel in a sulfate medium of high cobalt to nickel ratio, but their application in industry is limited because they offer a very low or no degree of selectivity between nickel and cobalt.[49] The chelating ion exchangers such as the DOWEX M4191 which are functionalized with *bis*-picolylamine (BPA) are more popular in industry and they have been used for extraction of base metal ions, however, no serration is observed with BPA.[50]

Literature studies [51] have shown that metal Ni(II) can be recovered by macroporous weak acid resin. Recent studies conducted by Chunchua *et. al.* have indicated that nickel(II) can be absorbed on the macroporous weak acid resin (D151 resin) in acetic acid-sodium acetate (HAc-NaAc) medium at pH = 6.90 in presence of cobalt(II).

1.3.4. Solvent extraction

Solvent extraction is a widely applied technique for the recovery of base metals.[25,52,53] The method continues to advance due to the continuous research in the area and development of new extractants, the improvements on the existing techniques and the low cost of the process involved. The method is highly applied as cleaning or purification step and for quick separation

of metal ions. SX involves the selective transfer of the targeted species from aqueous to the immiscible organic solvent. In hydrometallurgical separation of base metals, an organic extractant is dissolved in an organic solvent and is used to selectively extract the targeted metal ion from an aqueous solution, and with a favorable distribution ratio the metal ion is thus loaded into the organic phase. The metal ion is then recovered in its purer state through back extraction into a suitable aqueous solution. The formation constants for metal ion complexes and their relative distribution ratios are more important for effective separation factor to be achieved.

1.4. Separation of cobalt and nickel

The separation of cobalt from nickel has been practiced for many years. There are number of processes that have been used commercially for cobalt separation from nickel in both chloride and sulfate medium, but currently the favoured process is the selective solvent extraction of cobalt from nickel using phosphoric acid derivatives, such as CYANEX 272.[54]

1.4.1. Chloride leach liquor

In a chloride solution cobalt forms a tetrahedral anionic complex, $CoCl_4^{2-}$, and is extracted by protonated amine or quaternary ammonium extractants[55,56] as shown in **Equation 1**.

$$CoCl_4^{2-}{}_{(aq)} + 2R_4N^+Y^-{}_{(org)} \rightarrow (R_4N^+)_2CoCl_4^{2-}{}_{(org)} + 2Y^-{}_{(aq)} \quad (1)$$

where R denotes an alky group or hydrogen and Y is a univalent anion. The nickel species formed remain behind because it is in the neutral form $NiCl_2$. This separation principle has been

applied commercially at Falconbridge Nikkelverk in Norway[57] and at Sumitomo Metal Mining Co in Japan.[58]

1.4.2. Sulfate leach liquor

In a sulfate medium cobalt is commonly extracted in commercial plants from nickel using dialkylphosphorous extractants (CYANEX reagents) presented in **Figure 1.3**.

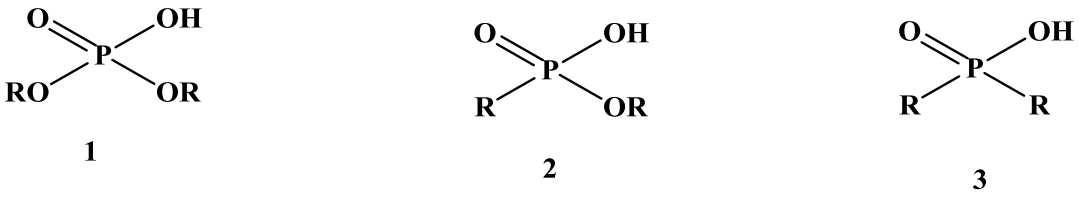

Figure 1.3: Comparison of dialkylphosphoric (**1)**, -phosphonic (**2)**, and -phosphinic acid (**3)** extractants

It is known that the basicity of these reagents increases with decreasing distance of the alkyl chains from the central phosphorus atom, from the phosphoric acid structure (represented by D_2EPHA), to the phosphonic acid (PC-88A, lonquest 801), to the phosphinic acid (CYANEX 272, lonquest 290). This resulted in improved Co:Ni separation factors from 14 to 280 to 7000 respectively.[59] The extraction reactions of the cobalt and nickel are presented in **Equations 2** and **3**.[60]

$$Co^{2+}_{(aq)} + 2H_2A_{2(org)} \rightarrow CoA_2{\cdot}H_2A_{2(org)} + 2H^{+}_{(aq)} \quad (2)$$

$$Ni^{2+}_{(aq)} + 2H_2A_{2(org)} + H_2O \rightarrow NiA_2{\cdot}H_2A_2xH_2O_{(org)} + 2H^{+}_{(aq)} \quad (3)$$

The selective extraction of cobalt over nickel is achieved due to the formation of the tetrahedral cobalt species, however the extraction takes place in the high pH range. This species is more favoured in the organic phase than the octahedral nickel complex (which has two water molecules coordinated). The nature of the complexes formed by these reagents allows the separation of cobalt. The cobalt complex is hydrophobic while the nickel complex can contain one or more coordinated water molecules in its inner sphere making it more hydrophilic.[61] Currently, however, the most preferred reagents for the separation of cobalt from nickel are organophosphinic acid based ligands such as CYANEX 272 due to the fact that they are more stable with respect to the oxidative degradation and are also more selective for cobalt(II) over calcium(II) and lastly any co-extraction of Fe^{3+} can be easily stripped by sulfuric acid.

This study explores the selective extraction of nickel(II) from cobalt(II) and other base metals. It is well known that the improvements of the chemical processes in the solvent extraction system require a thorough knowledge of base metal ions chemistry and an investigation of the chemistry involved in order to achieve a meaningful advancement of this technology. The innovative approaches to ligand design become the key factor in the advancement of the extraction chemistry.

1.5. Approaches for ligand design

1.5.1. Metal ion specificity

The basis of base metal ion separation is a unique property of the coordination chemistry of the particular metal ion. In the development of a metal ion-specific extractant, it is necessary to

consider the characteristics of the metal ions from which the desired metal ion must be removed as well as its own.

As far as base metals are concerned there are still some problems which deserve attention. In most base metal ores, iron is always present. Iron can be easily oxidized in the presence of oxygen to Fe^{3+}. This trivalent metal ion is a stronger Lewis acid than any other divalent ions, and due to this the ferric ion is preferentially extracted[62,63,64,65] than the other element. Currently, there is no extractant that can reject iron(III) and at the same time recover nickel or cobalt at pH < 4. All the commercial available extractants extract cobalt and nickel between pH values of 4-6.[6] In order to avoid the extraction of Fe^{3+} its removal by precipitation is carried out at pH of 3 in which very little of the other base metal ions co-precipitate with it.[5] Fe^{3+} is known to exist in aqueous solution in its spin-free form ($t_{2g}^3e_g^2$). This electronic structure prefers ionic interaction with oxygen-donor atoms and fluoride ligands. Most of the popular extractants currently available in industry such as organophosphorus extractants (Cyanex reagents) and oxime-type extractants (LIX reagents) have oxygen donor atoms.[66,67] The major drawback with the O-donor extractants is that they have high affinity for Fe^{3+} and other A-type metal ions such as Mg^{2+}, Mn^{2+} and Ca^{2+}, and this necessitates for the precipitation of Fe^{3+} prior to the extraction of nickel and cobalt[5,68] as explained above. However, the N-donor ligands are known to form stable complexes with borderline hard/soft metal ions such as the later 3d metal ions, and less stable complexes with A-type metal ions such as ferric ions.[69, 70] This motivates for the exploitation of N-donor ligands as potential extractants in the separation of base metals. Since the emphasis of this project is to design a base metal specific separating agent particularly for nickel ion in the presence of other base metal ions, it is important to investigate not only the preferred

coordination behavior of $Ni^{2+}$with the chosen ligands, but also the coordination behaviour of other base metal ions that are present during the separation process.

It is well known that specificity for metal ions can be tuned through stereochemical "tailor-making".[71] Nickel(II) forms the most stable spin free octahedral (O_h) complexes of all base metal ions (Fe^{2+}, Co^{2+}, Cu^{2+} and Zn^{2+}),[72]therefore to achieve nickel specificity it is important for the ligand to force the formation of six-coordination. It must also be pointed out that the square planar nickel(II) complexes also exhibit good crystal field stabilization energy gain in their formation and are therefore stable despite being uncommon. Ligands with mild sigma donor character and good pi acceptor capability have the ability to stabilize the spin-paired square planar nickel(II) complexes. The copper(II) ion, on the other hand, forms stable tetrahedral (T_d) and square planar complexes while octahedral complexes are less common.[69,73] Cobalt and zinc also tend to form more stable T_d complexes compared with O_h complexes. It is observed that Cu^{2+}, Co^{2+} and Zn^{2+} behave similarly in their tendency to form tetrahedral complexes. But Co^{2+} and Zn^{2+} are weaker Lewis acids hence four-coordination is sometimes satisfactory for stabilization and the probability of Co^{2+} to form T_d as compared to O_h complexes is quite smaller than Cu^{2+}. It is important to ensure that a six-coordinate complex is formed for nickel(II) or alternatively a square planar complex. It is equally important that the selected donor atoms of the neutral ligand do not form stable complexes with Fe^{3+}. Again it is known that, firstly the formation constants of O_h amine complexes increase from Mn^{2+} to Ni^{2+} and decrease towards Cu^{2+} and Zn^{2+}.[69] Secondly the amine based ligands do not form stable complexes with iron(III).[74] For this project it was therefore decided to investigate the possibility of using aromatic amine ligands as extractants.

1.5.2. Ligand design

The most popular commercial extractants are organophosphorus extractants and oxime-type extractants. These organic extractants have managed to address the separation of cobalt from nickel in the presence of other metal ions [67,75,76,77,78,79] but the selective extraction of nickel from cobalt has not yet been resolved.[6] The separating agents that will be suitable for the separation of these two metals in a strongly acidic medium must also not extract Fe^{3+} and in addition it must be specific to the metal ion of interest. To achieve this, the donor atom of the ligand becomes a very strong consideration in the choice of extractant for a specific metal ion separation. Factors such as steric effects, nature of the donor atoms, selectivity, low aqueous solubility, high metal ion loading capacity and rapid extraction kinetics are very important when designing metal specific ligands.[80, 81]

1.5.2.1. The oxygen donors

The oxygen donor ligands are the most used separating agents at the moment, but the drawback of these extractants is their inability to reject impurities such as Fe^{3+}, hence in many flow-sheet processes an additional precipitation stage is required prior to solvent extraction.[82] In addition the O-donor extractants have high affinity for other A-type metal ions such as Mg^{2+}, Mn^{2+} and Ca^{2+} [70,75,76], and their poor selectivity result to the co-extraction of the A-type metal ions.[83]

1.5.2.2. The sulfur donors

The sulfur donor ligands are soft Lewis bases, and are known to form stable complexes with the divalent 3d transition metal ions such as Co^{2+} and Ni^{2+} than the oxygen donor ligands. One of the most popular commercially available sulfur-donor extractants is the sulfur-containing

derivative.[84] These ligands can extract both cobalt and nickel at very low pH, and the disadvantage of using them is that a very strong acid is required for the stripping.[84]

1.5.2.3. The nitrogen donors

N-donor ligands are known to form stable complexes with borderline hard/soft metal ions such as the later 3d metal ions, and less stable complexes with A-type metal ions such as ferric ions.[77,78] There has been an envisaged shift towards amine-based extractants, and this is motivated by the favourable properties that are offered by the nitrogenous ligands especially the aromatic amines as compared with oxygen-based extractants.[71,77,79]

The application of amines as extractants in metal ion separation is well known. For the last two decades amines have been used in their ammonium form and in the neutral N-donor form.[85] Research and development of these ligands has allowed them to be applied as functional reagents in ion exchange techniques. The use of alkylated ammonium derivatives as extractants has resulted in an understanding of a number of effects namely perchlorate effect, the parent acid effect and the secondary cation effect. [86] The perchlorate effect results in the lowering of the activity of the bulky cationic extractant in the organic phase while the secondary cation effect causes a lowering of the activity of the anion to be extracted in the aqueous phase through increasing strong ion paring with decrease in charge density and increasing the size of the cations in aqueous medium.[86] Amines in their cationic form, such as alkylammonium cations, are organic phase compatible and they act as counter cations for the bulky anionic chlorido metal ion species such as $CoCl_4^{2-}$, $FeCl_4^{2-}$, and $FeCl_4^{-}$, and they readily phase transfer from the aqueous to the organic phase. The ion-pairing ammonium-type extractants are divided into the tertiary and

the secondary ammonium cations. These extractants have been used to extract Co(II) from higher chloride concentration and even separate Co(II) from Ni(II) in chloride medium since the latter does not form similar chlorido complexes.

Amines in their neutral form have been exploited in the separation of Ni^{2+} from other base metals but not exhaustively. The diamines as extractants have been developed and investigated including aliphatic, aromatic and the combination of the two. The properties offered by the aromatic nitrogenous ligands are attractive; some of these properties include the intermediate pK_a values as well as σ and π bonding capabilities resulting in extractions in the low pH range and in a possibility of separation through bonding preferences respectively. Aliphatic amines as extractants (R-NH_2, where R is an alkyl or aryl group) tend to form metal complexes at relatively high pH values due to their high protonation constants which lead to the hydrolysis of metal ions even under slightly acidic conditions. These strong ligands with σ-donor only character also show lack of relative preference for the metal ions, however, this can be improved if chelates are used for example the alkylated derivatives of ethylenediamine.[87] The studies indicated that separation of different metals may be achieved by altering the pH of the aqueous phase since each metal has different affinities for a particular nitrogen donor extractant.[88] It must be noted that the nature of the selected amine as extractant is governed by the nature of the metal ion as well as its affinity for the ligand and by the phase transferability of the complexes formed with the metal ion of interest.[89]

Research studies conducted on the behaviour of various classes of neutral amines as metal ion extractants shows that alkylated aliphatic amines, e.g. monodentate amine with only sigma donor

capability such as ammonia (pK_a = 9.63) and bidentate amine also with only sigma donor capability, e.g. ethylenediammine (en) (pK_a = 9.98 and 7.21) have limitations in their applications as extractants in acidic medium due to their ease of protonation (**Figure 1.4**).

(9.63) **(9.98, 7.21)**

Figure 1.4: Chemical structures of aliphatic amines as possible neutral donor ligands, ammonia and ethylenediammine (en) and the protonation constant values are presented in brackets

The two ligand systems have similar protonation constants and for ethylenediammine the "chelate effect" leads to the formation of a stronger metal-ligand bond than with ammonia. Nonetheless, the σ donor only bonding capability of aliphatic amines cannot influence discrimination between the later 3d metal ions and can only then best act as counter cations (as alkylammonium cations) for anionic metal complexes and not as N-donors in metal ion separation even under mild acidic conditions. [90] Again the high protonation constants of the two ligand systems dictate that complex formation occurs at high pH values which is not satisfactory for application in strongly acidic solutions.

The aromatic nitrogenous ligands, however, have an apparent relative preference for metal ions which could relate to the possibility of σ and π bonding capability resulting in an improved metal ion extraction capacity in slightly acidic medium through their N-donor atoms, and in addition allow for complexation to occur even in strongly acidic solutions due to their lower pK_a

values.[53,71] In the light of the above there is need to investigate the aromatic amines with both sigma donicity as well as π interactions in the search for amine extractant for metal ion separation. A series of possible aromatic N-donor monodentate ligands such as imidazole (pK_a = 7.31), benzimidazole (pK_a = 5.60), pyridine, (pK_a = 5.31) and pyrazole (pK_a = 2.78) are shown in **Figure 1.5**.

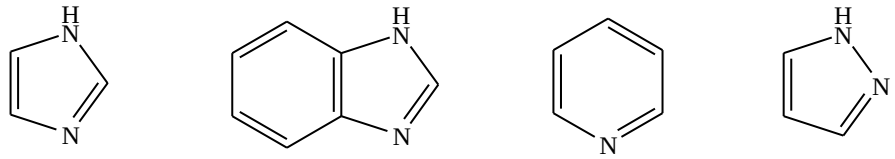

(7.13) **(5.60)** **(5.13)** **(2.78)**

Figure 1.5: Chemical structures of monodentate aromatic amines. (a) Imidazole, (b) benzimidazole, (c) pyridine and (d) pyrazole

Aromatic N-donor ligands and their derivatives are known not to be readily protonated due to their lower proton affinity. The sigma donor strength of these aromatic *N*-donor monodentate ligands is as follows; imidazole > benzimidazole > pyridine > pyrazole. The application of pyridine as an extractant for metal ion separation in strongly acidic solution can be attempted but with consideration for the reversibility of the extraction reaction. In the case of pyrazole, this system is limited as a metal extractant because of its character as a poor σ donor, challenge of back-extraction inherent from its interaction with metals at low pH, and due to the possibility of steric hindrance arising from alkylation at the α-position to the coordinating nitrogen. Imidazole with stronger σ donicity, smaller cone angle, and less stereochemical crowding offers an opportunity in the development of separating agents for the later 3d transition metal ions.[87]

Benzimidazole is intermediate between imidazole and pyridine in its proton affinity, and has an enhanced pi-backbonding capability compared with imidazole due to the additional benzene ring.

Bidentate aromatic amine such as dipyridyl (pK_a = 4.42) (**Figure 1.6**) on the other hand forms a more stable complex with the 3d metal ion owing to the chelate effect compared with the monodentate aromatic amines but its limitation as an extractant in a strongly acidic medium arises from the possible difficulty of back-extraction.

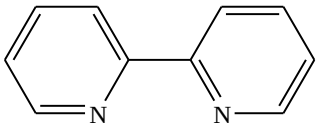

(4.42)

Figure 1.6: Chemical structure of 2,2-bipyridine

The chelate effect has been exploited effectively in a bidentate aromatic system (1-octyl-2,2′-pyridylimidazole) providing for effective separation of nickel from other base metals in strongly acidic sulfate solutions with a possibility of back-extraction.[53] An extension of the bidentate systems to tridentate ligands would have an additional advantage of increasing the extraction equilibrium constants[91] due to the high complex formation constants for reactions of base metals and tridentate ligands,[92, 93] thereby requiring relatively low extractant-to-metal ratios to achieve quantitative extractions.[93] The only example of a tridentate amine solvent extractant in the literature is that of a derivative of diethylenetriamine (pK_a = 9.88, 9.08, 4.42) (**Figure 1.7**),[94] but extractions occurred at relatively high pH values as expected due to high pK_a values of aliphatic amines,[93] and the small $\Delta pH_{0.5}$ values (0.2 for Ni/Co and ~1 for Cu/Zn and Zn/Co respectively)

implied a lack of pH-metric separation of the later 3d metal ions.[94] The famous Dow resins which are based on the tridentate *bis*-picolylamine ligand also showed lack of pH-metric separation of the base metals but extractions occurred at low pH values due to the low protonation constant of the pyridine group[95,50]

It would be hoped that good separation factors of the metal chelates for these tridentate systems would be achieved through stereochemical considerations since nickel(II) is known to form the most stable spin free octahedral (O_h) complexes of all base metal ions[72] while the copper(II) and cobalt(II) ions tend to form stable tetrahedral (T_d) complexes.[69,73]

This lack of selective separation may be attributed to thermodynamic and stereochemical factors. In this study we explore the use of a potentially tridentate aromatic amine ligands, namely *bis*((1*H*-benzimidazol-2-yl)methyl)sulfide and *bis*((1*H*-benzimidazol-2-yl)methyl)amine as extractants for the separation of the base metals, especially nickel from other later 3d metal ions.

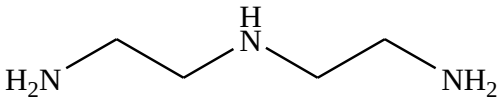

(9.88, 9.08, 4.42)

Figure 1.7: Chemical structure of diethylenetramine

1.6. Properties and behavior of imidazole and benzimidazole

Imidazole is a five-membered planar diazole ring with a pyrole-type nitrogen (N-1) at position 1 and a pyridine-type nitrogen (N-3) at position 3 (**Figure 1.8**). It exists in two equivalent tautomeric forms due to the hydrogen atom at N-1 which can be located on either of the nitrogen

atoms.[96] It is classified as aromatic due to the presence of a sextet π electrons made up of the lone pair ππ electrons at the N-1 and one from each of the remaining four atoms of the ring. Since the acidic proton is located on N-1, the bonding of a proton or metal-ion at N-1 is unfavourable at this position, however N-3 can easily form a stable sigma bond and imidazole is a good pi acceptor of electrons making it favorable to interact with electron-rich metal centers. The benzimidazole ring has enhanced pi acceptor capability compared with imidazole due to extended conjugation introduced by the benzene ring. This also has an effect of lowering the energy of the lone pair of electrons on N-3 giving benzimidazole a weaker sigma donor character compared with imidazole.

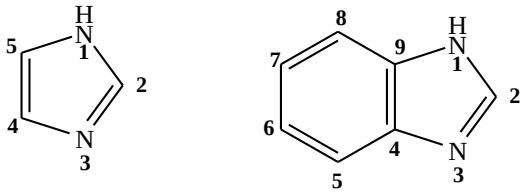

1 **2**

Figure 1.8: The basic chemical structures of imidazole **(1)** and benzimidazole **(2)**

In an acidic medium imidazole forms cationic imidazole while in a very strongly basic solutions it forms an anionic imidazole. Its basic nature can be further enhanced by the attachment of an alkyl chain at N-1. Since imidazole-based systems are capable to bind *via* σ and π bonding, this indicates their potential as metal ion extractants.[97]

Recent literature studies have shown that in order to gain insight on the behavior of the imidazole as the possible extractant for base metal ion separation, protonation constant studies of system of

interest is very important. The imidazole and its derivatives extract base metals at a pH of about 2 and the back-extraction achieved within a pH range of 0.5-1,[98] while the ammonia derivatives form extractible species at high pH due to the high pK_a values making them unsuitable for extraction at low pH since hydrolysis of metal ions would occur. The species distribution plots for the interaction of nickel(II) with ammonia, imidazole and benzimidazole respectively were generated from the protonation, stability and hydrolysis constants obtained from the literature,[99,100] and are presented in **Figure 1.9**. These plots provide insight on the pH-metric aspects of coordination of the *N*-donor ligands. The complexation studies of these *N*-donor ligands indicate that the complex formation of ammonia derivatives with nickel would occur at very high pH, while the complexation of imidazole derivatives with nickel is observed at relatively low pH as compared to ammonia derivatives. On the other hand, the benzimidazole derivatives forms more stable complex with nickel at lower pH as compared to imidazole derivatives.

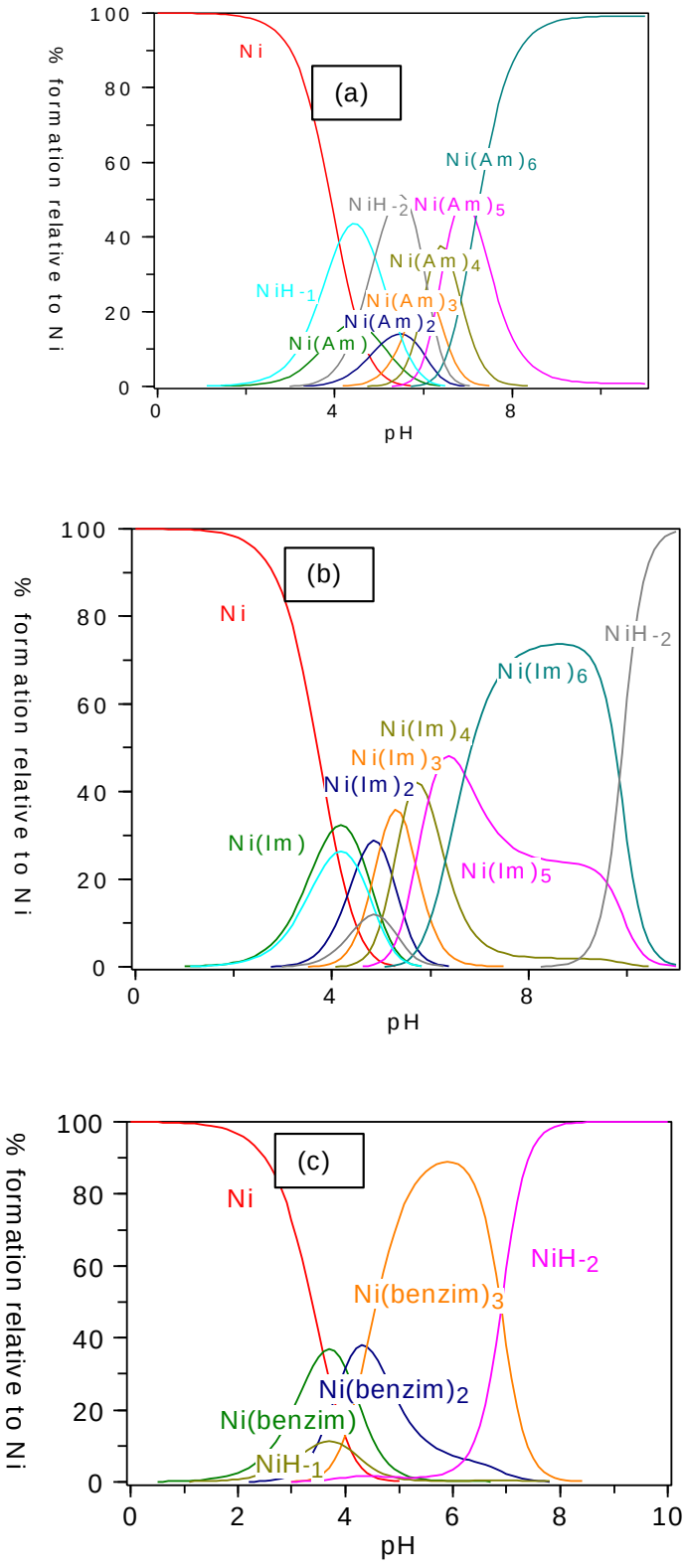

Figure 1.9: The species distribution plots for the step-wise formation of Ni(II) complexes with (a) ammonia (Am), (b) imidazole (Im) and (c) benzimidazole (benzim)[99,100]

1.7. Stability of base metal complexes

The stability constants formed between the extractant and each of the metal ions in solution is a very important factor in the separation of the metal ions *via* solvent extraction. It provides information on the strength of the interaction between the reagents that come together to form the complex. The coordination chemistry of each metal ion is still the leading factor for the metal ion separation. The Irving and Williams series on the stability of the high-spin octahedral complexes of bivalent ions indicates the following order; Mn < Fe < Co < Ni < Cu > Zn.[101] This order was to hold for the stability of all complexes known then. The theoretical background of this order is based on the ionic radii and the second ionisation potentials of the metal as well as the crystal field stabilization energy (CFSE). It is well known that variations of the coordination numbers, stereochemical considerations and entropy factors may affect this stability order.

The formation of a metal complex is represented by ML_n from a metal (M) and a ligand (L) in a stepwise process. The equilibria of the successive stages are denoted by **Equations 4-6**;

$$M + L \rightleftharpoons ML \quad (4)$$

$$ML + L \rightleftharpoons ML_2 \quad (5)$$

$$ML_{n-1} + L \rightleftharpoons ML_n \quad (6)$$

with all the species ML_n in mutual equilibrium and n denoting the maximum coordination number. The equilibrium constant termed as formation constant is given by **Equation 7**;

$$K_n = \frac{[ML_n]}{[ML_{n-1}][L]} \quad (7)$$

The overall stoichiometric stability constant is given as in **Equation 8**;

$$\beta = K_1.K_2.K_3 \ldots\ldots K_n \quad (8)$$

As shown in **Table 1.1**, the logarithm value of either K_n or β are often used to express the degree of the stability of the metal complex or the protonated ligand.

Table 1.1: Literature values of the protonation constants of imidazole and pyridine, and the first formation constants of their nickel (II) complexes[102]. The differences between these constants is also presented

Ligand (L)	**LogK_H^{+1}**	**Logβ_1Ni(II)**	**LogK_H-logβ_1**
Imidazole	7.31	3.02	4.29
Pyridine	5.31	1.88	3.34

Factors that contribute to the stability of a given metal complex are: the chelate effect, the geometrical effect, ionic radius of the metal and the classification of the metal ions. The chelate effect predominantly depends on the entropy change [103] while other factors such as solvation changes and ring formation also play a significant role. The chelate rings such as 5-membered and 6-membered are known to give the most stable complexes. The concentration of free metal ion [M] in solution in a system where the total metal concentration is C_M and the free ligand concentration is [L] can be shown to be

$$[M] = C_M / \sum_o \beta_n [L]^n \quad (9)$$

The subsequent change that occurs during the complex formation is considered of great importance in analytical chemistry where the equilibria are shifted to achieve quantitative

reactions.[103] It is well known that two or more different metals will form complexes of unequal stability with one and the same ligand, the separation of the metal ions is dependent on the formation of a strong chelate complex with few metal ions or at best with only one of the metal ions by the ligand. This makes the given extractant as a selective or "singular" reagent or better put a truly specific reagent realisable.

It can be concluded that in a given metal ion extraction system, to achieve a metal ion specificity, the stability constant (log β) of the complex formed between the extractant and the metal ion of interest must not only be higher than the protonated species but must also be significantly higher than that of the other metal ions present. Therefore, the position of the extraction curves relative to each other in an extraction isotherm would be in order with the relative formation constants.

1.8. Review of N-donor extractants for separation of base metals

The solvent extraction studies on the application of *N*-donor extractants for separation of base metals have been carried out for many decades. Research and development of these reagents was of interest due to the demand for pure metals through hydrometallurgical means. A huge amount of research and development of amine as separating agents for base metals occurred during 1940s to 1960s.[71] The aspects that were a major focus for research were: synthesis of amines,[104,105] the relationship between number of carbon atoms present in high molecular weight amine and aqueous solubility,[106] compatibility with organic solvents, aggregation and micelle formation in organic phase,[107] and extraction capabilities. All these topics have been researched and reviewed. The studies have shown that amine separating agents can be employed for metal ion extraction in slightly acidic medium through their *N*-donor action.

The monodentate aromatic, such as 4-(1-butylpently)pyridine has been employed as extractants for Cu^{2+} under conditions of high chloride ion concentrations (see **Table 1.2**).[108] The 1-alkyl-2-methylimidazole system has been used for the recovery of Zn(II).[109] While derivatives of imidazole such as octyl- or decylimidazole have been proven to be suitable extractants for Co(II), Ni(II), Cu(II) and Zn(II) from aqueous solutions having pH values above 2.[110, 111, 112, 113, 114, 115]

Research studies on bidentate aromatic amines have shown that the nature of the donor atom onto the extractant system plays a significant role in selective extraction of the metal ion of interest. The extractants such as *N*,*N'*-dioctylaminoethylpyridine, (2-(1'-methylthiomethyl)pyridine,[116] 2-((octylthio)methyl)pyridine,[69] *N*-octyl-2,2'-pyridylimidazole,[53,117] and *N*,*N*,*N'*,*N'*-tetraoctylethylene diamine[88,118] have also been of interest.

Table 1.2 .A review of *N*-donor extractants for separation of base metals from the monodentate to tridentate systems

Extractant name	Chemical structure	Explanatory notes
4-(1-Butylpentyl)pyridine[10] [8,87]	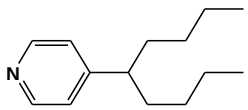	Extraction of Cu(II) under high chloride ion concentrations using chloroform organic solvent. It was observed that the high chloride ion concentration hinders the specificity for copper(II) since under these conditions is easily lost since many metal ions form stable chlorido complexes that may hinder the specificity of copper(II).
1-Alkyl-2-methylimidazole[109]	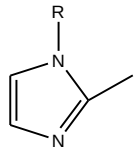 R = C_5H_{11}, C_8H_{13}, C_8H_{17}, $C_{10}H_{21}$, $C_{12}H_{25}$	Extraction of zinc(II) from nitric solution, using three organic solvents, namely, p-xylene and 1,2,3,4-tetrahydronaphthalene, has been carried out with this ligand. The purpose of the study was to determine whether steric effects could create conditions for the selectivity towards zinc(II). They observed that nature of solvent does not influence the stability constant of the Zn(II) complex. The steric hindrance (methyl group) prevents the penetration of the heterocyclic ligands into the sphere of the central ion, and less stable tetrahedral species were found to be more readily extracted.

Table 1.2 Continued

Extractant name	Chemical structure	Explanatory notes
N-Decylimidazole[87]	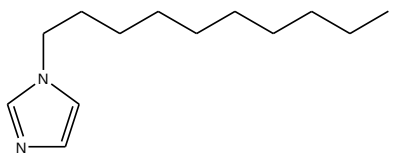	Extraction of Co(II), Ni(II), Cu(II) and Zn(II) from aqueous solutions having pH values above 2. It was observed that the metal ions can readily be stripped at lower pH values. From the study, it was observed that the extractant had a high affinity for copper (75% extraction ~0.08 M), and the system had a very convenient pH region for leaching and stripping, 2.5 and 1 respectively. Because of these characteristics the extractants was recommended for its application as extractant of Cu(II) from leach solutions obtained from the new biotech leach process
(2-(1'-Methylthiomethyl)pyridine)[116]	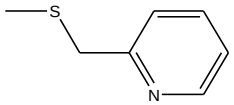	The ligand was employed in the extraction of Ni(II) in the presence of Fe(III). The studies indicated that the system has greater preference for Ni(II) than Fe(III) due to the presence of the soft donor atoms. The coordination chemistry showed that both Ni(II) and Co(II) form six-coordinate complexes but the relative preference for nickel(II) to cobalt(II) was favored.

Table 1.2 Continued

Extractant name	Chemical structure	Explanatory notes
2((Octylthio)methyl)pyridie[69]	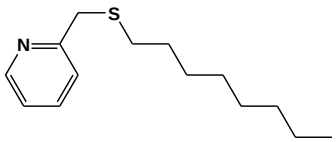	Separation of later 3d metal ions in diluted acid medium in the presence of chloride and thiocyanate ions was carried out. It was observed that in the chloride medium the extraction order of the metals was: Cu(II)>>Ni>Fe>Co>Zn>. In the thiocyanate media the extraction order was observed to behave fairly similar to the chloride medium.
N-Octyl-2,2'-pyridylimidazole[88]	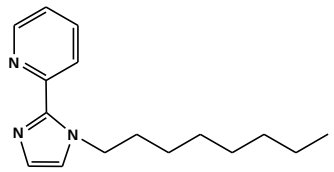	Selective extraction of nickel in the presence of other base metals from chloride or sulfate medium was done. The studies indicated that the nature of the medium (chloride or sulfate medium) does not affect the extraction pattern and its efficiency. A case of Cu(II) separation was demonstrated in a chloride medium. The studies showed that the stripping of Cu(II) metal ion was difficult due to the irreversible extraction of copper by this extractant.

Table 1.2 Continued

Extractant name	Chemical structure	Explanatory notes
N,N,N',N'-Tetraoctylethylene diamine[88,118]	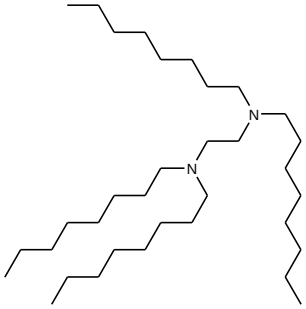	It was observed that the extractant poorly extracted copper as $CuCl_2$·tetoc complex in a narrow pH region (3-4). However, in more concentrated chloride media the protonation occurs and the orange yellow $CuCl_4^{2-}$ species are extracted *via* ion-pair formation. The studies indicated Cu(II) can be extracted at pH value higher than 4, from aqueous solution in which the chloride ion to copper(II) ratio is >100.
Bisacylated diethylenetriamine[94]	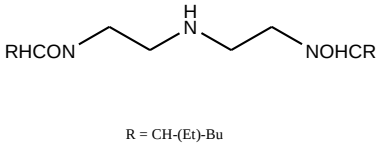 R = CH-(Et)-Bu	Selective extraction of nickel in the presence of other base metals from chloride or sulfate medium. The studies indicated that the nature of the medium (chloride or sulfate medium) does not affect the extraction pattern and its efficiency. Extractions occurred in the high pH range and there was lack of pH-metric separation of the metal ions (Figure 1.11).

The tridentate aromatic amine have not been fully investigated as separating agents and applied commercially for the extraction of base metals as compared to aliphatic tridentate amines. Tridentate aliphatic amine systems such as bisacylated diethylenetriamine (BAD) have been proposed for use in the extraction of non-ferrous metals from ammoniac, sulfate, and low-acidity chloride solutions (**Figure 1.10**).[94] These systems form very stable complexes in which stripping may not be readily achieved. It is advisable to use tridentate extractant of which the enthalpy contribution is smaller which will make it possible for back-extraction process to occur.

An application of tridentate ligands would have an additional advantage of increasing the extraction equilibrium constants[91] due to the high complex formation constants for reactions of base metals and tridentate ligands[92,93] thereby requiring relatively low extractant-to-metal ratios to achieve quantitative extractions.[94] The only example of a tridentate amine extractant in the literature is that of a derivative of diethylenetriamine[94] but extractions occurred at relatively high pH values as expected due to high p*K*a values of aliphatic amines [93] and the small ΔpH0.5 values implied a lack of pH-metric separation of the later 3d metal ions.[94] It would be hoped that good separation factors of the metal chelates would be achieved through stereochemical considerations since nickel(II) is known to form the most stable spin free octahedral (O_h) complexes of all base metal ions [72] while the copper(II) and cobalt(II) ions tend to form stable tetrahedral (T_d) complexes.[69,73] This study, therefore, also interrogates the coordination chemistry aspects of base metals that influence the extractions, with tridentate amine-based ligands.

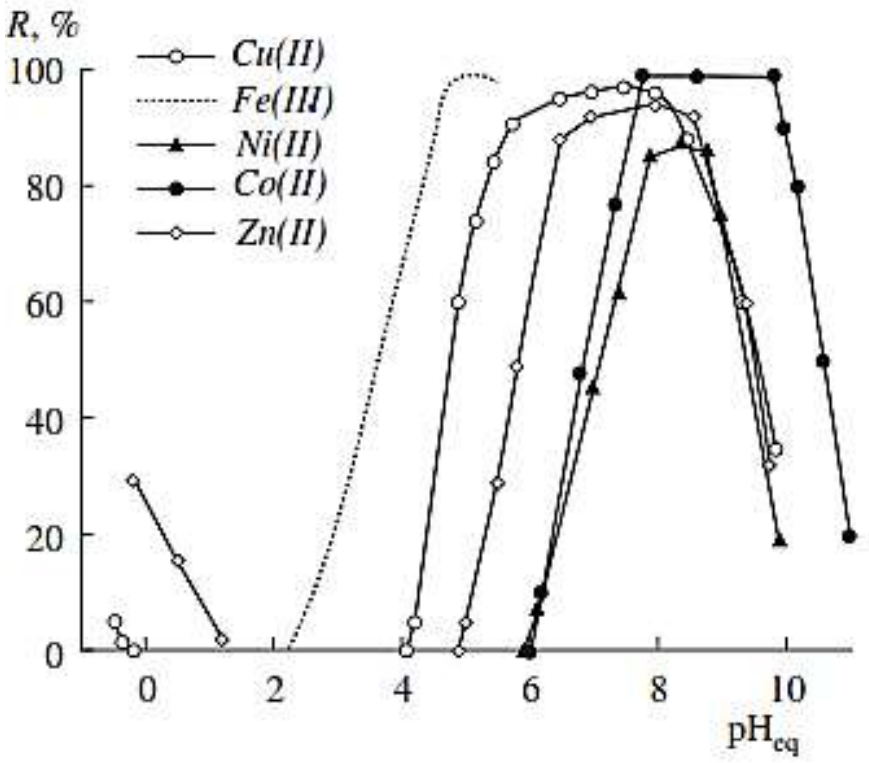

Figure 1.10: Extraction of nonferrous metals by BAD vs. aqueous acidity. BAD concentration: 0.1 mol/L (15% octanol in Nefras); starting metal concentrations in the aqueous solution: 0.02 mol/L; NaCl concentration: 1.0 mol/L.[94]

The diamine ligands, having two aromatic nitrogen donor atoms, such as *N*-octyl-2,2'-pyridylimidazole, have provided empirical evidence that this system can successfully recover nickel(II) from other base metals in solvent extraction process. The investigation of *N*-octyl-2,2'-pyridylimidazole as extractant for nickel have shown that the nature of the medium (chloride or sulfate medium) does not affect the extraction pattern and its efficiency.[53,69]

In the view of the above it was of interest to continue the investigation of the behaviour of similar extractants, with the variations being the σ-donor and the π-acceptor character of the nitrogen donors as well as the denticity of the ligand.

CHAPTER 2

2. MATERIALS, PHYSICAL METHODS AND EXPERIMENTAL SECTION

2.1 Materials

Table 2.1: List of chemicals and reagents used

Chemicals	**% Purity**	**Suppliers**
HCl	0.0364 g/mL	Merck Chemicals
HNO_3	≥69	Sigma-Aldrich
H_2SO_4	98	Merck Chemicals
$CaSO_4 \cdot 7H_2O$	98.5	UniLab
$CdSO_4 \cdot H_2O$	98+	BDH
$CoSO_4 \cdot 7H_2O$	97.5	Fluka
$CuSO_4 \cdot 5H_2O$	99	Merck Chemicals
$FeSO_4\ 7H_2O$	70	Merck Chemicals
$NiSO_4 \cdot 6H_2O$	98	Merck Chemicals
$MgSO_4 \cdot 7H_2O$	99.7	Merck Chemicals
$MnSO_4 \cdot H_2O$	99.2	Holpro Analytics
$ZnSO_4 \cdot 7H_2O$	99.5	BDH
$Co(ClO_4)_2 \cdot 6H_2O$	99	Merck Chemicals
$Cu(ClO_4)_2 \cdot 6H_2O$	99	Merck Chemicals
$Ni(ClO_4)_2 \cdot 6H_2O$	99	Merck Chemicals
$Zn(ClO_4)_2 \cdot 6H_2O$	99	Merck Chemicals

Table 2.1: Continued

Chemicals	**% Purity**	**Suppliers**
KOH	98	Sigma Aldrich
Na_2CO_3	98	Merck Chemicals
NaClO	99	Merck Chemicals
NaOH	99	Merck Chemicals
Acetone	98	Sigma -Aldrich
Ammonia	28	Merck Chemicals
Diethyl ether	99	Merck Chemicals
DMF	99	Merck Chemicals
Ethanol	99	Sigma-Aldrich
Alkyl halides	97	Sigma-Aldrich
Ethyl acetate	98	Sigma-Aldrich
Methanol	99.9	Sigma-Aldrich
Triethylamine	99	Merck Chemicals
N-Methylglycine	99	Merck Chemicals
2,2'-thiodiacetic acid	99	Merck Chemicals
Iminodiacetic acid	99	Merck Chemicals
o-Phenylenediamine	99	Merck Chemicals
DNNSA	50 wt in heptane	Sigma-Aldrich
2-Octanol	98	Sigma-Aldrich
Shellsol 2325	17-22 v/v aromatic	Shell Chemicals (SA)
Toluene-4-sulfonic acid	98	Sigma-Aldrich

2.2. Spectroscopic techniques

2.2.1. NMR spectrometry

The purity of the extractants was determined by ^{1}H NMR spectroscopy on a Bruker AMX 400 MHz spectrometer. All samples were prepared using deuterated solvents. Chemical shifts are reported in parts per million (ppm) relative to an internal standard tetramethylsilane (TMS).

2.2.2. Infrared spectroscopy

The metal complexes were analyzed using infrared spectroscopy. The infrared spectra were recorded on either Perkin-Elmer spectrum 400 FT-IR spectrometer in the mid-IR range (4000-400 cm^{-1}) as KBr pellets or as neat compounds with a Perkin Elmer 100 FTIR-ATR (4000 – 650 cm^{-1}) spectrometer.

2.2.3. UV-Vis electronic spectroscopy (solid reflectance)

The solid reflectance spectra of ligands and complexes were recorded on a Shimadzu UV-VIS-NIR Spectrophotometer UV-3100 with a MPCF-3100 sample compartment with samples mounted between two quartz discs which fit into a sample holder coated with barium sulfate. The spectra were recorded over the wavelength range of 2000-250 nm, and the scans were conducted at a medium speed using a 20 nm slit width.

2.3. Analytical Methods

2.3.1. Elemental analysis

Elemental analysis was carried out with a Vario Elementary ELIII Microcube CHNOS elemental analyser.[119] Calibration of the instrument was done with the use of the following standards in a linear curve adjustment within the total working range.

Standard 1: Sulfanilamide – C; 41.81, H; 4.65, N; 16.25, S; 18.62%

Standard 2: Acetanilide – C; 71.09, H; 0.67, N; 10.36, O; 12.0%

The basic principle of quantitative CHNOS analysis is high temperature combustion of organic and many inorganic solid or liquid samples.[120] The gaseous combustion products are purified, separated into their various components and analyzed with a suitable detector such as thermal conductivity detector (TCD) and optional infrared detector (IR) for sulfur.

2.3.2. Inductively coupled plasma (ICP) spectrometry

Metal ion analyses were carried out with a Thermo Electron (iCAP 6000 Series) inductively coupled plasma (ICP) spectrometer equipped with an OES detector. The ICP/AAS metal standards, dissolved in 0.5 M nitric acid, were used to prepare standard solutions for the construction of calibration curves using distilled, deionized, milliQ water for the dilutions. The elements were analysed at the following US-EPA[121] specified wavelengths (nm) for minimal interferences; 231.6 (Ni^{2+}), 237.80 (Co^{2+}), 324.75 (Cu^{2+}), 334.50 (Zn^{2+}), 259.99 (Fe^{2+}, Fe^{3+}), 413.70 (Cd^{2+}), 315.88 (Ca^{2+}), 257.61 (Mn^{2+}), and 279 (Mg^{2+}). The detector type was RACID charge injection device.

The Thermo Electron iCAP 6000 Series-optical emission spectrometer was operated with the parameters in **Table 2.2**. The elements (atoms) are excited and when they return to low energy status, emission rays are released and the emission rays that correspond to the photon wavelength are measured.[122] The element type is determined based on the position of the photon rays, and the content of each element is further determined based on the rays' intensity. To generate plasma, argon gas is supplied to the torch coil, and high frequency electric current is applied to the work coil at the tip of the torch tube. Using the electromagnetic field created in the torch tube by the high frequency current, argon gas is ionized and plasma is generated. This plasma has high electron density and temperature (10000 K) and this energy is used in the excitation-emission of the sample. Solution samples are introduced into the plasma in an atomized state through the narrow tube in the center of the torch tube.[123]

Table 2.2: ICP-OES method and operating parameters

Parameter	Setting
Applied radio frequency (RF) power	1150 W
Plasma (Ar) gas Flow rate	5.0 L/min
Auxiliary gas flow rate	0.5 L/min
Nebulizer Ar gas flow rate	1.5 L/min
Sampling depth	8.5 mm
Sample pump rate	50 rpm
Time scan acquisition	50 ms/point
Cooled spraying chamber temperature	4 ^{o}C
The camera temperature	46.63 ^{o}C
Generator temperature	24 ^{o}C
Optics temperature	36.9 ^{o}C
Total integration time	30 s per analyte
Sample flush time	30 s
Number of replicates	3

2.4. *Crystal structure determination*

X-ray diffraction studies were performed at 200K using a Bruker Kappa Apex II diffractometer with graphite monochromated Mo Kα radiation (λ = 0.71073 Å). The crystal structures were solved by direct methods using SHELXTL.[124] All non-hydrogen atoms were refined anisotropically. Carbon-bound hydrogens were placed in calculated positions and refined as riding atoms with bond lengths 0.95 (aromatic CH), 0.99 (CH_2), and 0.98 (CH_3) Å and with

Uiso(H) = 1.2 (1.5 for methyl) Ueq(C). Hydrogens bonded to nitrogen were located on a Fourier map and allowed to refine freely. Hydrogens on water were restrained to an O–H bond length of 0.84Å and H–O–H angle of 110°. Diagrams and publication material were generated using SHELXTL, PLATON,[125] and ORTEP-3.[126]

2.5. Potentiometry and HYPERQUAD

Potentiometry is an electroanalytical method which is based on measurement of potential of an electrode system and is used to calculate stability constants and determine protonation constants. In this regard, potentiometric studies are based primarily on measurements of at least one of the species involved in protonation or metal–ligand equilibria. The essence of the potentiometric experiment involving a glass electrode is the monitoring of the change in the hydrogen ion concentration, $[H^+]$, throughout the experiment. The experimentally known quantities in a potentiometric titration are: (a) the initial analytical concentrations of the reactants in the solution; (b) the added volumes of the titrant solution of known concentration; and (c) the free concentration of one (or more) reactants in the solution, *e*.g., $[H^+]$ in the case of Glass Electrode Potentiometry (GEP).

The concentration stability constants (β_{pqr}) were calculated using the computer program HYPERQUAD[127] (extension of SUPERQUAD). This program makes use of the following assumptions to calculate the formation constants.

(i) For each chemical species $M_pL_qH_r$ in the solution equilibra there is a chemical constant which is expressed as:

$$\beta_{pqr} = \frac{[M_pL_qH_r]}{[M]^p[L]^q[H]^r} \qquad (10)$$

where M, L and H represent a metal, ligand and proton respectively.

(ii) The electrodes used, have a pseudo-Nernstian behaviour.

(iii) Careful calibration of the electrode, accurate standardization of reagents, elimination of weighing and dilution errors, elimination of carbonate impurities, elimination of temperature variance and purity of water minimise the systematic errors. All statistical tests are based on the assumption that systematic errors are absent.

(iv) The program assumes that the independent variables (such as titre volume) are not subject to errors and that the dependent variables (such as measured potential) have a normal distribution. If this is the case then the calculated residuals should not show systematic trends.

(v) For any equilibrium system, a model exists that will fit the experimental data. All least-square refinements are performed in terms of the assumed model. The model that is found may not be the true model, but it will be the one that fits the observed data. It will have no ill-defined constant and the standard deviation. A constant is considered ill-defined if its standard deviation is more than 33% (such standard deviations are labeled "Excessive") or if its value is negative.

The program calculates the stability constants using a non-linear least-square refinement algorithm based on following the acid concentration in complex acid-base equilibria using the proton sensitive glass electrode. The concentration of the hydrogen ion in solution is related to the potential measured with the electrode by the modified Nernst equation, $E = E^{o} + RT/F \ln[H^{+}]$. The standard potential, E^{o}, must be determined for the specific conditions of operation *via* the calibration of an electrode for a strong acid-base titration using the Gran method.[128]

The concentrations of the chemical species are determined by solving the non-linear simultaneous equations of mass-balance using the Newton-Raphson method. The program allows for up to four reactants and up to 18 species. The equilibria for the specific interactions of the reagents, M (metal) and L (ligand), with H (proton) are:

$$M + iH = H_iM; \; L + jH = H_jL \tag{11}$$

and the total concentrations (T_M, T_L, T_H) of the species are given by:

$$T_M = [M] + \sum_{pqr} p\beta_{pqr}[M]^p[L]^q[H]^r + \sum_i \beta_{10i}[M][H]^i \tag{12}$$

$$T_L = [L] + \sum_{pqr} q\,\beta_{pqr}[M]^p[L]^q[H]^r + \sum_j \beta_{10j}[L][H]^j \tag{13}$$

$$T_H = [H] + \sum_{pqr} r\,\beta_{pqr}[M]^p[L]^q[H]^r + \sum_i \beta_{10i} i[M][H]^i + \sum_j \beta_{10j} j[L][H]^j[OH^-] \tag{14}$$

Mass-balance equations must be satisfied and hence the total concentration of a reagent is the sum of its concentrations in all the chemical species in the mixture. Once the free reactant concentrations ([M], [L], [H]) have been calculated, the concentrations of the complexes are derived from them and the equilibrium constants (during model fitting, the constants must be estimated). The best fit to the experimental data is determined by minimizing the error which is expressed as the square sum of the residuals,

$$U = \sum w_i \, (E_I^{Obs} - E_I^{cal})^2 \tag{15}$$

where w_i is the weighting factor.

The model adequately accounts for the experimental observations and can be proposed for the equilibrium system. The model is specified by a set of coefficients (p,q,r), one for each species in terms of the assumed model. Choice of the "best" model is based on the statistical value, sigma (σ). Ideally σ should be equal to one but it has been proposed that any fit with $\sigma < 3$ is satisfactory. If σ is large, then the experimental data points with larger residuals must be removed during the refinement if the specified model is a promising fit.

2.6. Other Instruments

2.6.1. pH determinations

The pH measurements were performed on a Metrohm 827 pH meter using a combination electrode with 3 M KCl as electrolyte. Calibration of the electrode was maintained at intervals of two weeks using standard buffer solution of pH 4.0, 7.0 and 9.0 from Metrohm.

2.6.2. Conductivity measurements

The conductivity measurements were carried out on A.W.R. Smith Process Instrumentation cc Laboratory Bench Meter Model AZ 86555. The ABS graphite cell probe was used along with an aqueous standard which has a conductivity value of 135 $ohm^{-1}.cm^{-1}.mole^{-1}$ at 20°C for the calibration. All the complexes were prepared in water as solvent at a concentration of 10^{-3} M for the conductivity measurements.

2.6.3. Melting point determination

The melting points of the solid complexes were determined with the Electrothermal IA 9000 digital measuring point apparatus.

2.6.4. Lab Shaker

The Labcon micro-processor controlled orbital platform shaker model SPO-MP 15 was used for contacting the two phases in the solvent extraction experiments.

CHAPTER 3

3. SOLVENT EXTRACTION WITH TRIDENTATE AND BIDENTATE AMINE-BASED EXTRACTANTS

3.1. Overview

Benzimidazole-based tridentate and bidentate ligands used as extractants in this study were *bis*((1*H*-benzimidazol-2-yl)methyl)sulfide, *bis*((1*H*-benzimidazol-2-yl)methyl)amine and (1*H*-benzimidazol-2-yl)-*N*-methylmethanamine (**Figures 3.1, 3.2** and **3.4**). The benzimidazole-based tridentate were derived from iminodiacetic acid or 2,2-thiodiacetic acid and *o*-phenylenediamine,[92] while the bidentate ligand was prepared from *N*-methylglycine and *o*-phenylenediamine. [129] These ligand systems were of interest because they could offer three advantages, namely; interaction with metal ions at relatively low pH, higher stability of the chelates, and a possibility of specificity for metal ions through stereochemical "tailor-making".

The low p*K* benzimidazole group should allow for interaction of the ligands with base metal ions at the low pH range while it forms a strong M-L bond due to pi-backbonding. The pi acidity character of benzimidazole is higher than that of imidazole or pyridine due to the presence of the additional benzene ring in benzimidazole.

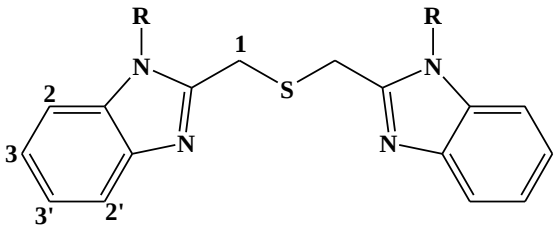

R = Heptyl, Octyl, Decyl (BRNSN)

Figure 3.1: The chemical structures of *bis*((1*H*-benzimidazol-2-yl)methyl)sulfide (BNSN) and *bis*((1-alkylbenzimidazol-2-yl)methyl)sulfide (RNSN)

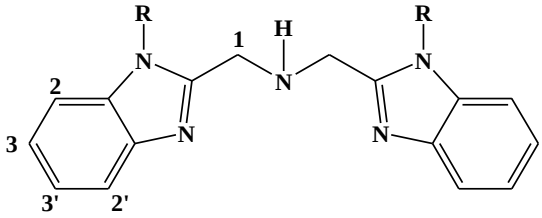

R = Heptyl, Octyl, Decyl (BRNNN)

Figure 3.2: The chemical structures of *bis*((1*H*-benzimidazol-2-yl)methyl)amine (BNNN) and *bis*((1-alkylbenzimidazol-2-yl)methyl)amine (RNNN)

The application of benzimidazole tridentate ligand systems as separating agents for metal ions have not been investigated, and only one example appears in the literature for a tridentate extractant using the ligand diethylenetriamnine.[94] However, extractions occurred at relatively high pH values as expected due to high pK_a values of aliphatic amines,[93] and the small $\Delta pH_{0.5}$ values implied a lack of pH-metric separation of the later 3d metal ions.[131] It would be hoped that good separation factors of the metal chelates would be achieved through stereochemical considerations since nickel(II) is known to form the most stable spin free octahedral (O_h) complexes of all base metal ions[72] while the copper(II) and cobalt(II) ions tend to form stable tetrahedral (T_d) complexes.[69,73]

This thesis will, in part, also attempt to uncover some of the contributing factors to the lack of pH-metric separation of base metal ions with neutral tridentate extractants through coordination chemistry studies (Chapter 4) and thermodynamics of the complexation reaction (Chapter 5). In this chapter, the application of tridentate ligands, containing benzimidazole groups as well as a secondary amine or sulfur donor atoms, for the extraction of base metals has been advanced. The strong chelate effect of tridentate ligands should allow stable complex formation with base metal ions and result in high extraction efficiencies (even at low metal-to-ligand (M-L) ratios). This chapter presents a case for the extraction of base metal ions, from highly acidic sulfate solutions, using *bis*((1-alkylbenzimidazol-2-yl)methyl)sulfide and *bis*((1-alkylbenzimidazol-2-yl)methyl)amine (**Figures 3.1 and 3.2**) as extractants, respectively, and dinonylnaphthalenesulfonic acid (DNNSA) (**Figure 3.3**) as a synergist in Shellsol 2325. Further studies were conducted using a bidentate ligand, (1*H*-benzimidazol-2-yl)-*N*-methylmethanamine (**Figure 3.4**).

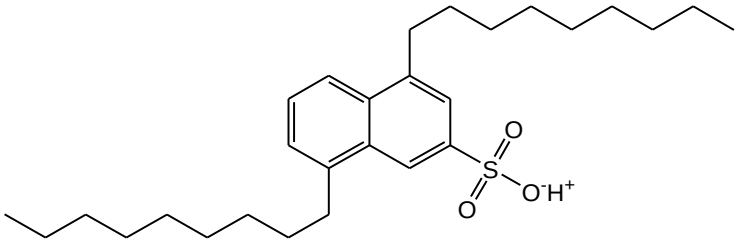

Figure 3.3: The chemical structure of dinonylnaphthalene sulfonic acid (DNNSA)

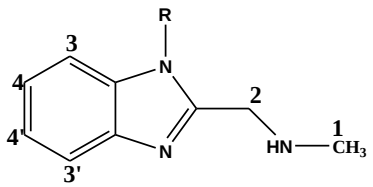

R = Heptyl, Octyl, Decyl (RBIMA)

Figure 3.4: The chemical structure of (1-alkylbenzimidazol-2-yl)-*N*-methylmethanamine

3.2. Experimental

3.2.1. Preparative work

3.2.1.1. Synthesis of bis((1H-benzimidazol-2-yl)methyl)sulfide (BNSN)

The NSN ligand was synthesized as reported elsewhere,[129] except that 2,2'-thiodiacetic acid was used and the decolorization step using activated charcoal was not necessary. The characterization data for the white precipitate of the free base was as follows: Yield: 71%, m.p., 210–212 °C. Anal. Calcd for $C_{16}H_{16}N_4OS$ (%): C, 61.52; H, 5.16; N, 17.93; S, 10.26. Found: C, 61.15; H, 5.34; N, 17.97; S, 10.15. ^{1}H-NMR ($CDCl_3$) δ (ppm) : 4.06 (4H, s, H1), 7.17 (4H, m, H3, H3′), 7.53 (4H, m, H2, H2′). IR (cm^{-1}): 3377 ν(N–H), 1534 ν(C=N), 1128 δ(C-S-C).

3.2.1.2. Synthesis of bis((1-alkylbenzimidazol-2-yl)methyl)sulfide (BRNSN)

Bis((1-alkylbenzimidazol-2-yl)methyl)sulfides, the alkylated derivatives of the ligand, were prepared according to a literature method.[130] However, the purification step was carried out as follows: the resulting solution after removal of the KBr salt was concentrated via rotary evaporation and purified using a silica gel chromatographic column with ethyl acetate/methanol (4:1). After removal of the solvent by rotary evaporator, the products were obtained as white precipitates. The characterization data for the heptyl, octyl as well as decyl derivatives is presented below:

3.2.1.2.1. Bis((1-heptylbenzimidazol-2-yl)methyl)sulfide (BHNSN)

Yield = 69%, m.p., 71–72 °C. Anal. Calcd for $C_{30}H_{46}N_4O_2S$ (%): C, 68.40; H, 8.80; N, 10.64; S, 6.09. Found: C, 68.37; H, 9.12; N, 10.58; S, 6.13. ^{1}H-NMR ($CDCl_3$) δ (ppm): 0.81 (6H, t, CH3), 1.18 (20H, m, $CH_3(CH_2)_5$), 1.67 (4H, t, CH_2–CH_2N), 4.16 (4H, t, CH_2–N), 4.23 (4H, s,H1), 7.21

(4H, q, H3 & H3′), 7.53 (2H, d, H2), 7.62 (2H, d, H2′). IR (cm^{-1}): 1505 ν(C=N), 1135 δ(C–S–C).

3.2.1.2.2. Bis((1-octylbenzimidazol-2-yl)methyl)sulfide (BONSN)

Yield = 63%, m.p., 76–78 °C. Anal. Calcd for $C_{32}H_{50}N_4O_2S$ (%): C, 69.27; H, 9.08; N, 10.10; S, 5.78. Found: C, 68.83; H, 9.45; N, 10.04; S, 5.83. ^{1}H-NMR ($CDCl_3$) δ (ppm): 0.81 (6H, t, CH3), 1.17 (20H, m, $CH_3(CH_2)_5$), 1.65 (4H, t, CH_2–CH_2N), 4.14 (4H, t, CH_2–N), 4.21 (4H, s,H1), 7.19 (4H, q, H3 & H3′), 7.51 (2H, d, H2), 7.59 (2H, d, H2′). IR (cm^{-1}): 1503 ν(C=N), 1137 δ(C–S–C).

3.2.1.2.3. Bis((1-decylbenzimidazol-2-yl)methyl)sulfide (BDNSN)

Yield = 71%, m.p., 76–78 °C. Anal. Calcd for $C_{36}H_{58}N_4O_2S$ (%): C, 70.77; H, 9.57; N, 9.17; S, 5.25. Found: C, 70.74; H, 9.63; N, 9.23; S, 5.28. ^{1}H-NMR ($CDCl_3$) δ (ppm): 0.81 (6H, t, CH3), 1.15 (20H, m, $CH_3(CH_2)_5$), 1.63 (4H, t, CH_2–CH_2N), 4.12 (4H, t, CH_2–N), 4.22 (4H, s,H1), 7.18 (4H, q, H3 & H3′), 7.50 (2H, d, H2), 7.58 (2H, d, H2′). IR (cm^{-1}): 1507 ν(C=N), 1139 δ(C–S–C).

3.2.1.3. Synthesis of bis((1H-benzimidazol-2-yl)methyl)amine (BNNN)

The *bis*((1*H*-benzimidazol-2-yl)methyl)amine (NNN) was synthesized as reported elsewhere, [131] except that iminodiacetic acid was used and the decolorization step using activated charcoal in methanol was not necessary. The characterization data for the white precipitate of the free base was as follows: Yield: 84%, m.p., 268 - 270ºC. Anal. Calcd. for $C_{16}H_{16}N_4OS$ (%): C, 65.10; H, 5.80; N, 23.70. Found: C, 65.78; H, 5.80; N, 23.07. ^{1}H NMR ($CDCl_3$) δ (ppm): 3.17 (2H, s,

NHC), 4.06 (4H, s, *H*1), 7.15 (4H, m, *H*3, *H3′*), 7.52 (4H, m, *H*2, *H2′*). IR (cm^{-1}): 3208 ν(N-H), 3049 ν(sec N-H), 1592 ν(C=N).

3.2.1.4. Synthesis of bis((1-alkylbenzimidazol-2-yl)methyl)amine (BRNNN)

The alkylated derivatives of the ligand were prepared according to a literature method.[130] However, the purification step was carried out as follows: The resulting solution after the removal of the KBr salt was concentrated *via* rotary evaporation, and purified using a silica gel chromatographic column with ethyl acetate/methanol (4:1) solvent system. After the removal of the solvent by rotary evaporation the products were obtained as oils. The characterization data appears below:

3.3.1.4.1. Bis((1-heptylbenzimidazol-2-yl)methyl)amine (BHNNN)

Yield = 60%. Anal. Calcd. for $C_{30}H_{47}N_5O_2$ (%): C, 70.69; H, 9.29; N, 13.74. Found: C, 70.72; H, 9.31; N, 13.79. ^{1}H NMR ($CDCl_3$) δ (ppm): 0.89 (6H, t, CH_3), 1.15 (24H, m, CH_3**$(CH_2)_3$**), 1.03(4H, t, **CH_2**-CH_3), 1.57(4H, t, **CH_2**-CH_2N), 3.98 (4H, t, **CH_2**-N), 4.04 (4H, s, *H*1), 7.28 (4H, q, *H3 & H3'*), 7.29 (2H, d, *H2*), 7.77 (2H, d, *H2'*). IR (cm^{-1}): 1520 ν(C=N).

3.3.1.4.2. Bis((1-octylbenzimidazol-2-yl)methyl)amine (BONNN)

Yield = 72%. Anal. Calcd. for $C_{32}H_{51}N_5O_2$ (%): C, 71.47; H, 9.56; N, 13.02. Found: C, 71.44; H, 9.59; N, 13.07. ^{1}H NMR ($CDCl_3$) δ (ppm): 0.89 (6H, t, CH_3), 1.14 (24H, m, CH_3**$(CH_2)_6$**), 1.02(4H, t, **CH_2**-CH_3), 1.56(4H, t, **CH_2**-CH_2N), 3.97 (4H, t, **CH_2**-N), 4.03 (4H, s, *H*1), 7.27 (4H, q, *H3 & H3'*), 7.29 (2H, d, *H2*), 7.76 (2H, d, *H2'*). IR (cm^{-1}): 1525 ν(C=N).

3.3.1.4.3. Bis((1-decylbenzimidazol-2-yl)methyl)amine (BDNNN)

Yield = 67%. Anal. Calcd. for $C_{36}H_{59}N_5O_2$ (%): C, 72.81; H, 10.01; N, 11.79. Found: C, 72.95; H, 10.61; N, 11.86. ^{1}H NMR ($CDCl_3$) δ (ppm): 0.89 (6H, t, CH_3), 1.13 (24H, m, CH_3**$(CH_2)_6$**), 1.01(4H, t, **CH_2**-CH_3), 1.55(4H, t, **CH_2**-CH_2N), 3.96 (4H, t, **CH_2**-N), 4.02 (4H, s, *H*1), 7.26 (4H, q, *H3 & H3'*), 7.28 (2H, d, *H2*), 7.75 (2H, d, *H2'*). IR (cm^{-1}): 1522 ν(C=N).

3.2.1.5. Synthesis of (1H- benzimidazol-2-yl)-N-methylmethanamine (BIMA)

The preparation of the ligand, (1*H*-benzimidazol-2-yl)-*N*-methylmethanamine, was done according to the method developed elsewhere,[132] except that N-methylglycine was used and (1*H*-benzimidazol-2-yl)-*N*-methylmethanamine dihydrochloride was washed with acetone. The product was deprotonated with sodium bicarbonate. The sodium bicarbonate was added portion wise while the (1*H*-benzimidazol-2-yl)-*N*-methylmethanamine dihydrochloride solution was stirring at -5^{o}C. The pH of the free base solution mixture was further increased to 11 using an ammonium hydroxide solution. The resulting solution was concentrated *via* rotary evaporation. The product was purified using a silica gel chromatographic column with ethyl acetate/methanol (4:1) solvent system. Yield: 71%, m.p., 126-128^{o}C. Anal. Calcd. for $C_9H_{11}N_3$ (%): C, 67.06; H, 6.88; N, 26.07. Found: C, 67.13; H, 6.03; N, 26.13. ^{1}H NMR ($CDCl_3$) δ (ppm): 2.31 (3H, s, *H*1), 3.84 (2H, s, *H*2), 7.12 (4H, m, *H3′*, *H*4), 7.43 (4H, m, *H*3, *H*5). IR (cm^{-1}): 3318 ν(imdN-H), 1622 ν(C=N).

3.2.1.6. (1H-Benzimidazol-2-yl)-N-methylmethanamine (RBIMA)

The alkylated compounds were synthesized by alkylation of the benzimidazole ring with heptyl, octyl and decyl groups respectively according to a literature method.[130] However, the

purification step was carried out as follows: the resulting solution after removal of the KBr salt was concentrated via rotary evaporation and purified using a silica gel chromatographic column with ethyl acetate/methanol (4:1). After removal of the solvent by rotary evaporator, the products were obtained as white precipitates.

3.2.1.6.1. (1-Heptylbenzimidazol-2-yl)-N-methylmethanamine (HBIMA)

Yield = 77%. Anal. Calcd. for $C_{17}H_{29}N_4O$ (%): C, 69.27; H, 9.81; N, 15.15. Found: C, 69.34; H, 9.85; N, 15.12. ^{1}H NMR ($CDCl_3$) δ (ppm): 0.96 (3H, t, CH_3), 1.32 (10H, m, $CH_3(CH_2)_3$), 1.56(4H, t, CH_2-CH_2N), 2.36 (3H, s, *H*1), 2.53 (4H, t, CH_2-N), 3.87 (2H, s, *H*2), 7.28 (4H, m, *H*3′, *H*4), 7.30 (4H, s, *H*5), 7.63 (4H, s, *H*3). IR (cm^{-1}): 1625 ν(C=N).

3.2.1.6.2. (1-Octylbenzimidazol-2-yl)-N-methylmethanamine (OBIMA)

Yield = 71%. Anal. Calcd. for $C_{17}H_{29}N_4O$ (%): C, 70.06; H, 10.03; N, 14.42. Found: C, 70.75; H, 10.18; N, 14.16. ^{1}H NMR ($CDCl_3$) δ (ppm): 0.91 (3H, t, CH_3), 1.31 (10H, m, $CH_3(CH_2)_5$), 1.55 (4H, t, CH_2-CH_2N), 2.34 (3H, s, *H*1), 2.51 (4H, t, CH_2-N), 3.85 (2H, s, *H*2), 7.26 (4H, m, *H*3′, *H*4), 7.29 (4H, s, *H*5), 7.61 (4H, s, *H*3). IR (cm^{-1}): 1620 ν(C=N).

3.2.1.6.3. (1-Decylbenzimidazol-2-yl)-N-methylmethanamine (DBIMA)

Yield = 81%. Anal. Calcd. for $C_{19}H_{33}N_4O$ (%): C, 71.43 H, 10.41; N, 13.15. Found: C, 71.46; H, 10.47; N, 13.09. ^{1}H NMR ($CDCl_3$) δ (ppm): 0.90 (3H, t, CH_3), 1.32 (10H, m, $CH_3(CH_2)_5$), 1.53 (4H, t, CH_2-CH_2N), 2.32 (3H, s, *H*1), 2.50 (4H, t, CH_2-N), 3.86 (2H, s, *H*2), 7.26 (4H, m, *H*3′, *H*4), 7.28 (4H, s, *H*5), 7.62 (4H, s, *H*3). IR (cm^{-1}): 1629 ν(C=N).

3.2.2. Extraction procedure

All the extractions were carried out in a temperature controlled laboratory at 25(±1)^{o}C. Equal volumes (10 mL) of 0.001 M metal ion solution (aqueous layer) and 80% 2-octanol/shellsol extractant solution (organic layer) were pipette into 50 mL conical separating funnels. They were shaken with an automated orbital platform shaker for 30 mins at an optimised speed of 200 rpm. A minimum period of 60 mins was observed before harvesting the raffinates. The raffinates were filtered through a 33 mm millex-HV Millipore of 0.45 µm and diluted appropriately for analysis by ICP-OES. The percentage extractions (%E) of the metal ions were calculated from the concentrations of the metal ions in the aqueous phase using **Equation 16** below:

$$\%E = (C_i - C_s)/C_i \times 100 \qquad (16)$$

where C_i is the initial solution concentration (mg/L) and C_s is the solution concentration after extraction.

The extraction efficiencies were investigated as a function of pH, and all the extraction curves were plotted with SigmaPlot 11.0.

3.3. Results and discussion

3.3.1. Synthesis of extractants and general considerations

3.3.1.1. Bis((1-alkylbenzimidazol-2-yl)methyl)sulfide

The ligand, BNSN, was synthesized by condensation/cyclization between 2,2'-thiodiacetic acid and *o*-phenylenediamine[129] while the extractants, *bis*((1-heptylbenzimidazol-2-yl)methyl)sulfide (BHNSN), *bis*((1-octylbenzimidazol-2-yl)methyl)sulfide (BONSN) and *bis*((1-decylbenzimidazol-2-yl)methyl)sulfide (BDNSN), were prepared by alkylation of NSN in the presence of a base.[130] The purity of the ligand and the extractants was confirmed by elemental analyses and ^{1}H NMR. The alkyl groups of the extractants (BHNSN, BONSN and BDNSN) are positioned away from the coordination sphere and, therefore, the use of the ligand (NSN) would not change the coordination chemistry from a steric hindrance point of view.

3.3.1.2. Bis((1-alkylbenzimidazol-2-yl)methyl)amine

The preparation of the ligand BNNN was achieved by condensation between iminodiacetic acid and *o*-phenylenediamine.[131] The extractants, *bis*((1-heptylbenzimidazol-2-yl)methyl)amine (BHNNN), *bis*((1-octylbenzimidazol-2-yl) methyl)amine (BONNN) and *bis*((1-decylbenzimidazol-2-yl)methyl)amine (BDNNN), were prepared by alkylation of BNNN in the presence of a base.[130] The purity of the ligand and the extractants were confirmed by elemental analyses and ^{1}H NMR.

3.3.1.3 (1H-benzimidazol-2-yl)-N-methylmethanamine

The benzimidazole-based bidentate ligand and the extractants, *bis*(*1-alkylbenzimidazol-2-yl*)-*N*-methylmethanamine (RBIMA), (1-heptylbenzimidazol-2-yl)-*N*-methylmethanamine (HBIMA),

(1-octylbenzimidazol-2-yl)-*N*-methylmethanamine (OBIMA), and (1-decylbenzimidazol-2-yl)-*N*-methylmethanamine (DBIMA), were prepared by condensation/cyclization between *N*-methylglycine and *o*-phenylenediamine, followed by alkylation of the benzimidazole in the case of extractants.

Alkylation of benzimidazole for the tridentate and bidentate systems were achieved under mild temperature conditions (40°C) with the deprotonation of the pyrrole-type nitrogen of benzimidazole using potassium hydroxide as a base and subsequent substitution with the alkyl group. This was enhanced by the nature of benzimidazole as a pi-electron-excessive heterocycle. The products were purified using a silica column with ethyl acetate/methanol (4:1) as solvent mixture yielding a pure product. The longer chain 1-alkylbenzimidazole products solidified into a wax-like transparent product after a few days.

The mechanism for the cyclization reaction in the formation of benzimidazoles in *bis*((1-alkylbenzimidazol-2-yl)methyl)sulfide, *bis*((1-alkylbenzimidazol-2-yl)methyl)amine and (1H-benzimidazol-2-yl)-N-methylmethanamine formation goes by the usual acid catalysed initial formation of diamides followed by ring closure and elimination of water molecules. The reactions were therefore conducted at elevated temperature and in acid medium. The necessary purification for alkylbenzimidazole was achieved by the removal of residual water *in vacuo*, at a temperature of 45°C and subsequent column chromatographic separation on silica with ethyl acetate/methanol (4:1) as solvent mixture yielding a pure product. The longer chain 1-alkylimidazole products solidify into a wax-like transparent product after a few days.

The purity of the benzimidazole ligands and their corresponding extractants were ascertained by elemental analyses and ^{1}H NMR characterization (see **Figures 3.5-3.7**). The alkylation of the imidazole ring by electrophilic substitution at N(1) was successfully achieved as signified by the emergence of the alkyl group peaks as shown in spectra in **Figures 3.5(B), 3.6(B)** and **3.7(B)**. The formation of the extractants was confirmed by the appearance of the peaks between the region 0.81 to 2.51 ppm in the ^{1}H NMR spectra of these compounds which signifies the presence of the alkyl chain (see **Figures 3.5(B), 3.6(B) and 3.7(B)**). The purity of the extractant was further confirmed by the agreement of the elemental micro-analysis results to the theoretical values.

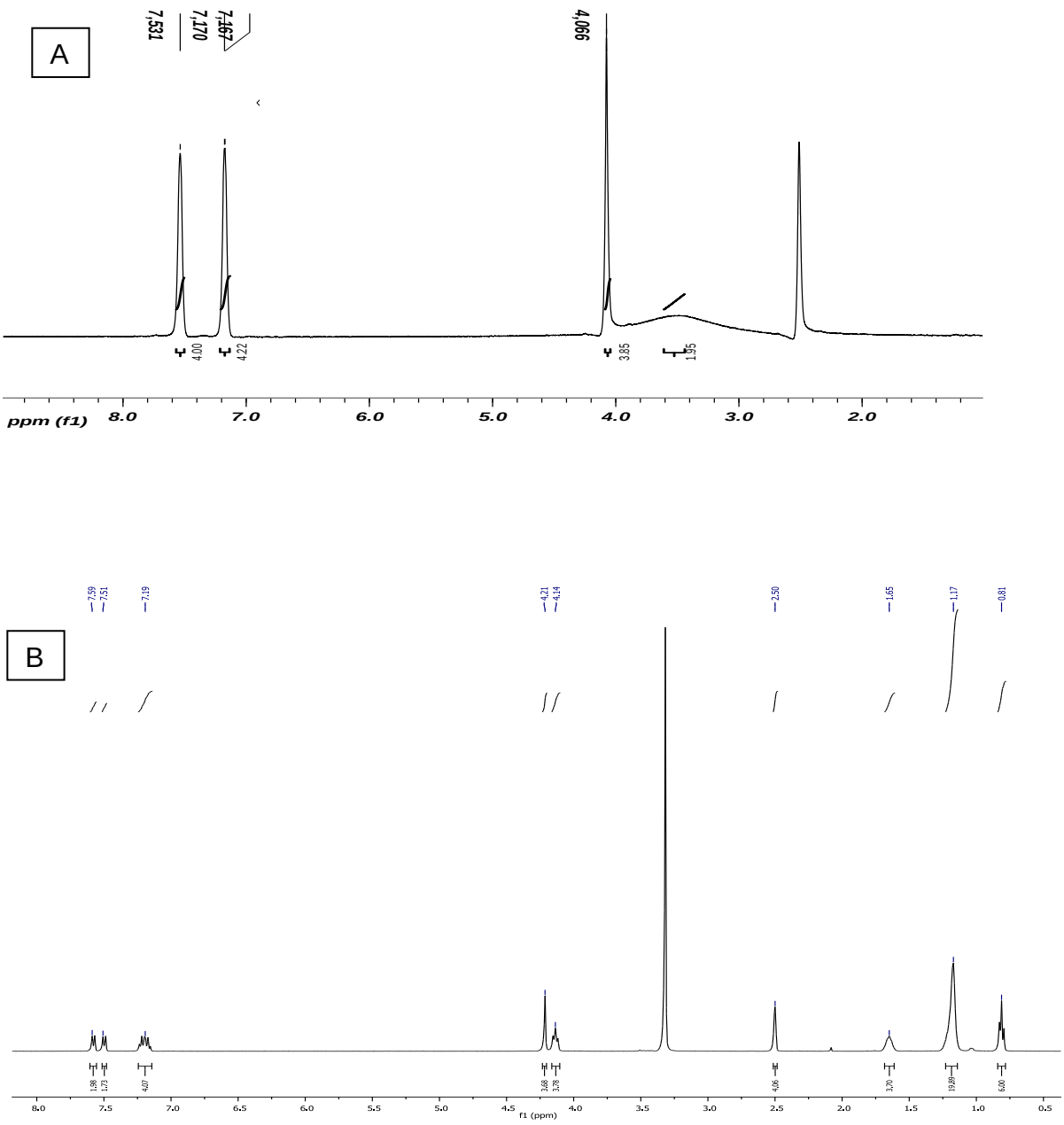

Figure 3.5: The ^{1}H NMR spectra of *bis*((1-alkylbenzimidazol-2-yl)methyl)sulfide (A) and *bis*((1-octylbenzimidazol-2-yl)methyl)sulfide (B)

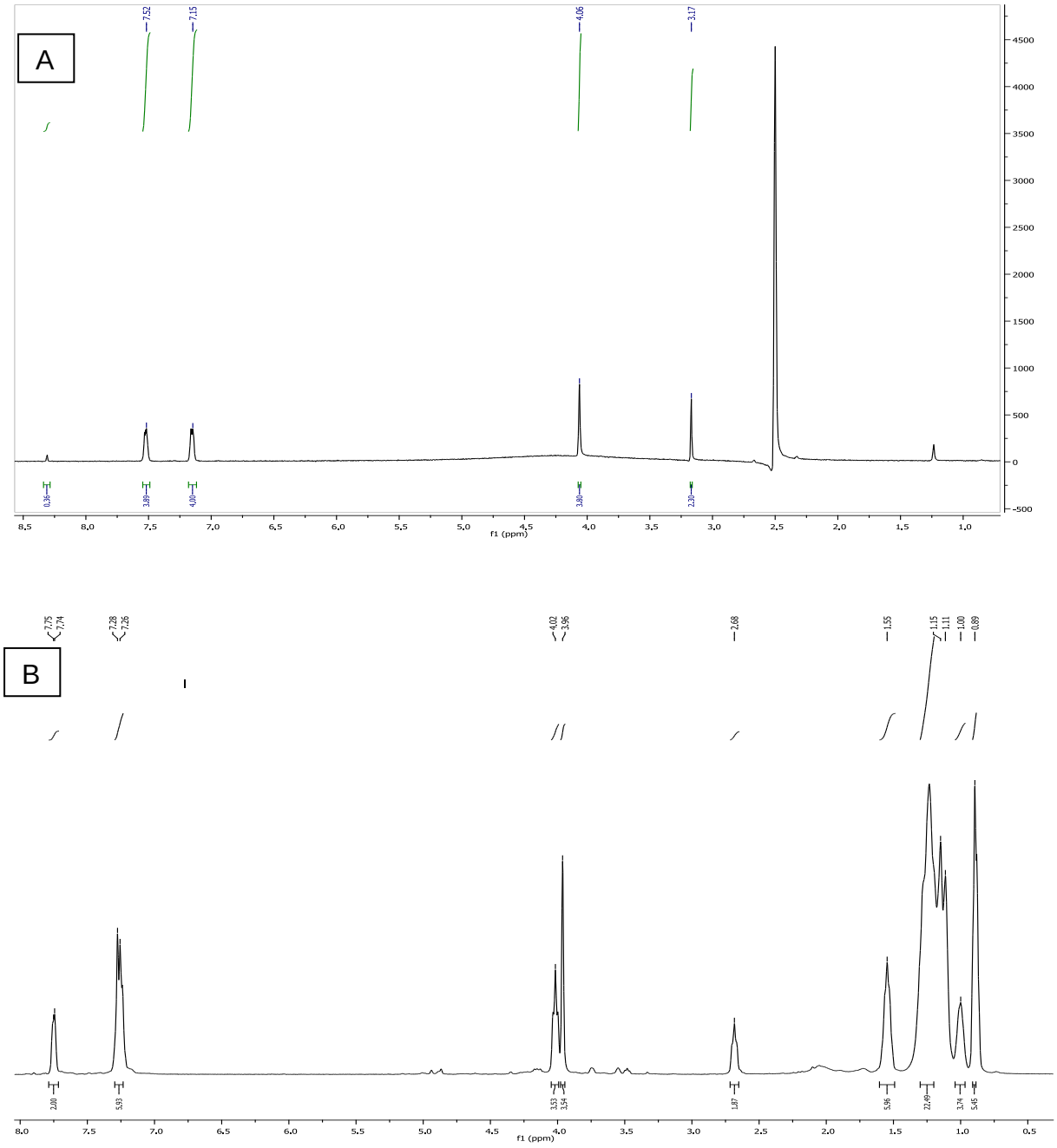

Figure 3.6: The ^{1}H NMR spectra of *bis*((1-alkylbenzimidazol-2-yl)methyl)amine (A) and *bis*((1-octylbenzimidazol-2-yl)methyl)amine (B)

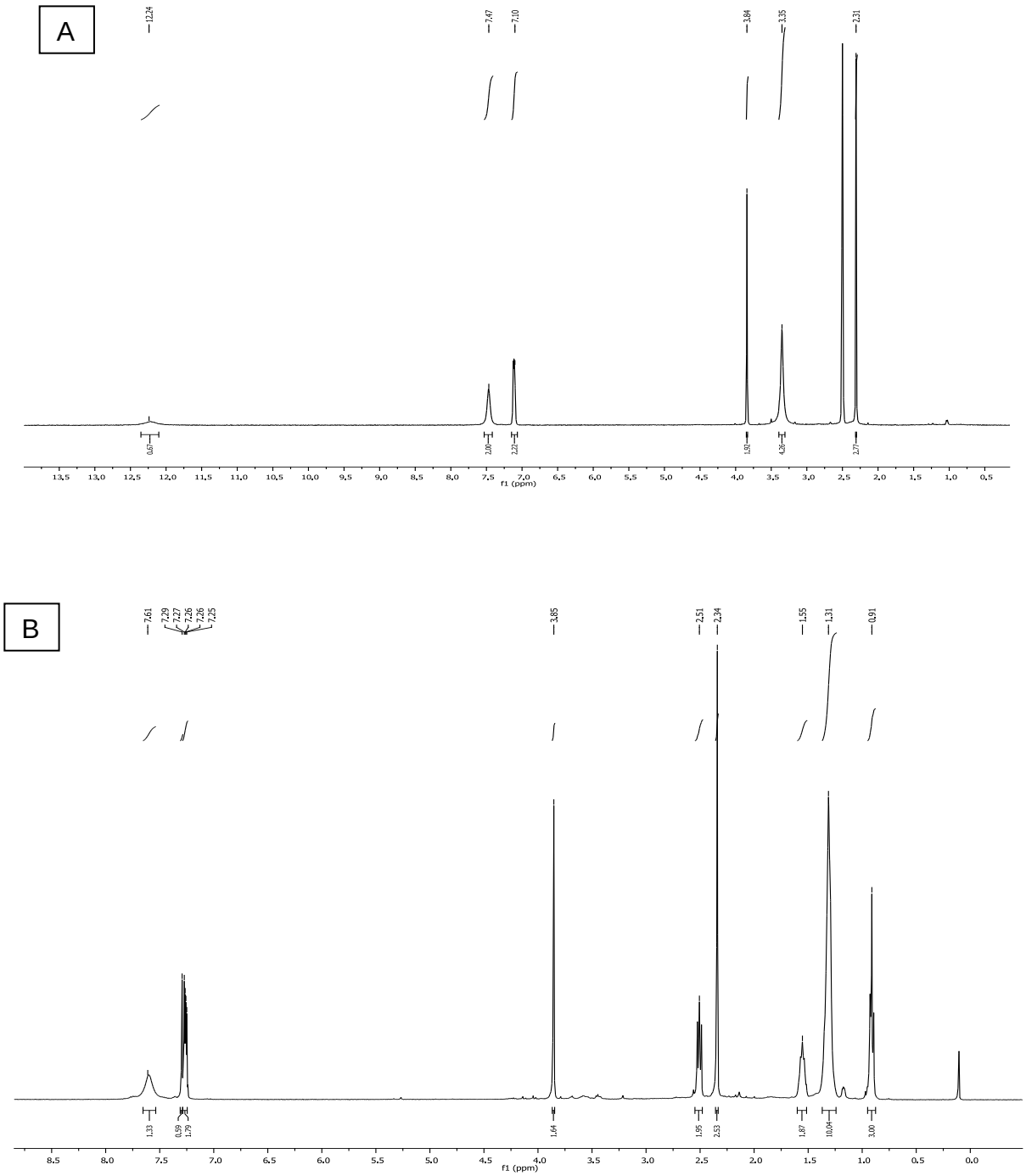

Figure 3.7: The ^{1}H NMR spectra of (1*H*-benzimidazol-2-yl)-*N*-methylmethanamine (A) and (1-octylbenzimidazol-2-yl)-*N*-methylmethanamine (B)

3.3.2. Extraction studies

The extraction studies were performed using individual synthetic sulfate solutions of Ni(II), Co(II), Cu(II), Fe(II), Zn(II), Mn(II), Mg(II), Cd(II) and Fe(III). The purpose of this study was to investigate selectivity towards nickel(II) through forcing six-coordination while the other metal ions adopt other geometries. In these studies, the conditions for the extraction of nickel were optimized through investigating the required concentration of the extractant, the suitable alkyl chain on the benzimidazole as well as the concentration of the synergist (DNNSA). The kinetics of the extraction process for the benzimidazole-based tridentate system were also investigated through varying the equilibration time. Typical results of percentage extraction versus pH are presented for the extraction studies.

3.3.2.1. Extraction with bis((1-alkylbenzimidazol-2-yl)methyl)sulfide

3.3.2.1.1. The effect of the alkyl chain on extraction of nickel (constant DNNSA)

The following experiments were carried out to determine effect of the alkyl chain. This allows for the identification of the chain that makes the extractant organic compatible and aqueous phase recognizable. The extraction studies pertaining to the effect of the alkyl chain are graphically represented in **Figures 3.8, 3.9** and **3.10**. The experimental data are given in **Tables 3.1, 3.2** and **3.3**. The extraction studies indicated that the BONSN and BDNSN resulted in higher extraction of nickel(II) than (BHNSN) (**Figure 3.8**). The decision to select the octyl derivative was based on the fact that the decyl derivative resulted into a formation of third phase. Again the octyl derivative result into slight separation between nickel and cobalt as shown in **Figure 3.9.**

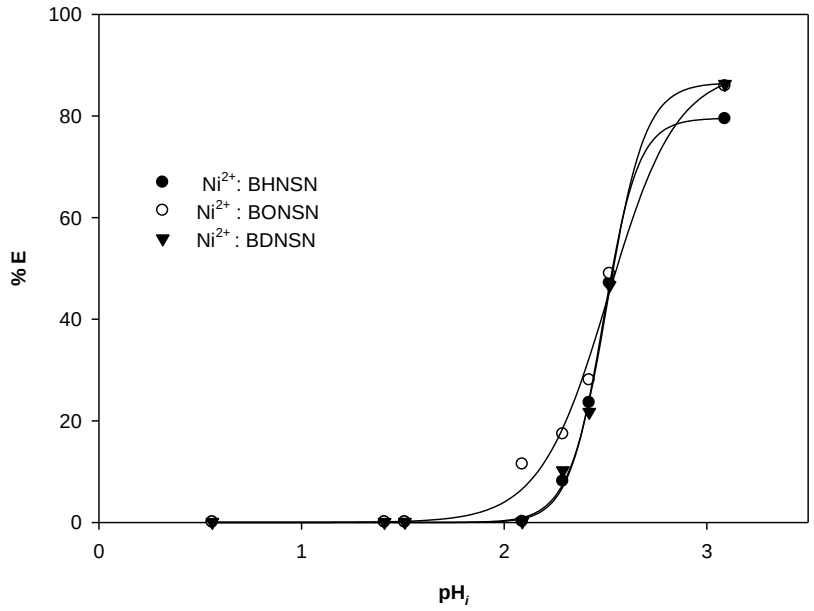

Figure 3.8: A plot of %E vs initial pH in the extraction of 0.001M Ni^{2+} from a dilute sulfate medium with BHNSN, BONSN and BDNSN at M:L ratio of 1:20 and in the presence of 0.02 M DNNSA in 2-octanol/Shellsol 2325 (8:2)

Table 3.1: %E vs initial and equilibrium pH in the extraction of 0.001 M Ni^{2+} from dilute sulfate medium with BHNSN, BONSN and BDNSN at M:L molar ratio of 1:20 in the presence of DNNSA, in 80% 2-Octanol/Shellsol 2325

BHNSN			**BONSN**			**BDNSN**		
pH$_i$	**pH$_e$**	**% E**	**pH$_i$**	**pH$_e$**	**% E**	**pH$_i$**	**pH$_e$**	**% E**
0.56	0.60	0.06	0.56	0.59	0.07	0.56	0.58	0.08
1.41	1.45	0.07	1.41	1.43	0.07	1.41	1.49	0.08
1.51	1.50	0.08	1.51	1.50	0.08	1.51	1.40	0.09

Table 3.1: Continued

BHNSN			BONSN			BDNSN		
pH_i	pH_e	% E	pH_i	pH_e	% E	pH_i	pH_e	%E
2.09	1.94	0.19	2.09	2.01	11.47	2.09	1.98	0.18
2.29	2.06	8.11	2.29	2.17	17.39	2.29	2.03	10.23
2.42	2.21	23.59	2.42	2.21	28.03	2.42	2.15	21.71
2.52	2.19	47.12	2.52	2.37	48.97	2.52	2.50	46.66
3.09	2.93	79.43	3.09	2.95	85.90	3.09	2.97	86.27

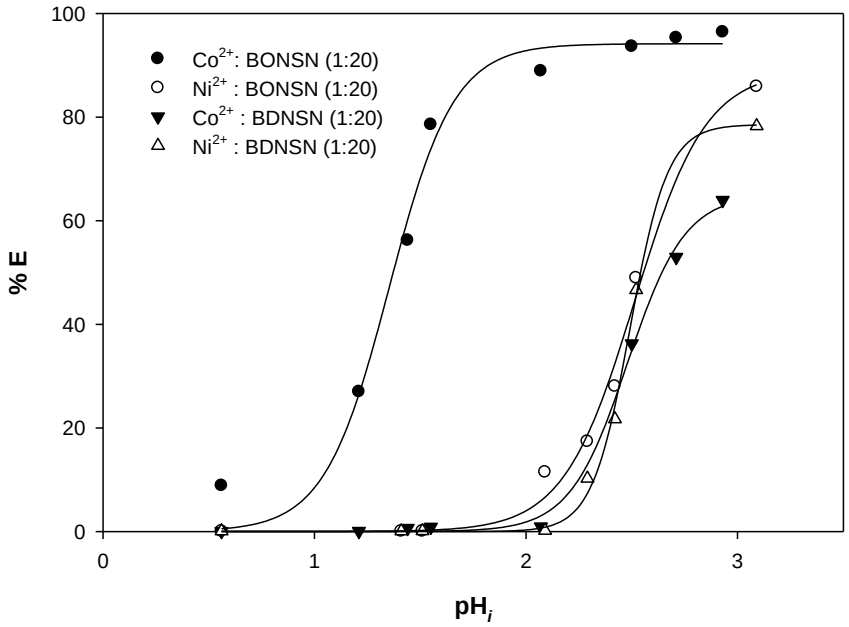

Figure 3.9: A plot of %E vs initial pH in the extraction of 0.001M Ni^{2+} and Co^{2+} from a dilute sulfate medium with BONSN and BDNSN at M:L ratio of 1:20 and in the presence of 0.02 M DNNSA in 2-octanol/Shellsol 2325 (8:2)

Table 3.2: %E vs initial and equilibrium pH in the extraction of 0.001 M Ni^{2+} and Co^{2+} from dilute sulfate medium with BONSN and BDNSN at a M:L molar ratio of 1:20 in the presence of DNNSA, in 80% 2-Octanol/Shellsol 2325

Ni^{2+} BONSN			Co^{2+}:BONSN			Ni^{2+}:BDNSN			Co^{2+}:BDNSN		
pH_i	pH_e	% E	pH_i	pH_e	% E	pH_i	pH_e	% E	pH_i	pH_e	% E
0.56	0.59	0.07	0.56	0.58	8.87	0.56	0.57	0.08	0.56	0.57	0.04
1.41	1.46	0.07	1.21	1.19	26.99	1.41	1.40	0.08	1.21	1.24	0.07
1.51	1.44	0.08	1.44	1.38	56.22	1.51	1.48	0.09	1.44	1.40	0.64
2.09	1.81	11.47	1.55	1.51	78.56	2.09	2.11	0.18	1.55	1.47	0.87
2.29	2.17	17.39	2.07	2.01	88.91	2.29	2.15	10.23	2.07	2.01	0.94
2.42	2.21	28.03	2.50	2.49	93.65	2.42	2.31	21.71	2.50	2.36	36.2
2.52	2.47	48.97	2.71	2.38	95.31	2.52	2.39	46.66	2.71	2.43	52.9
3.09	2.75	85.90	2.93	2.76	96.41	3.09	2.98	78.27	2.93	2.65	63.9

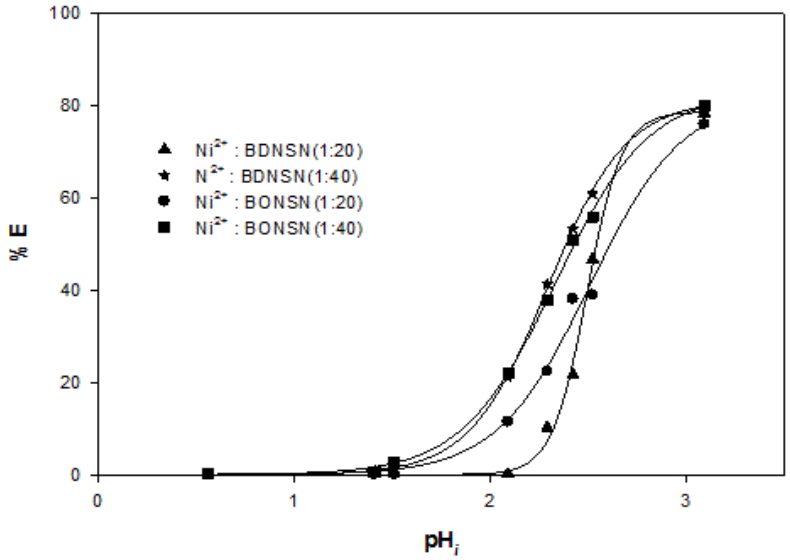

Figure 3.10: A plot of %E vs initial pH in the extraction of 0.001 M nickel from dilute sulfate medium with BONSN and BDNSN at M:L molar ratio of 1:20 and 1:40 with 0.02 M DNNSA in 2-octanol/Shellsol 2325 (8:2)

Table 3.3: %E vs initial and equilibrium pH in the extraction of 0.001 M nickel from dilute sulfate medium with BONSN and BDNSN at M:L molar ratio of 1:20 and 1:40 with 0.02 M DNNSA in 2-octanol/Shellsol 2325 (8:2)

Ni^{2+}:BONSN (1:20)			**Ni^{2+}:BDNSN(1:20)**			**Ni^{2+}:BONSN(1:40)**			**Ni^{2+}:BDNSN(1:40)**		
pH_i	**pH_e**	**% E**	**pH_i**	**pH_e**	**% E**	**pH_i**	**pH_e**	**% E**	**pH_i**	**pH_e**	**% E**
0.56	0.59	0.07	0.56	0.58	0.075	0.56	0.59	0.09	0.56	0.54	0.10
1.41	1.36	0.074	1.41	1.49	0.083	1.41	1.37	0.62	1.41	1.38	0.93
1.51	1.24	0.079	1.51	1.40	0.086	1.51	1.46	2.73	1.51	1.39	1.33
2.09	1.95	11.47	2.09	2.01	0.18	2.09	2.01	22.02	2.09	1.98	21.04
2.29	2.07	22.39	2.29	2.08	10.23	2.29	2.07	37.72	2.29	2.03	41.28
2.42	2.11	38.03	2.42	2.25	21.71	2.42	2.31	50.67	2.42	2.07	53.29
2.52	2.27	38.97	2.52	2.46	46.66	2.52	2.26	55.74	2.52	2.23	60.85
3.09	2.85	75.90	3.09	2.73	78.27	3.09	2.85	79.97	3.09	2.93	79.98

3.3.2.1.2. Effect of the extractant concentration on extraction of nickel (constant DNNSA)

The effect of the concentration of the extractant was studied within the extractible M:L ratio range of 1:20 to 1:60 in the extraction of 0.001 M nickel as shown by the results in **Figure 3.11** and **Table 3.4**. The results indicated that the variation of the M:L ratio does not significantly change the extraction pattern of nickel. There is a slight shift of the extraction curves to lower pH values with an increase in the concentration of the extractant.

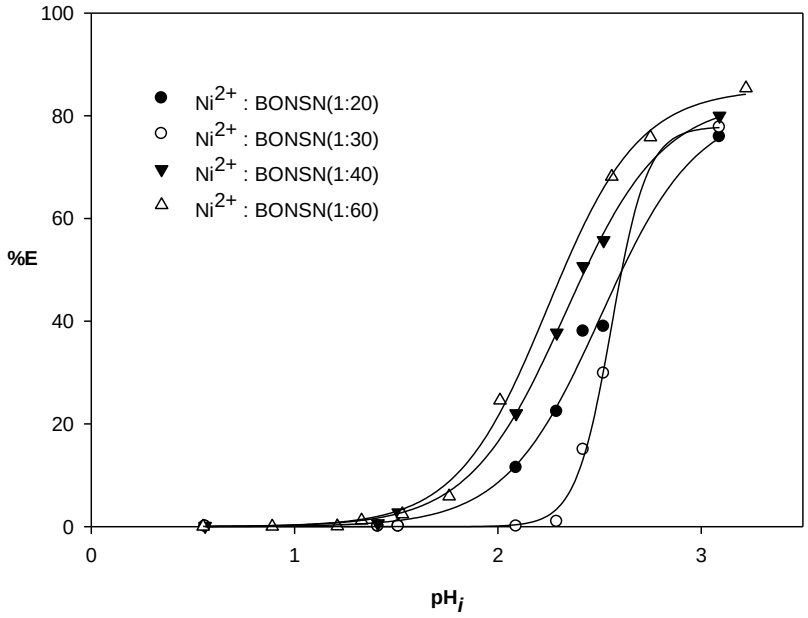

Figure 3.11: A plot of %E vs initial pH in the extraction of 0.001 M nickel from dilute sulfate medium with BONSN at various M:L molar ratio of 1:20, 1:40 and 1:60 with 0.02 M DNNSA in 2-octanol/Shellsol 2325 (8:2)

Table 3.4: %E vs initial and equilibrium pH in the extraction of 0.001 M nickel from dilute sulfate medium with BONSN at various M:L molar ratio of 1:20, 1:40 and 1:60 with 0.02 M DNNSA in 2-octanol/Shellsol 2325 (8:2)

Ni^{2+} : BONSN (1:20)			**Ni^{2+}: BONSN(1:40)**			**Ni^{2+}: BONSN(1:60)**		
pH$_i$	**pH$_e$**	**% E**	**pH$_i$**	**pH$_e$**	**% E**	**pH$_i$**	**pH$_e$**	**% E**
0.56	0.59	0.07	0.56	0.59	0.09	0.55	0.57	0.59
1.41	1.36	0.07	1.41	1.37	0.62	0.88	0.87	0.88
1.51	1.34	0.08	1.51	1.26	2.73	1.20	1.08	1.41

Table 3.4: Continued

Ni^{2+} : BONSN (1:20)			Ni^{2+}: BONSN(1:40)			Ni^{2+}: BONSN(1:60)		
pH_i	pH_e	% E	pH_i	pH_e	% E	pH_i	pH_e	% E
2.09	2.01	11.47	2.09	2.03	22.02	1.32	1.06	1.98
2.29	2.07	22.39	2.29	2.07	37.72	1.53	1.13	2.79
2.42	2.11	38.03	2.42	2.21	50.67	1.76	1.32	6.41
2.52	2.17	38.97	2.52	2.26	55.74	2.00	1.92	25.03
3.09	2.85	75.90	3.09	3.05	79.97	2.56	2.37	68.67
						2.74	2.43	76.72
						3.22	2.81	85.89

3.3.2.1.3. Effect of the synergist concentration on extraction of nickel (constant BONSN)

The involvement of dinonylnaphthalene sulfonic acid (DNNSA) as a synergist has proven to be vital to this extraction method since there is very low extraction efficiency observed in its absence (**Figure 3.12**), and this could be attributed to the fact that sulfate ions do not readily phase-transfer the cationic complexes formed in the extraction system from the aqueous to the organic layer.[133] The presence of DNNSA, which is a bulky organic acid with a very low pK_a, provides significant ion pairing with the cationic complex species thus eliminating the hindrance of the sulfate ion.

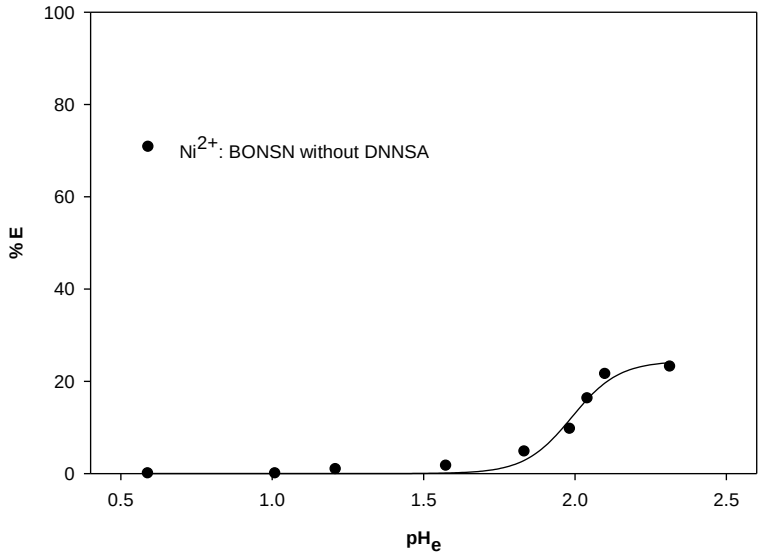

Figure 3.12: A plot of %E vs pH_e for without DNNSA in dilute sulfate medium with BONSN at M:L molar ratio of 1:40 without DNNSA in 2-octanol/Shellsol 2325 (8:2)

Table 3.5: A plot of %E vs initial pH_e for without DNNSA in dilute sulfate medium with BONSN at M:L molar ratio of 1:40 without DNNSA in 2-octanol/Shellsol 2325 (8:2)

pH_i	0.56	1.14	1.33	1.51	2.09	2.24	2.52	3.09	3.52
pH_e	0.59	1.01	1.21	1.58	1.83	1.98	2.04	2.10	2.31
% E Ni^{2+} (No DNNSA)	0.00	0.00	0.93	1.66	4.75	9.67	16.29	21.56	23.17

This tentative explanation can be illustrated by considering the following chemical equilibria that are possible under the pH conditions employed with these two extractants:

$$BONSN + 3H^+ + 3HSO_4^- \rightleftharpoons (BONSNH_3^{3+})(HSO_4^-)_3 \quad (17)$$

$$2(BONSN + 3H^+) + 3SO_4^{2-} \rightleftharpoons (BONSNH_3^{3+})_2(SO_4^{2-})_3 \quad (18)$$

$$BONSN + 3H^+ + 3A^- \rightleftharpoons (BONSNH_3^{3+})(A^-)_3 \quad (A^- = \text{deprotonated DNNSA}) \qquad (19)$$

$$Ni^{2+} + xBONSN + (BONSNH_3^{3+})(HSO_4^-)_3 \rightleftharpoons [Ni(BONSN)_{(x+1)}](HSO_4)_3 + 3H^+ \qquad (20)$$

$$Ni^{2+} + xBONSN + (BONSNH_3^{3+})_2(SO_4^{2-})_3 \rightleftharpoons [Ni(BONSN)_{(x+2)}]SO_4 + 6H^+ + 2SO_4^{2-} \qquad (21)$$

$$Ni^{2+} + xBONSN + (BONSNH_3^{3+})(A^-)_3 \rightleftharpoons [Ni(BONSN)_{(x+1)}](A)_2 + 3H^+ \qquad (22)$$

Equations 17, **18**, **20** and **21** illustrate the functioning chemistry in the absence of DNNSA, while **Equation 22** depicts the loading of nickel ions in the presence of DNNSA. The low pK_a of DNNSA and its bulky nature ensures that it acts as a non-coordinating ion pairing agent and an organic compatible anion respectively, thus facilitating an effective transfer of metals ions.

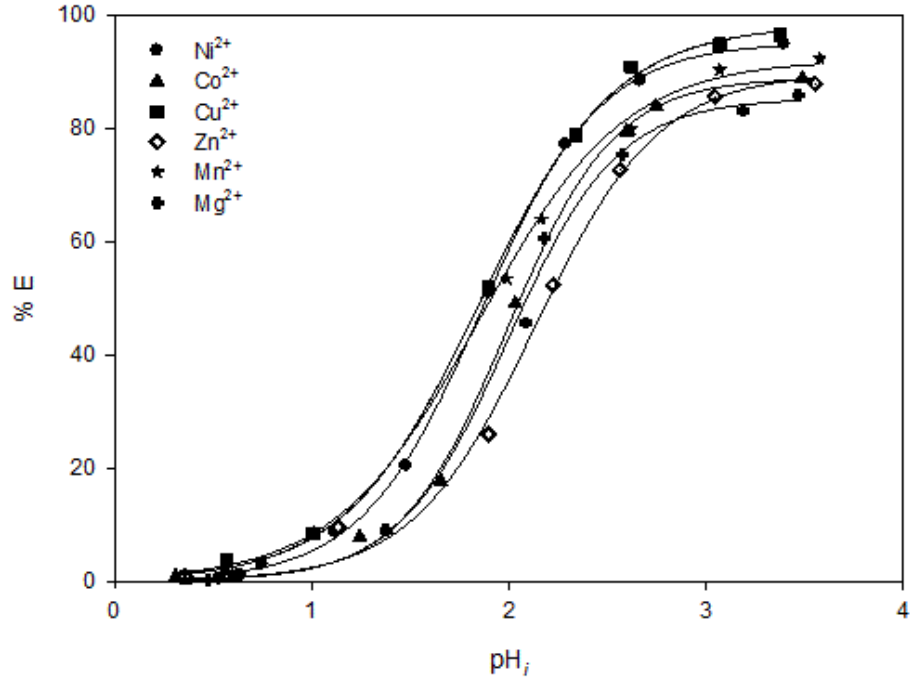

Figure 3.13: A plot of %E vs initial pH of 0.001 M Ni^{2+}, Co^{2+}, Cu^{2+}, Zn^{2+}, Mn^{2+} and Mg^{2+}, extracted from dilute sulfate medium with 0.02 M DNNSA alone in 100% Shellsol 2325[134]

It must be borne in mind, however, that DNNSA on its own does not show selectivity between metal ions (including the hard ions, Mn^{2+} and Mg^{2+}) since there is no separation observed as a function of pH with this extractant as reported in a patent publication by Schaekers and du Preez,[135] and also discussed by Preston and du Preez.[136] This effect is also demonstrated in **Figure 3.13**,[134] and it merely illustrates that the bulky counterion extracts the metals through the formation of extractible metal sulfonate salts. This necessitates the use of a ligand which has been carefully designed to discriminate between the metal ions *via* the bonding preferences with respect to coordination numbers, stereochemistry and type of bonding involved.

The optimization of the concentration of DNNSA was conducted for the extraction of 0.001 M nickel(II) ions with BONSN, and the results are shown in **Figure 3.14 and Table 3.6**. It was found out that 0.04 M DNNSA gave the most efficient extraction of the nickel ion as the pH was increased above 2.5.

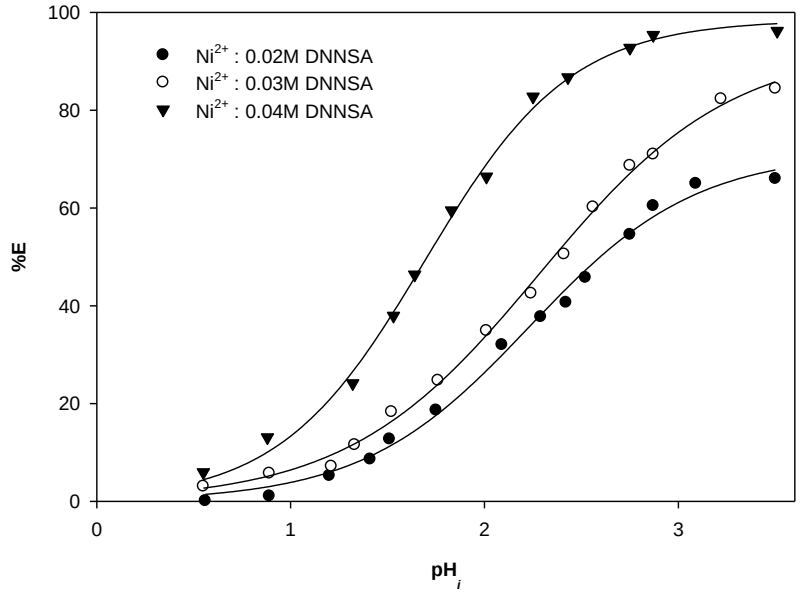

Figure 3.14: A plot of %E vs initial pH in the extraction of 0.001 M nickel from a dilute sulfate medium with BONSN at molar ratio of 1:40 with various DNNSA concentrations of 0.02 M, 0.03 M and 0.04 M in 2-octanol/Shellsol 2325 (8:2)

Table 3.6: %E vs initial and equilibrium pH in the extraction of 0.001 M nickel from dilute sulfate medium with BONSN at M:L molar ratio of 1:40 with various DNNSA concentrations of 0.02 M, 0.03 M and 0.04 M in a 2-octanol/Shellsol 2325 (8:2)

0.02 M DNNSA			**0.03 M DNNSA**			**0.04 M DNNSA**		
pH_i	**pH_e**	**% E**	**pH_i**	**pH_e**	**% E**	**pH_i**	**pH_e**	**% E**
0.55	0.56	1.46	0.54	0.55	3.71	0.54	0.57	6.51
0.88	0.89	2.03	0.89	0.86	6.51	0.86	0.81	13.29
1.18	1.06	6.26	1.21	1.24	7.95	1.31	1.26	24.54
1.40	1.24	9.63	1.32	1.15	12.43	1.52	1.36	38.34
1.50	1.45	13.57	1.51	1.36	19.20	1.64	1.57	47.06
1.74	1.63	19.77	1.75	1.45	25.11	1.83	1.62	59.74
2.08	1.95	33.29	2.00	1.69	35.80	2.01	1.98	66.77
2.28	2.01	38.63	2.23	1.96	43.11	2.25	2.04	83.40
2.41	2.10	41.71	2.40	2.26	51.57	2.42	2.19	87.06
2.51	2.29	46.80	2.56	2.41	60.86	2.75	2.43	93.51
2.74	2.41	55.51	2.74	2.35	69.03	2.86	2.69	95.77
2.86	2.56	61.71	2.86	2.55	71.86	3.51	2.31	96.63
3.08	2.91	65.94	3.21	3.04	82.83			
3.89	3.02	66.77	3.50	3.01	84.80			

3.3.2.1.4. Extraction of other base metals with BONSN and DNNSA

The effect of other metal ions such as Cu^{2+}, Fe^{2+}, Zn^{2+}, Mn^{2+}, Mg^{2+} and Fe^{3+} were also investigated under the conditions optimized for the extraction of Ni^{2+} (**Figure 3.15**). The

experimental data is presented in **Table 3.7**. The extraction curves obtained from this study showed that all elements (Ni^{2+}, Co^{2+}, Cu^{2+}, Fe^{2+}, Zn^{2+}, Mn^{2+}, Mg^{2+} and Fe^{3+}) are extracted at pH above 2 and slightly below, while Fe^{3+} is completely rejected below this pH. The hard ions Mn^{2+} and Mg^{2+} are also extracted significantly at pH above 2. This indicated that the system does not discriminate between the hard, soft and borderline metal ions. The observation of the lack of pH-metric separation of base metals with the NSN-based extractant warranted us to look at the effect of a related *bis*-benzimidazole-based tridentate extractant, *bis*((1-alkylbenzimidazol-2-yl)methyl)amine.

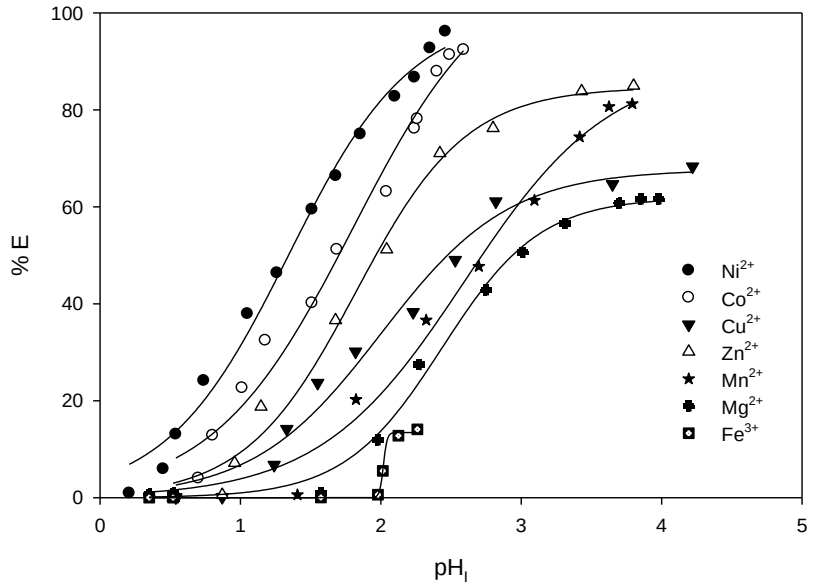

Figure 3.15 : A plot of %E vs initial pH in the separation of 0.001 M, Ni^{2+}, Co^{2+}, Cu^{2+}, Fe^{2+}, Zn^{2+}, Mn^{2+}, Mg^{2+} and Fe^{3+} from dilute sulfate medium with BONSN (M:L ratios of 1:40), and 0.04 M DNNSA in 2-octanol/Shellsol 2325 (8:2)

Table 3.7: A plot of %E vs initial pH in the separation of 0.001 M Ni^{2+},Co^{2+}, Cu^{2+},Fe^{2+}, Zn^{2+}, Mn^{2+}, Mg^{2+} and Fe^{3+} from dilute sulfate medium with BONSN (M:L ratios of 1:40), and 0.04 M DNNSA a 2-octanol/Shellsol 2325 (8:2)

Ni^{2+}								
pH_i	0.21	0.45	0.54	1.26	1.85	2.10	2.35	2.46
pH_e	0.29	0.48	0.51	1.19	1.72	1.98	2.03	2.25
% E	0.91	5.94	13.07	46.35	75.00	82.76	92.74	96.18
Co^{2+}								
pH_i	0.54	0.80	1.51	2.04	2.40	2.49	2.59	
pH_e	0.57	0.83	1.57	1.97	2.12	2.23	2.31	
% E	0.03	12.85	40.16	63.12	87.94	91.35	92.38	
Cu^{2+}								
pH_i	0.54	0.87	1.55	2.23	2.53	2.82	3.65	4.22
pH_e	0.58	0.89	1.50	2.01	2.27	2.59	2.73	2.97
% E	0.08	0.13	23.67	38.28	49.02	61.10	64.66	68.30
Zn^{2+}								
pH_i	0.52	0.87	1.15	1.68	2.04	2.42	3.43	3.80
pH_e	0.50	0.83	1.07	1.42	2.01	2.16	2.91	2.96
% E	0.03	0.56	18.74	36.60	51.20	71.04	83.81	84.96
Mn^{2+}								
pH_i	0.54	1.41	1.82	2.32	3.09	3.42	3.63	3.80
pH_e	0.51	1.26	1.54	2.01	2.72	2.93	2.91	3.04
% E	0.21	0.60	20.26	36.61	61.31	74.40	80.66	81.26

Table 3.7: Continued

Mg^{2+}								
pH_i	0.52	1.57	1.98	2.27	3.01	3.70	3.85	3.98
pH_e	0.47	1.56	1.76.	2.03	2.86	2.96	2.83	3.27
% E	0.94	0.99	11.91	27.43	50.60	60.71	61.62	61.64
Fe^{3+}								
pH_i	0.35	0.52	1.57	1.98	2.01	2.12	2.26	
pH_e	0.31	0.50	1.52	1.87	1.63	1.95	1.98	
% E	0.00	0.00	0.03	0.62	5.53	12.80	14.10	

3.3.2.2. Extractions with bis((1-alkylbenzimidazol-2-yl)methyl)amine (BRNNN)

*3.3.2.2.1. The effect of the alkyl chain on extraction of nickel (constant DNNSA***)**

The results obtained from the investigation showed (**Figure 3.12** and **Table 3.7**) that all three alkyl derivatives (BHNNN, BONNN and BDNNN) extract Ni^{2+} similarly, but the decyl chain was selective among other alkyl chains because the heptyl and octyl derivatives resulted into the third phase formation indicating the lack of organic compatibility of the extracted species.

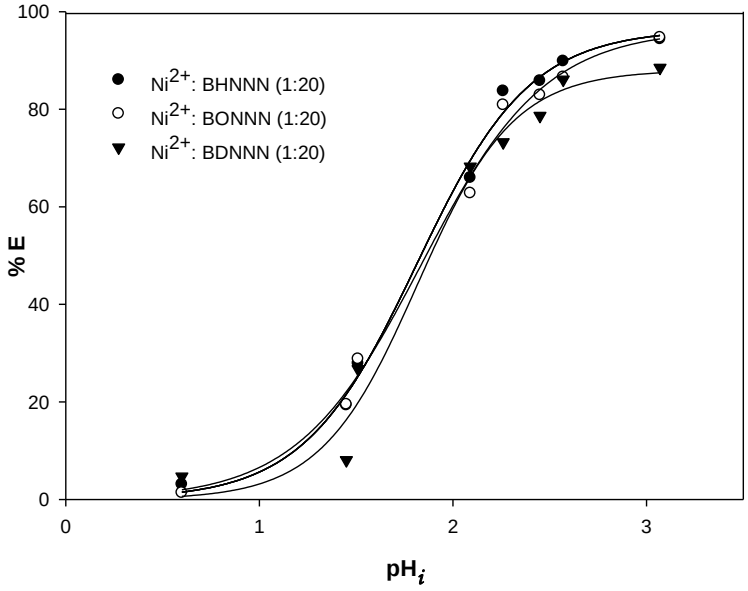

Figure 3.16: A plot of %E vs initial pH in the extraction of 0.001 M Ni^{2+} from a dilute sulfate medium with BHNNN, BONNN and BDNNN at M:L ratio of 1:20 and in the presence of 0.02 M DNNSA in 2-octanol/Shellsol 2325 (8:2)

Table 3.8: A plot of %E vs initial pH in the extraction of 0.001 M Ni^{2+} from a dilute sulfate medium with BHNNN, BONNN and BDNNN at M:L ratio of 1:20 and in the presence of 0.02 M DNNSA in 2-octanol/Shellsol 2325 (8:2)

BHNNN			**BONNN**			**BDNNN**		
pH_i	**pH_e**	**% E**	**pH_i**	**pH_e**	**% E**	**pH_i**	**pH_e**	**% E**
0.60	0.35	3.10	0.60	0.42	1.37	0.60	0.31	4.71
1.45	1.26	19.33	1.45	1.41	19.50	1.45	1.34	8.05
1.51	1.47	27.89	1.51	1.43	28.80	1.51	1.46	26.72
2.09	1.87	65.94	2.09	1.90	62.78	2.09	1.85	68.24
2.26	2.08	83.72	2.26	2.14	80.89	2.26	2.10	73.24
2.45	2.35	85.83	2.45	1.86	82.91	2.45	1.89	78.63
2.57	2.41	89.87	2.57	2.21	86.58	2.57	2.25	86.08
3.07	2.87	94.39	3.07	2.78	94.71	3.07	3.19	88.49

3.3.2.2.2. Effect of the synergist concentration on extraction of nickel (constant BDNNN)

The investigation of synergist was necessitated by the poor extraction of nickel in the absence of DNNSA as shown in **Figure 3.17** and **Table3.9**. The results indicated the poor phase transferability of the sulfate complexes of the extractant from the aqueous to the organic phase and it was evident that the presence of the bulky anion (DNNSA) as a co-extractant is crucial for the satisfactory extraction of the metals. Further studies on the effect of synergist were carried out to obtain a complete extraction as illustrated in **Figure 3:14**. The studies indicated that 0.02 M DNNSA gave the most efficient extraction of the nickel ion as shown in **Figure 3.14** (and **Table 3.9**)

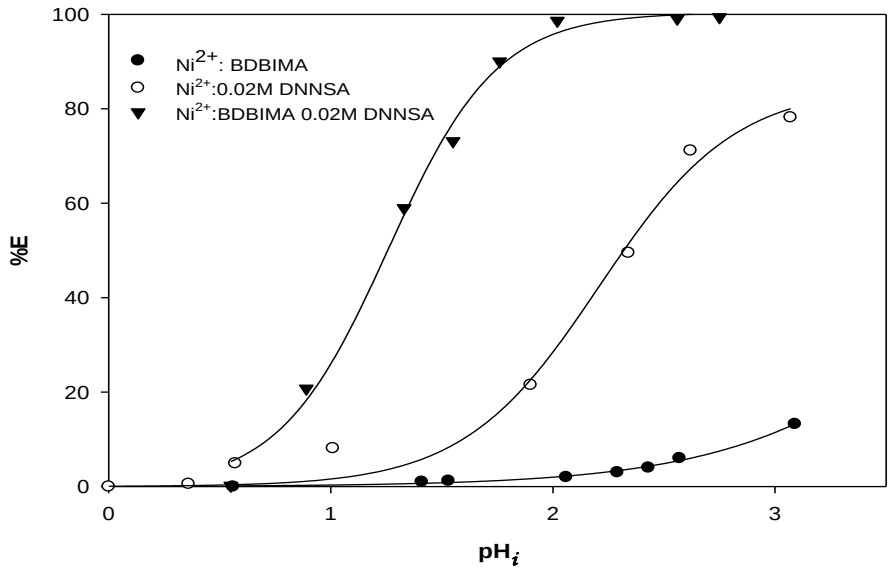

Figure 3.17: A plot of %E vs initial pH in the extraction of 0.001 M nickel from a dilute sulfate medium with BDNNN at molar ratio of 1:40 in the absence of DNNSA, and with 0.02M DNNSA, and with BDNNN at molar ratio of 1:40 in the presence of DNNSA (0.02 M) in 2-octanol/Shellsol 2325 (8:2)

Table 3.9: A plot of %E vs initial pH in the extraction of 0.001 M nickel from a dilute sulfate medium with BDNNN at molar ratio of 1:40 in the absence of DNNSA, and with 0.02 M DNNSA, and with BDNNN at molar ratio of 1:40 in the presence of DNNSA (0.02 M) in 2-octanol/Shellsol 2325 (8:2)

Ni (No DNNSA)			**DNNSA only**			**Ni (with DNNSA)**		
pH_i	**pH_e**	**% E**	**pH_i**	**pH_e**	**% E**	**pH_i**	**pH_e**	**% E**
0.56	0.58	0.00	0.01	0.03	0.56	0.55	0.65	0.19
1.41	1.43	1.01	0.36	0.39	4.91	0.89	0.97	20.75
1.53	1.46	1.22	0.57	0.54	4.94	1.33	1.47	58.98
2.06	1.87	2.03	1.01	1.04	8.11	1.55	1.53	73.16
2.29	2.10	3.05	1.90	1.84	21.51	1.76	1.63	90.04
2.43	2.35	4.02	2.34	2.29	49.50	2.02	1.76	98.65
2.57	2.40	6.04	2.62	2.42	71.14	2.56	1.84	99.09
3.09	2.96	13.23	3.07	2.13	78.19	2.75	1.95	99.41

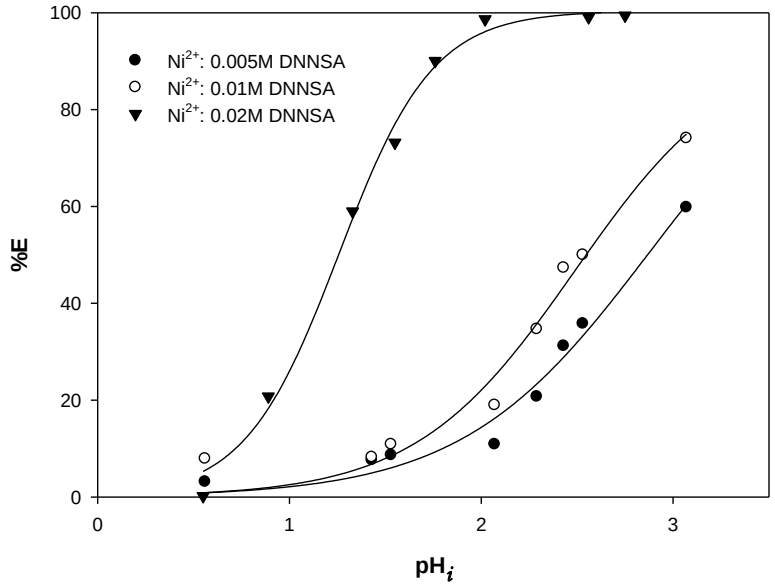

Figure 3.18: A plot of %E vs initial pH in the extraction of 0.001 M nickel from a dilute sulfate medium with BDNNN at molar ratio of 1:40 with various DNNSA concentrations of 0.005 M, 0.01 M and 0.02 M in 2-octanol/Shellsol 2325 (8:2)

Table 3:10: %E vs initial and equilibrium pH in the extraction of 0.001 M nickel from dilute sulfate medium with BDNNN at M:L molar ratio of 1:40 with various DNNSA concentrations of 0.005 M, 0.01 M and 0.02 M in in 2-octanol/Shellsol 2325 (8:2)

0.005 M DNNSA			**0.01 M DNNSA**			**0.02 M DNNSA**		
pH_i	**pH_e**	**% E**	**pH_i**	**pH_e**	**% E**	**pH_i**	**pH_e**	**% E**
0.56	0.59	3.15	0.56	0.58	7.92	0.56	0.60	0.19
1.43	1.35	7.64	1.43	1.49	8.23	1.43	1.32	20.75
1.53	1.45	8.65	1.53	1.56	10.89	1.53	1.44	58.98
2.07	2.01	10.87	2.07	2.02	18.98	2.07	1.97	73.16
2.29	2.14	20.74	2.29	2.17	34.68	2.29	2.13	90.04
2.43	2.18	31.20	2.43	2.29	47.36	2.43	2.21	98.65
2.53	2.48	35.79	2.53	2.32	50.01	2.53	2.46	99.09
3.07	2.95	59.82	3.07	2.96	74.11	3.07	2.89	99.41

3.3.2.2.3. Effect of the extractant concentration on extraction of nickel (constant DNNSA)

The effect of the concentration of the extractant was studied within the extractible M:L ratio range of 1:20 to 1:40 in the extraction of 0.001 M nickel as shown by the results in **Figure 3.19 and Table 3.11**. The M:L ratio of 1:40 extracted nickel more than the 1:20 ratio. Further studies were then conducted using M:L ratio of 1:40 for the extraction of nickel and cobalt.

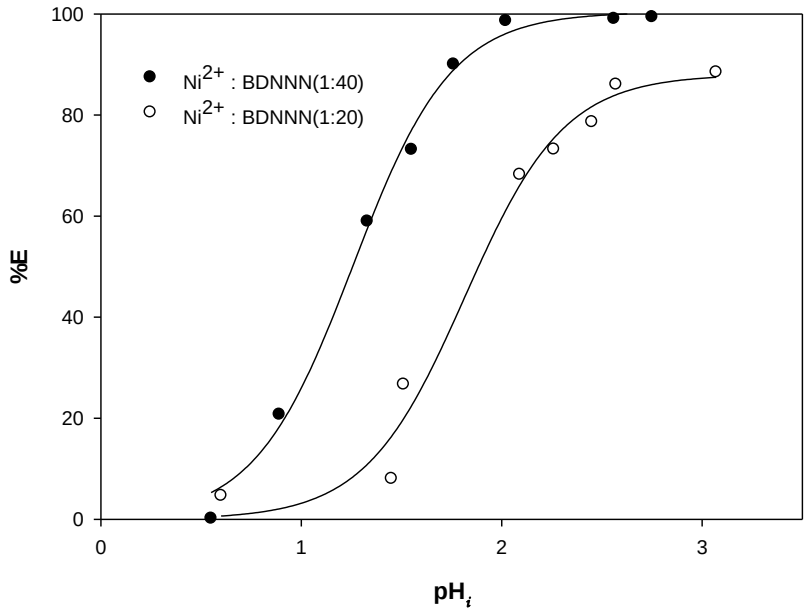

Figure 3.19: A plot of %E vs initial pH in the extraction of 0.001 M nickel from dilute sulfate medium with BDNNN at various M:L molar ratio of 1:20 and 1:40 with 0.02 M DNNSA in 2-octanol/Shellsol 2325 (8:2)

Table 3.11: %E vs initial and equilibrium pH in the extraction of 0.001 M nickel from dilute sulfate medium with BDNSN at various M:L molar ratio of 1:20 and 1:40 with 0.02 M DNNSA in 2-octanol/Shellsol 2325 (8:2)

BDNNN (1:20)			**BDNNN(1:40)**		
pH_i	**pH_e**	**% E**	**pH_i**	**pH_e**	**% E**
0.55	0.61	0.19	0.64	0.83	0.19
0.89	1.06	20.75	1.45	1.36	20.75
1.33	1.24	58.98	1.51	1.77	58.98
1.55	1.43	73.16	2.09	1.83	73.16
1.76	1.81	90.04	2.26	2.12	90.04
2.02	2.04	98.65	2.45	2.33	98.65
2.56	2.32	99.09	2.57	2.41	99.09
2.75	2.56	99.41	3.07	2.64	99.41

3.3.2.2.4. Separation of nickel and cobalt with BDNNN (constant DNNSA)

To assess the separation between nickel and cobalt parameter such as equilibration time and concentration of extractant were investigated. The optimised conditions for the separation of nickel and cobalt are presented by the extraction curve in **Figures 3.20**. Nickel and cobalt were extracted at various equilibration times (**Figure 3.20** and **Figure 3.21**). The results show that the two various equilibration times do not provide a significant separation between the two metal ions

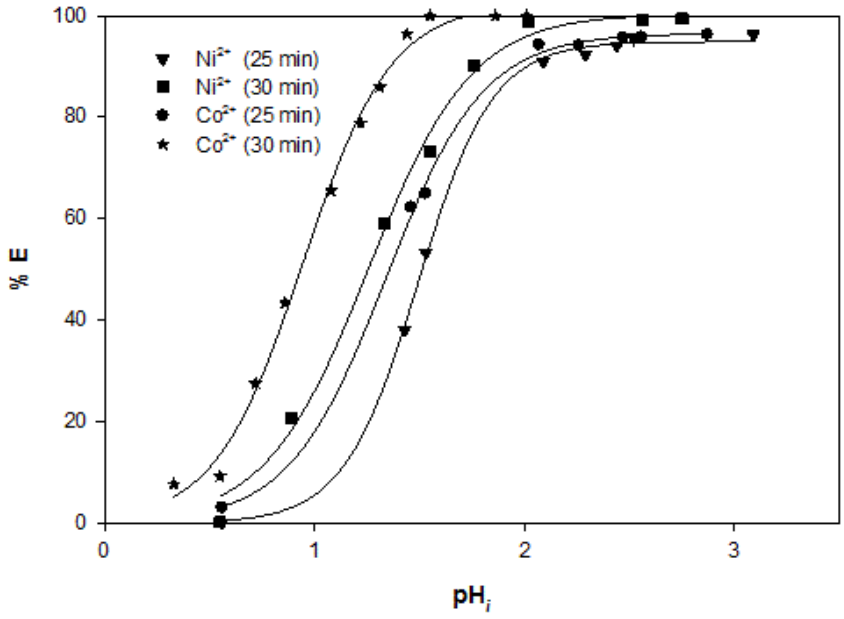

Figure 3.20: A plot of %E vs initial pH in the extraction of 0.001 M nickel and cobalt from dilute sulfate medium with BDNNN at various equilibration time of 25 and 30 mins and M:L molar ratio of 1:40 with 0.02 M DNNSA in 2-octanol/Shellsol 2325 (8:2)

Table 3.12: %E vs initial pH equilibrium pH in the extraction of 0.001 M nickel and cobalt from dilute sulfate medium with BDNNN at various equilibration time of 25 and 30 mins and M:L molar ratio of 1:40 with 0.02 M DNNSA in 2-octanol/Shellsol 2325 (8:2)

25 min						**30 min**					
Ni^{2+}			**Co^{2+}**			**Ni^{2+}**			**Co^{2+}**		
pH_i	**pH_e**	**% E**	**pH_i**	**pH_e**	**% E**	**pH_i**	**pH_e**	**% E**	**pH_i**	**pH_e**	**% E**
0.56	0.59	0.09	0.56	0.58	2.99	0.55	1.59	0.19	0.33	0.36	7.68
1.43	1.45	38.08	1.43	1.49	62.22	1.14	1.03	36.61	0.55	0.54	9.25

Table 3.12: Continued

25 min						30 min					
Ni^{2+}			Co^{2+}			Ni^{2+}			Co^{2+}		
pH_i	pH_e	% E	pH_i	pH_e	% E	pH_i	pH_e	% E	pH_i	pH_e	% E
1.53	1.51	53.31	1.53	1.41	64.88	1.33	1.22	58.98	0.72	0.72	27.55
2.07	2.10	90.99	2.07	2.01	94.20	1.55	1.48	73.16	0.86	0.74	43.33
2.29	2.14	92.35	2.29	2.17	94.46	1.76	1.54	90.04	1.08	0.97	65.49
2.43	2.49	94.095	2.43	2.29	95.64	2.02	1.73	98.65	1.22	1.14	78.79
2.53	2.38	95.52	2.53	2.42	95.77	2.56	2.49	99.09	1.31	1.22	85.98
3.07	2.94	96.23	3.07	2.96	96.24	2.75	2.43	99.41	1.44	1.36	96.43
									1.55	1.43	99.95
									1.86	1.67	99.96
									2.01	1.86	99.99

*3.3.2.2.5. Extraction of other base metals with BDNNN and DNNSA (constant DNNSA***)**

The effect of the other metal ions including Mg^{2+}, Mn^{2+}, Fe^{3+}, Fe^{2+}, Cu^{2+} and Zn^{2+} were also investigated under the conditions investigated for cobalt and nickel extractions. The results of this study are shown in **Figure 3.21**. The extraction curves are pushed further into the acidic region compared with the BNSN-based extractant resulting in a lack of back-extraction of some metals (like Cu(II), Co(II) and possibly Ni(II)) at the "left legs" of the extraction curves. The lack of pH-metric separation of the base metal ions, however, was evident from the small $\Delta pH_{0.5}$ values (**Figure 3.21**). Interestingly, the order of the extraction of the metal ions somewhat followed the Irving-Williams stability order[101] in the shifting of the curves towards the acidic

region with the exception of Co(II) and Ni(II) extractions, which could be influenced by kinetic effects.[43] It is also noteworthy to report on the hard ions (Mn^{2+} and Mg^{2+}) extracting ability of this tridentate ligand but with rejection of Fe(III) in the pH range 0–2.6, which is attractive for the latter but not the former.

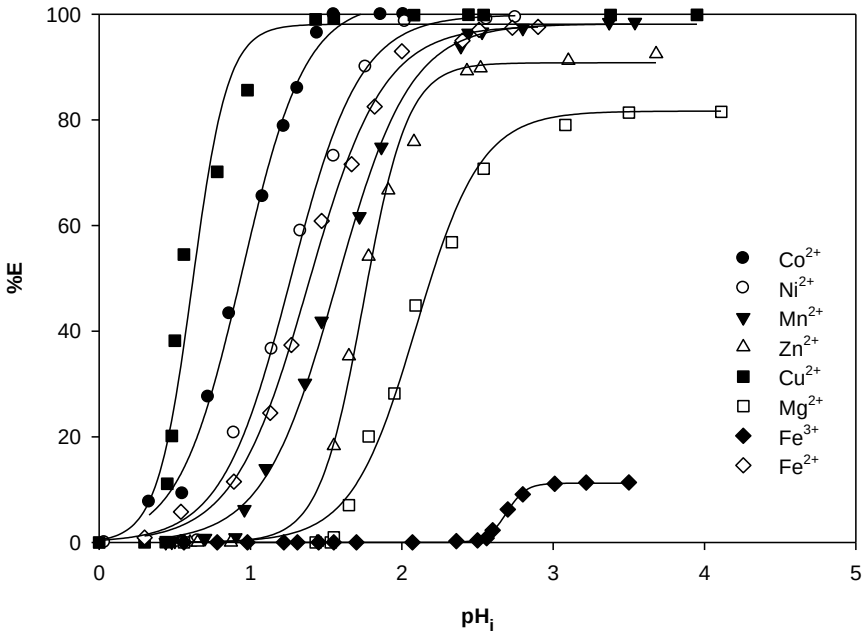

Figure 3.21: A plot of %E vs initial pH of equimolar concentrations (0.001 M) of Co^{2+}, Ni^{2+}, Mn^{2+}, Zn^{2+}, Cu^{2+}, Mg^{2+}, Fe^{3+} and Fe^{2+}, extracted with BDNNN (at M:L ratio 1:40) and 0.02 M DNNSA in 2-octanol/Shellsol 2325 (8:2) from a dilute sulfate medium

Table 3.13*:* Extraction data (%) with initial pH and equilibrium pH of %E vs initial pH in the separation of 0.001 M, Ni^{2+},Co^{2+}, Cu^{2+},Fe^{2+}, Zn^{2+}, Mn^{2+}, Mg^{2+} and Fe^{3+} from dilute sulfate medium with BDNNN (M:L ratios of 1:40), and 0.0 M DNNSA in 2-octanol/Shellsol 2325 (8:2)

Ni^{2+}								
pH_i	0.55	0.89	1.14	1.33	1.76	2.02	2.56	2.75
pH_e	0.57	0.85	1.03	1.18	1.43	1.94	2.43	2.65
% E	0.19	20.75	36.61	58.98	90.04	98.65	99.09	99.41
Co^{2+}								
pH_i	0.33	0.55	0.86	1.08	1.22	1.55	1.86	2.01
pH_e	0.37	0.60	0.71	1.01	1.16	1.32	1.75	1.89
% E	7.68	9.25	43.33	65.49	78.79	99.95	99.96	99.99
Cu^{2+}								
pH_i	0.44	0.50	0.78	1.43	2.08	2.54	3.38	3.95
pH_e	0.47	0.53	0.65	1.12	1.76	2.18	2.34	2.56
% E	0.04	38.20	70.16	99.01	99.83	99.95	99.96	99.98
Zn^{2+}								
pH_i	0.54	0.87	1.55	1.78	2.08	2.43	3.10	3.68
pH_e	0.52	0.83	1.32	1.59	1.78	1.95	2.87	2.91
% E	0.00	0.00	18.27	54.14	75.84	89.23	91.22	92.47
Mn^{2+}								
pH_i	0.50	0.96	1.36	1.87	2.39	2.44	3.37	3.54
pH_e	0.54	0.98	1.13	1.62	2.15	2.23	2.17	2.12
% E	0.26	6.25	30.15	74.84	93.92	96.41	98.44	98.48
Mg^{2+}								
pH_i	0.56	1.55	1.95	2.09	2.54	3.08	3.50	4.11
pH_e	0.51	1.58	1.67	1.85	2.21	2.56	3.09	3.73
% E	0.00	0.96	28.19	44.85	70.74	79.01	81.35	81.51

Table 3.13: Continued

Fe^{3+}								
pH_i	0.30	0.54	0.89	1.67	2.00	2.51	2.73	2.90
pH_e	0.37	0.56	0.76	1.34	1.73	1.96	2.34	2.41
% E	0.90	5.78	11.50	71.59	92.95	97.02	97.42	97.60
Fe^{2+}								
pH_i	0.56	2.36	2.50	2.70	2.80	3.01	3.22	3.50
pH_e	0.59	2.39	2.49	2.43	2.41	2.78	2.85	2.91
% E	0.0	0.23	0.80	6.25	9.10	11.10	11.32	11.35

3.3.2.2.6. Quantitative treatment of the extractions with BDNNN and DNNSA

In a quantitative treatment for this solvent extraction system, similar to that applied for a chelating system (HL),[91] the protonation, complexation and phase distribution equilibria can be used to describe the system mathematically with respect to the distribution ratio of a metal ion (M^{n+}), and also give insight into the coordination numbers involved in the extraction reaction. The protonation equilibria, which were studied using potentiometry in the pH range of 2 – 10 by Hay *et al.*,[92] showed two constants for *bis*((1*H*-benzimidazol-2-yl)methyl)amine (BNNN, L), and they were 5.64 and 10.12 respectively for the cumulative protonation steps (LH^+ and LH_2^{2+}). However, our calculation using potentiometric data gave three protonation constants which were 8.31, 14.70 and 17.60 (**Chapter 5, Section 5.5.1**). The species distribution plot, constructed from our constants using the computer program HYSS,[137] is given in **Figure 3.22** for the pH-metric speciation involved for L in the aqueous phase.

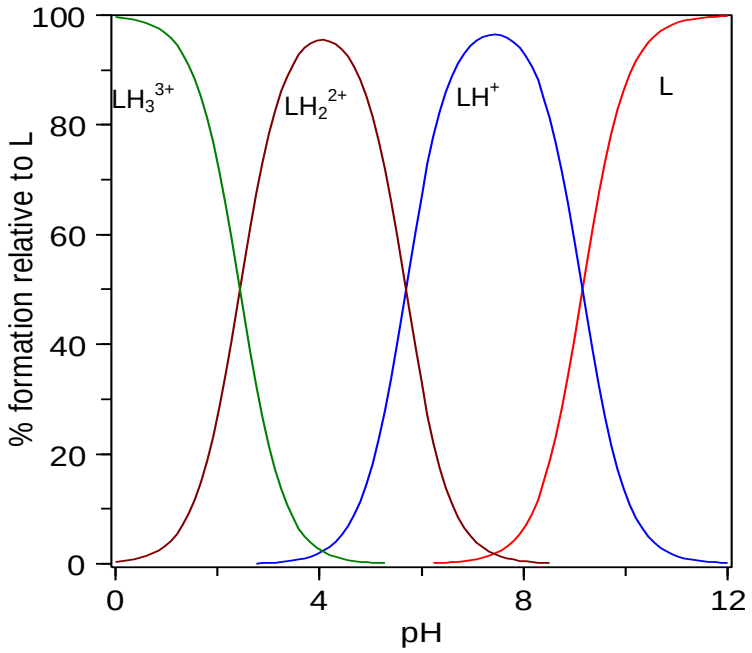

Figure 3.22: Protonation species distribution diagram for *bis*((1*H*-benzimidazol-2-yl)methyl)amine (BNNN, L)

The chelating agent (L) must distribute between the organic and aqueous phases to effect coordination in the aqueous phase, and that distribution coefficient is represented by K_D(L):

$$(L)_a \rightleftharpoons (L)_o \quad \text{and} \quad K_D(L) = \frac{[L]o}{[L]a} \tag{23}$$

However, in the aqueous phase the following three protonation equilibria may exist depending on pH:

$$LH_3^{3+} \rightleftharpoons H^+ + LH_2^{2+}, K_{a1} = \frac{[H^+]_a[LH_2^{2+}]_a}{[LH_3^{3+}]_a} \tag{24}$$

$$LH_2^{2+} \rightleftharpoons H^+ + LH^+, K_{a2} = \frac{[H^+]_a[LH^+]_a}{[LH_2^{2+}]_a} \tag{25}$$

$LH^+ \rightleftharpoons H^+ + L$, and $K_{a3} = \frac{[H^+]_a[L]_a}{[LH^+]_a}$ (26)

Then, the metal ion chelates react with the neutral ligand to form a cationic complex:

$M^{n+} + mL \rightleftharpoons ML_m{}^{n+}$ and $K_f = \frac{[ML_m{}^{n+}]_a}{[M^{n+}]_a\,[L]_a^m}$ (27)

It must be borne in mind, however, that the metal ion will replace proton(s) in the pH ranges under investigation but the protonation equilibria will accommodate this in the mathematical treatment. For example, $LH_3{}^{3+}$ and $LH_2{}^{2+}$ are most dominant in the pH range under investigation (**Figure 3.22**). Finally, the chelate which is ion-paired by an anion (in our case two sulfonate anions represented by X^{n-}) to form an extractible species, $[ML_m]X$, distributes itself between the organic and aqueous phases:

$(ML_m{}^{n+})_a + (X^{n-})_{o/a} \rightleftharpoons (ML_mX)_o$, and $K_D(ML_m{}^{n+}) = \frac{[ML_mX]o}{[ML_m{}^{n+}]a}$ (28)

The distribution ratio (D), defined as the ratio of the concentration of the total metal species in the organic phase to that in the aqueous (regardless of its mode), is given by expression 29, on the assumption that the metal chelate distributes largely in the organic phase and that the metal ion does not hydrolyse in the aqueous phase.

$D \approx \frac{[ML_mX]_o}{[M^{n+}]_a}$ (29)

Substituting **Equations 28** and **27** respectively into **Equation 29** yields **Equation 30**, depicting the formation constant and the concentration of the ligand in the aqueous phase as important parameters as well as the distribution coefficient of the chelate:

$$D = K_D(ML_m^{n+})\, K_f\, [L]_a^m \quad (30)$$

Equation 30 can be transformed to **Equation 31** if **Equation 23** is substituted into **Equation 30**, indicating that the concentration of L in the aqueous phase is dependent on its concentration in the organic phase and that its distribution between the two phases affects the distribution ratio of the complex formed:

$$D = \frac{K_D(ML_m^{n+})\, K_f}{K_D(L)^m}\, [L]_o^m \quad (31)$$

However, since the extractions are carried out at low pH, it is necessary to consider the two protonation equilibria (**Equations 24** and **25**) which dominate in the pH range under investigation and the free ligand (**Figure 3.22**), and competition of metal ions with protons for the ligand occurs early with pH due to the higher formation constants[91] compared with protonation constants thereby resulting in release of the protons from the ligand. Now, substituting **Equation 26**, and **Equations 25** and **26**, respectively, into **Equation 30** yields the following respective **Equations** (**32** and **33**):

$$D = K_D(ML_m^{n+})\, K_f\, K_{a3}{}^m\, \frac{[LH^+]_a^m}{[H^+]_a^m} \quad (32)$$

and $D = K_D(ML_m^{n+})\, K_f\, K_{a3}{}^m K_{a2}{}^m \frac{[LH_2^{2+}]_a^m}{[H^+]_a^{2m}}$ (33)

$D = K_D(ML_m^{n+})\, K_f\, K_{a3}{}^m K_{a2}{}^m K_{a1} \frac{[LH_3^{3+}]^m}{[H^+]_a^{3m}}$ (34)

Therefore, in the pH range where only one protonation equilibrium (**Equation 26**) is involved then a plot of log D vs pH (from taking the logarithms of both sides in **Equation 32**) should yield a straight line with slope m (number of ligands bonded to the metal ion M^{n+}). But in the highly acidic region where the second proton equilibrium (**Equation 25**) is also active, then a plot of log D vs pH should yield a straight line with slope (2m) (**Equation 33**), and the same applies for **Equation 34** where the slope should be 3m.

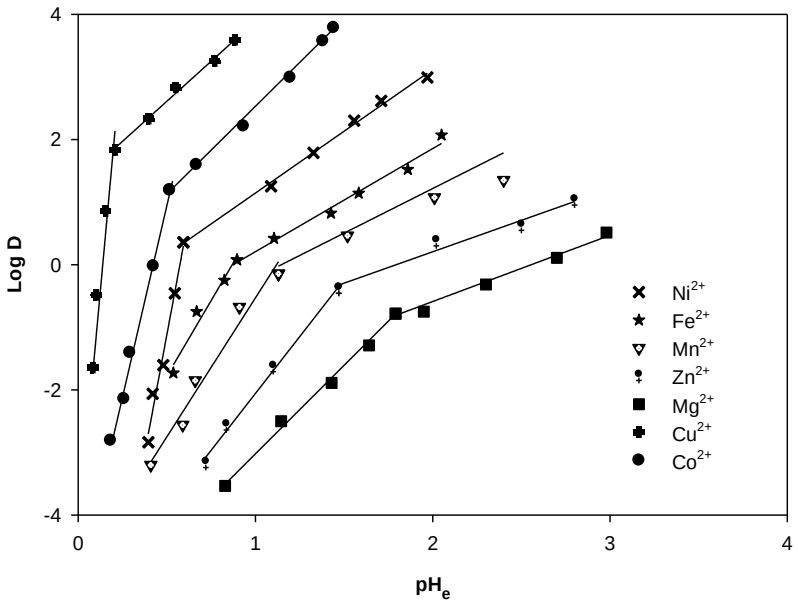

Figure 3.23: A plot of log D vs equilibrium pH (pH_e) for the extraction of 0.001 M M^{2+} (M = Mg^{2+}, Zn^{2+}, Mn^{2+}, Fe^{2+}, Ni^{2+}, Co^{2+} and Cu^{2+}) with 0.002 M BDNNN and 0.02 M DNNSA from sulfate medium

A plot of log D vs pH_e (since the extraction isotherms relate to the equilibrium condition) for this extraction system is presented in **Figure 3.23**. There is a clear change in the slope of each curve and respectively become steeper with an increase in the order of stabilization.[101] The higher pH range for Mg^{2+}, Zn^{2+}, Mn^{2+}, Fe^{2+} and Ni^{2+} is represented by a slope in the range 1 – 2 with nickel at m = 1.97 while it increases to 3–4 (≈ 2m) respectively at the lower pH range with the exception of nickel (slope = 15) which gets seriously affected by the extremely acidic medium. This observation is somewhat in agreement with the mathematical model described here for the complex equilibria systems suggesting two ligands per metal ion are involved in the coordination. These observations (as well as those discussed below) are also in line with the protonated ligand species observed in **Figure 3.22** (for the protonation equilibria).

According to our mathematical treatment (**Equation 34**), involving the third protonation equilibrium should result in a slope of 3m = 6 at the lower pH end for cobalt and copper (and to some extent nickel), however, it is much steeper with slopes of 12, 15 and 26 for cobalt, nickel and copper respectively. It is possible, however, that not only the double (slope = 2m) and the triple (slope = 3m) protonation equilibria dominate in the pH range where extractions of copper and cobalt ions occur but complex multiple protonations (*i*m, *i* = 1, 2, 3, ...) with *i* exceeding 3 from the hydrogen bonding with the rings' π electrons,[138] hence the coordination number (m) cannot be calculated accurately from data in that pH range. It seems though that a linear plot of the points (calculated at the intersections of the two lines from each metal ion extraction data) at the vertices of the two linear plots, respectively for each metal ion, gives a negative slope ≈ 1.6 which is in agreement with the coordination numbers of 2 involved for all the metal ions. A similar behaviour was observed for BONSN (**Figure 3.24**). The graph shows a negative slope ≈

1.5 which possibly indicates the coordination numbers of 2 which are involved for all the metals. This observation may be coincidental, and therefore one cannot conclude on an isolated study (i.e. with just two ligands). Once it is verified for other extraction studies, with extractants similar to the two extractants studied here, a mathematical function may be derived to link the slope to the extraction information.

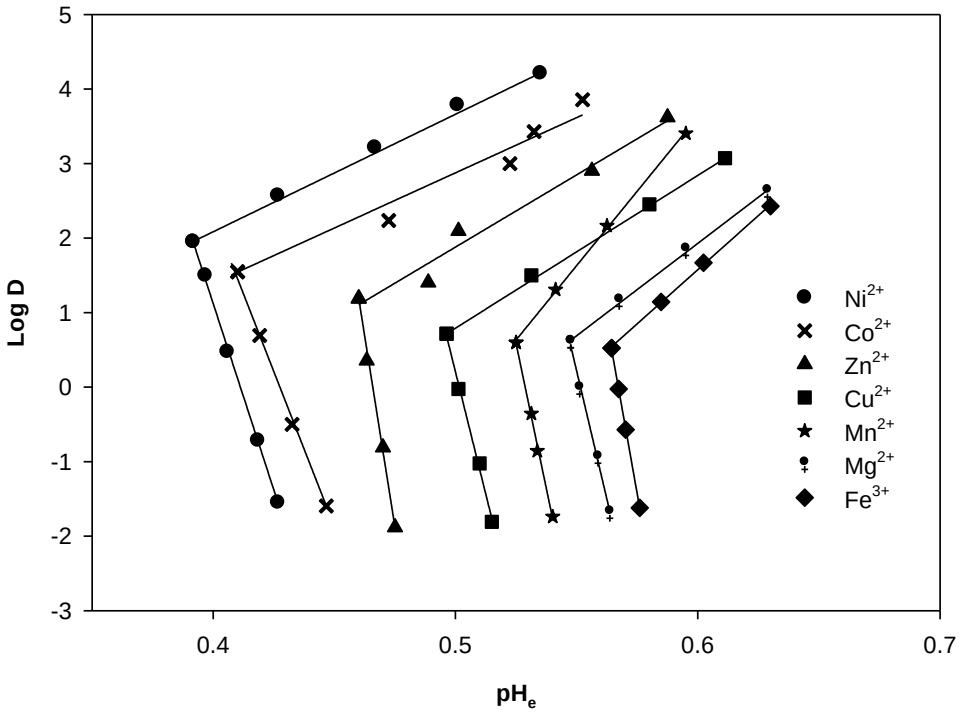

Figure 3.24: A plot of log D vs equilibrium pH (pH_e) for the extraction of 0.001 M, Ni^{2+}, Co^{2+}, Cu^{2+}, Fe^{2+}, Zn^{2+}, Mn^{2+}, Mg^{2+} and Fe^{3+} from dilute sulfate medium with BONSN (M:L ratios of 1:40), and 0.04 M DNNSA in 2-octanol/Shellsol 2325 (8:2)

3.3.2.3. Extractions with (1-alkylbenzimidazol-2-yl)-N-methylmethanamine (RBIMA)

The two tridentate systems, BONSN and BDNNN, were not able to selectively extract nickel and at the same time also extracted the hard ions, and thus a bidentate ligand system containing a benzimidazole and an aliphatic amine group, (1-alkylbenzimidazol-2-yl)-N-methylmethanamine, was designed as the alternative. The results of the extraction studies obtained from this investigation with OBIMA are shown in **Figure 3.20** and **Table 3.14**. The extraction data shows that the bidentate system selectively extracts nickel(II) from the rest of the other base metal ions in the pH above 1.2 and below 1.8 with only copper(II) as a co-extracted metal ion. The hard ions, Mn^{2+} and Fe^{3+}, were only extracted mildly at pH above 3. This result is very similar with what has been observed in our research group and presented by Okewole *et al.* using 1-octyl-2,2'-pyridylimidazole as an extractant (**Figure 3.26**).[53] The coordination of water molecules onto divalent metal ion is known to results into a less extractable complex. The coordination chemistry studies (**Section 4.3.3**) of the bidentate ligand (BIMA) and divalent metal ions confirmed the presence of coordinated water molecule(s) to Cu^{2+} and Co^{2+} hence the complexes were not readily extractable. In the case of cobalt, the coordination chemistry studies confirmed two water molecules attached onto the cobalt(II) complex ($[Co(BIMA)_2(H_2O)_2]^{2+}$). The possible six-coordination of the cobalt complex and the coordination of water molecules in addition to BIMA ligands may suggest the reason for the inextractibility of the cobalt complex in the range where nickel(II) complex extracts as a *bis*-coordinated complex that is not aquated. The Cu^{2+} anomaly is also explained similarly by the formation of the aquated $[Cu(BIMA)_2(H_2O)_2]^{2+}$ complex (**Chapter 4**).

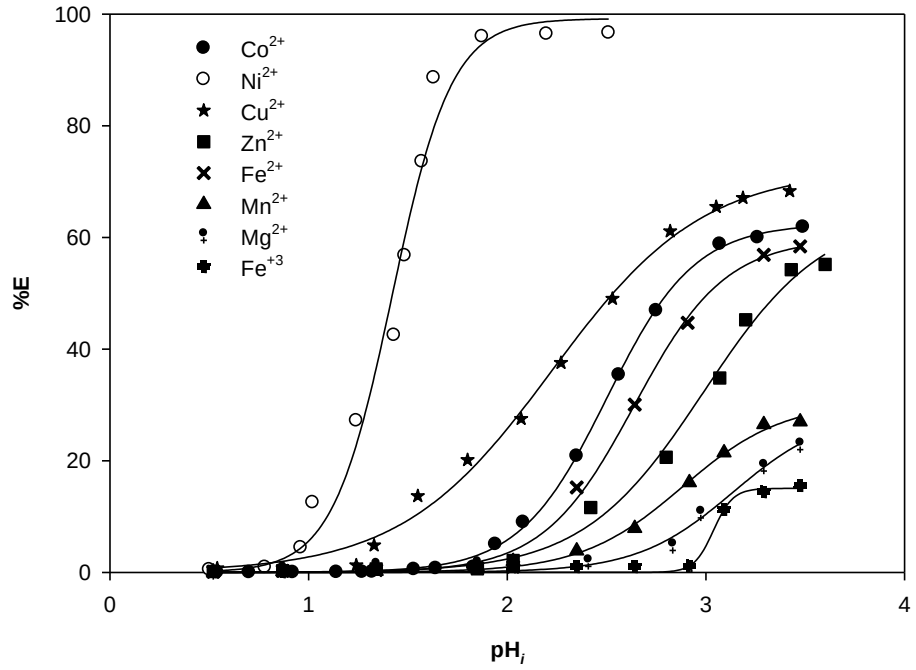

Figure 3.25: A plot of %E vs initial pH of equimolar concentrations (0.001 M) of Mg^{2+}, Mn^{2+}, Fe^{3+}, Fe^{2+}, Co^{2+}, Ni^{2+}, Cu^{2+} and Zn^{2+}, extracted with OBIMA (at M:L ratio 1:40) and 0.02 M DNNSA in 2-octanol/Shellsol 2325 (8:2) from a dilute sulfate medium

Table 3.14: A plot of %E vs initial pH in the separation of 0.001 M, Ni^{2+},Co^{2+}, Cu^{2+},Fe^{2+}, Zn^{2+}, Mn^{2+}, Mg^{2+} and Fe^{3+} from dilute sulfate medium with OBIMA (M:L ratios of 1:40), and 0.0 M DNNSA in 2-octanol/Shellsol 2325 (8:2)

Ni^{2+}								
pH_i	0.50	0.96	1.24	1.57	1.63	1.87	2.20	2.5
pH_e	0.59	0.98	1.17	1.39	1.41	1.64	2.19	2.15
% E	0.51	4.46	27.18	73.59	88.63	96.00	96.46	96.63
Co^{2+}								
pH_i	0.54	0.92	1.27	1.53	2.08	2.56	3.07	3.49
pH_e	0.51	0.97	1.13	1.47	1.73	2.32	2.71	2.92
% E	0.00	0.09	0.07	0.54	9.00	35.38	58.81	61.88
Cu^{2+}								
pH_i	0.54	1.24	1.55	2.07	2.27	2.53	3.05	3.42
pH_e	0.51	1.19	1.36	1.89	2.04	2.23	2.86	2.91
% E	0.74	1.27	13.67	27.51	49.02	61.10	67.06	68.30
Zn^{2+}								
pH_i	0.52	0.87	1.85	2.03	2.42	2.80	3.07	3.60
pH_e	0.55	0.89	1.74	1.97	2.17	2.23	2.73	2.88
% E	0.17	0.29	0.64	2.13	11.61	20.63	34.82	55.15
Mn^{2+}								
pH_i	0.52	0.87	1.85	2.03	2.35	2.92	3.29	3.47
pH_e	0.56	0.92	1.76	1.96	2.09	2.65	2.77	2.61
% E	0.10	0.18	0.90	2.00	3.86	16.09	26.51	27.00
Mg^{2+}								
pH_i	0.52	0.87	1.85	2.03	2.41	2.98	3.29	3.47
pH_e	0.56	0.91	1.64	1.87	2.25	2.62	2.98	2.76
% E	0.12	0.67	1.58	1.84	1.94	10.61	19.01	22.84
Fe^{3+}								
pH_i	0.52	0.87	1.85	2.03	2.35	2.92	3.29	3.47
pH_e	0.56	0.83	1.97	1.96	2.01	2.64	2.81	2.97
% E	0.08	0.09	0.85	0.94	0.98	1.10	14.43	15.54

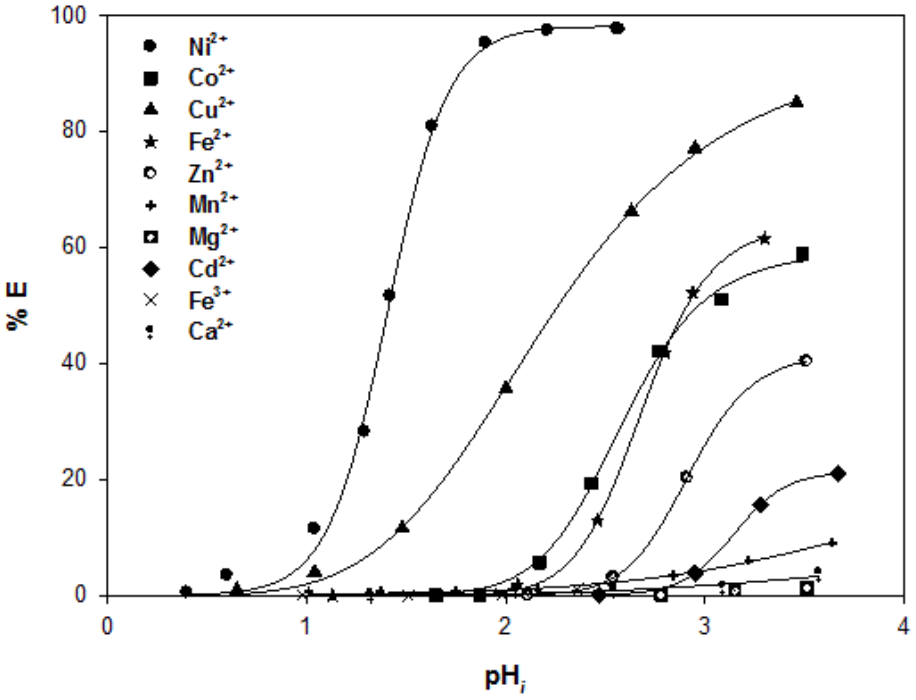

Figure 3.26: A plot of %E vs initial pH of equimolar concentration (0.001 M) of Ni^{2+}, Co^{2+}, Cu^{2+}, Fe^{2+}, Zn^{2+}, Fe^{3+}, Mn^{2+}, Mg^{2+}, Cd^{2+}, and Ca^{2+} extracted with OPIM (at M:L ratio of 1:25) and 0.015 M DNNSA in 2-octanol/Shellsol 2325 (8:2) from dilute sulfate medium[53]

The coordination chemistry studies as well as the quantitative treatment of the extraction data for 2,2'-pyridylimidazole[53] suggested *bis*-coordination of the bidentate ligand. A plot of log D vs pH_i for the extraction with OBIMA **(Figure 3.27)** also suggested similar coordination numbers for this ligand. It therefore appears that the coordination chemistry behavior of these two bidentate ligands with base metal ions is similar. Further work has been discussed (**Chapter 4**) with respect to the coordination chemistry of this new bidentate ligand, (1*H*-benzimidazol-2-yl)-*N*-methylmethanamine, through the isolation and characterization of the solid state complexes.

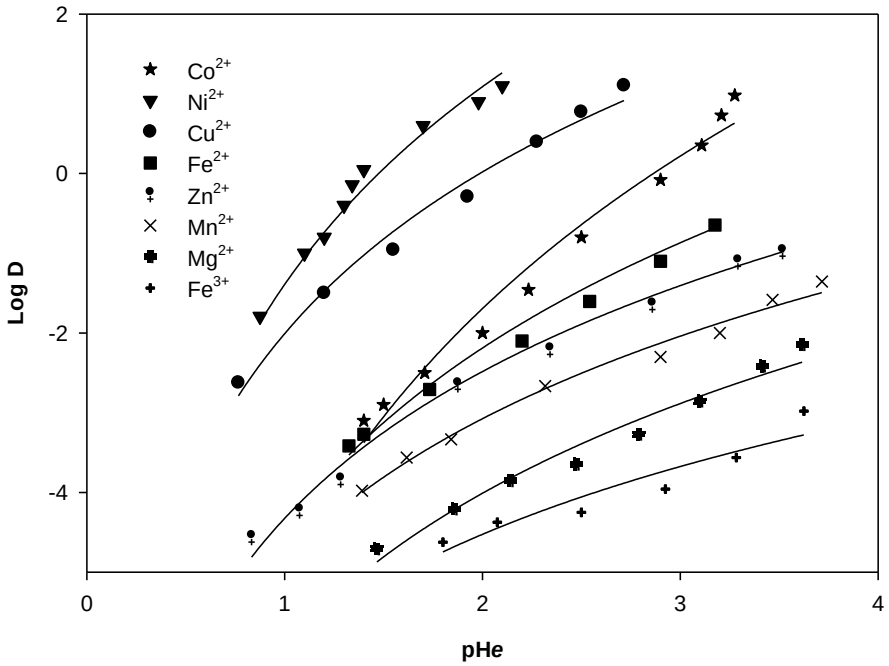

Figure 3.27: A plot of log D vs equilibrium pH for the extraction of 0.001 M Mg^{2+}, Mn^{2+}, Fe^{3+}, Fe^{2+}, Co^{2+}, Ni^{2+}, Cu^{2+} and Zn^{2+} with OBIMA (M-L = 1:40) and 0.02 M DNNSA from sulfate medium

3.4. Conclusions

The combination of two low pK_a aromatic nitrogenous groups of benzimidazole with a strong aliphatic amine or sulfur atom in the design of tridentate extractants, resulted in extraction curves that are pushed deep as a function of pH possibly due to the high complex formation constants of tridentate coordination and the relatively low protonation constants of the benzimidazole groups. This may compromise the stripping of the metal ions from the loaded organic phase through pH adjustment to lower pH. The Fe(III) rejection ability of these tridentate ligands in the range where the other later 3-d metal ions extract is remarkable. The quantitative treatment of the extraction data suggested that each of the metal ions react with two ligands, possibly tridentately.

It can be concluded that the exploitation of the subtle stereochemical aspects of coordination for the extraction of base metals is lacking with tridentate ligands (at least those of the nature presented here). This led to a consideration of the evaluation of a bidentate derivative, (1-octylbenzimidazol-2-yl)-*N*-methylmethanamine, as a potential extractant of base metal ions. This extractant was proven at separating nickel(II) from other base metals from an acidic sulfate medium in the presence of the hard ions which were rejected by this nitrogenous ligand in the range of extraction of nickel with only copper as a possible co-extracting metal ion albeit in lower quantities. Most interesting is the ability of this extractant to reject ferric ions, thus providing a shortened route for the recovery of nickel in acidic solutions without the need to precipitate ferric ions. This new bidentate extractant seems to behave in a similar manner as 2,2'-pyridylimidazole which has been studied in detail in our laboratory.[53] It is, however, desirable to study the coordination chemistry of this extractant through the isolation of solid state complexes formed with base metals (**Chapter 4**).

CHAPTER 4

4. COORDINATION CHEMISTRY

4.1 Overview

In an attempt to gain insight into the nature of the extracted complex species, the solid state complexes of *bis*((1*H*-benzimidazol-2-yl)methyl)sulfide (BNSN), *bis*((1*H*-benzimidazol-2-yl)methyl)amine (BNNN) and (1*H*- benzimidazol-2-yl)-*N*-methylmethanamine (BIMA) as the coordinating ligands to the metal ions Ni^{2+}, Co^{2+}, Cu^{2+}, Zn^{2+}, Mn^{2+} and Mg^{2+} were prepared and isolated. The nature of these complexes was determined by the usual characterization techniques such as infrared spectroscopy, electronic spectroscopy, conductivity measurements and single crystal X-ray diffraction. In view of the important role played by the coordinating ligands in a solvent extraction system for metal ion separation, it is desirable to understand the nature of compounds formed between extracting ligands and metal ions. It must be emphasized again that the alkyl groups on the extractants would be positioned away from the coordination sphere and therefore not change the coordination patterns hence the non-alkylated ligands were used for the isolation of the complexes.

The complex formation is classified based on two categories, namely chelate extraction system and ion association extraction system. The chelate system involves the formation of neutral complexes by ionisable ligands, while the ion association system involves the formation of either cationic complexes through the use of neutral ligands or anionic complexes through the use of anionic ligands which would then respectively be ion-paired by ions of opposite charge. The ligands (extractants) used in this study are neutral (since the NH of the benzimidazole has a very

high pKa) and therefore formation of cationic complexes is expected hence the use of dinonylnaphthalene sulfonic acid (DNNSA) as a counterion in the extraction studies presented in **Chapter 3**. But for the complexation studies a smaller sulfonate ion, toluene-4-sulfonate, was used instead of the bulky DNNSA ion. It would be hoped that separation could be achieved through formation of different geometries of the metal ion complexes since different metal ions show relative stabilization in different stereochemical environments.

The extraction of the metal chelate is described by the chelate reaction that occurs when an aqueous phase containing a metal ion is contacted with an organic phase containing the extractant. The steps leading to the extraction have been presented in **Chapter 3** (**Equations 23** to **34**). The distribution ratio (D) was presented by **Equation 34**, as follows:

$$D = K_D(ML_m^{n+})\, K_f\, K_{a3}{}^m K_{a2}{}^m K_{a1} \frac{[LH_3{}^{3+}]^m}{[H^+]_a^{3m}} \qquad (34)$$

The separation factor (β), which is equal to the ratio of the distribution ratios of the two metal chelates formed (in a competitive environment) with an extractant (L), can be predicted from **Equation 34**. Since only K_f and K_D (ML_m^{n+}) will be a function of the metal ion, then in cases where m (number of ligands bonded) is the same for both M-to-L reactions, then

$$\beta = \frac{D_1}{D_2} = \frac{K_{f1}\, K_D}{K_{f2}\, K_D} \frac{(M_1L_m^{n+})}{(M_2L_m^{n+})} \qquad (35)$$

The separation efficiency will, therefore, depend on the relative formation constants and on the relative solubilities of the chelates and is not pH dependent under these conditions. However,

when the number of the ligands coordinated with the metal ions differ, i.e. m ligands for metal ion 1 and *l* ligands for metal ion 2, then

$$\beta = \frac{[K_D](ML_m^{n+})K_{f1}[K_{a2}^{m-l}]K_{a1}^{m-l}}{[K_D](ML_m^{n+})K_{f2}} \cdot \frac{[LH_3{}^{3+}]_a^{m-l}}{[H^+]_a^{3m-3l}} \qquad (36)$$

Therefore, the separation efficiency is dependent not only on the relative formation constants and solubilities of the complexes but also on the pH and ligand concentration. This, therefore, illustrates that if different geometries of complexes are formed then it is possible to separate the complexes through pH tuning and varying ligand concentration as has been demonstrated in Chapter 3. This property is termed stereochemical "tailor making".[71] It must be acknowledged, however, that the isolated solid-state complexes between metal ions and the ligands may not be completely representative of the complex reaction equilibria that operate in the extraction system. However, on the basis of the metal ions having a defined preference for a particular ligand the chemistry observed in the solid-state studies (stereochemical aspects) may be dominant to some extent (despite the complex equilibria) since excess extractant amounts are used in the extraction studies. It is possible, therefore, that the subtle coordination chemistry of the isolated complexes can be inferred to the extraction isotherms observed in **Chapter 3**.

For instance nickel(II) forms the most stable spin-free octahedral (O_h) complexes of all base metal ions.[69] Therefore, to achieve nickel specificity, it is important for the ligand to force six-coordination. Copper(II), on the other hand, forms stable tetrahedral (T_d) and square planar complexes while octahedral complexes are less common.[139] Cobalt(II) and zinc(II) also tend to form more stable T_d complexes compared with O_h complexes. These subtle stereochemical

factors can be exploited when designing extractants for separation of base metals. The tridentate ligands used in this study were intended to achieve six-coordination for nickel(II) through *bis*-coordination while other metal ions adopt other preferred geometries. Another possible route for the stabilization of nickel(II) is through formation of the diamagnetic square planar complexes [69] hence the involvement of bidentate ligands with mild σ-donor and good pi-acceptor capability, in thus development of amine extractants.

With regard to chelate stability, the order of the stability of a number of metal ions is known to be fairly independent of the nature of the chelating reagent employed. Mellor and Maley list the following stability sequence for bivalent metal ions. Pd > Cu > Ni > Pb > Co > Zn > Cd > Fe > Mn > Mg.[140] For high spin octahedral metal complexes, Irving and Williams suggested, for a given ligand, that the stability of the divalent metal ions to be in the order: $Ba^{2+} < Sr^{2+} < Ca^{2+} < Mg^{2+} < Mn^{2+} < Fe^{2+} < Co^{2+} < Ni^{2+} < Cu^{2+} > Zn^{2+}$.[101] This is essentially due to decreasing ionic size as one moves across the 3d period, and in the case of the transition metal ions, also ligand field effects. In the case of Cu(II), its position is considered out-of-line with predictions based on Crystal Field Theory and is due to the consequence of the fact that Cu(II) often forms distorted octahedral complexes which are Jahn-Teller distorted.[101]

In the light of the above, the stereochemistry of inorganic elements is a very important parameter for a successful operation of extractants. In developing separating agents having greater nickel(II) specificity it is advantageous to have insight on the basic coordination chemistry of nickel(II) and other metal ions from which it should be separated. Herein, we describe the coordination chemistry of the ligands *bis*((1*H*-benzimidazol-2-yl)methyl)sulfide (BNSN),

bis((1*H*-benzimidazol-2-yl)methyl)amine (BNNN) and (1*H*-benzimidazol-2-yl)-*N*-methylmethanamine (BIMA) with base metal ions. Both the sulfate and sulfonate complexes were prepared in order to elucidate the nature of these anions respectively with respect to their innocence to coordination, and the full structural analyses are presented and discussed in **Sections 4.2.3 and 4.3**. Both the sulfate and sulfonate complexes were prepared since the extraction studies were carried out in a sulfate medium and a bulky sulfonate anion was also used to replace the sulfate ion.

4.2. Syntheses of metal complexes

4.2.1. Preparation of metal sulfonate salts, $M(RSO_3)_2{\cdot}6H_2O$ (M= Co, Ni, Cu and Zn)

A solution of toluene-4-sulfonic acid (RSO_3H) (10 mmol) was mixed with equimolar potassium hydroxide (10 mmol) in absolute ethanol to produce toluene-4-sulfonate salt (**Equation 37**) which was filtered and left to dry at room temperature.

$$RSO_3H + KOH \rightarrow K^+ RSO_3^- + H_2O(R = \text{toluene}) \quad (37)$$

$$2K^+ RSO_3^- + M(ClO_4)_2 \rightarrow M(RSO_3)_2 + 2KClO_4(s) \quad (38)$$

To potassium toluene-4-sulfonate (2 mmol) was added $M(ClO_4)_2{\cdot}6H_2O$ (1 mmol) dissolved in 30 mL absolute ethanol (**Equation 38**), after which, the potassium perchlorate salt was removed by centrifugation and filtration. The metal sulfonate salts were purified by slow recrystallization in acetone to form crystals. The analytical data for the metal(II)-toluene-4-sulfonates is presented below.

$Co(RSO_3)_2 \cdot 6H_2O$: Color: orange. Yield = 78%, M.p., 245–246 °C. Anal. Calcd for $C_{14}H_{26}CoO_{12}S_2$ (%): C, 33.01; H, 5.14; S, 12.59. Found: C, 33.00; H, 5.06; S, 12.53. IR (cm^{-1}): 1000–1250 $\nu_3(SO_3)$.

$Ni(RSO_3)_2 \cdot 6H_2O$: Color: light green. Yield = 75%, M.p., 245–246 °C. Anal. Calcd for $C_{14}H_{26}NiO_{12}S_2$ (%): C, 33.02; H, 5.15; S, 12.59. Found: C, 32.96; H, 5.10; S, 12.51. IR (cm^{-1}): 1000–1250 $\nu_3(SO_3)$.

$Cu(RSO_3)_2 \cdot 6H_2O$: Color: Light blue Yield = 82%, M.p., 245–246 °C. Anal. Calcd for $C_{14}H_{26}CuO_{12}S_2$ (%): C, 32.71; H, 5.10; S, 12.48. Found: C, 32.70; H, 5.10; S, 12.42. IR (cm^{-1}): 1000–1250 $\nu_3(SO_3)$.

$Zn(RSO_3)_2 \cdot 6H_2O$: Color: white. Yield = 79%, M.p., 245–246 °C. Anal. Calcd for $C_{14}H_{26}ZnO_{12}S_2$ (%): C, 32.60; H, 5.08; S, 12.43. Found: C, 32.54; H, 5.05; S, 12.63. IR (cm^{-1}): 1000–1250 $\nu_3(SO_3)$.

4.2.2. Preparation of sulfate and sulfonate complexes

All reactions for the preparation of coordination complexes (sulfonate and sulfate compounds) were conducted in absolute ethanol and under inert conditions. Hot ethanolic solution (10 mL at 60°C) containing 2 mmol of the ligand was added dropwise to 10 mL of the metal ion solution (1 mmol, respectively, for each metal ion). The mixture was heated at reflux overnight under a nitrogen atmosphere and the precipitate was filtered off and washed with ethanol.

4.2.2.1. Complexes of bis((1H-benzimidazol-2-yl)methyl)sulfide (BNSN)

4.2.2.1.1. Sulfate complexes

$[Co(BNSN)_2]SO_4 5H_2O$: Color: mauve. Yield = 57%, M.p., 242–243 °C. Anal. Calcd for $C_{32}H_{38}N_8CoO_9S_3$ (%): C, 46.09; H, 4.59; N, 13.44; S, 11.54. Found: C, 46.13; H, 4.68; N, 13.52; S, 11.79. IR (cm^{-1}): 3191 ν(N–H), 1547 ν(C=N), 1068–1095 $\nu_3(SO_4)$, 349 ν(M–N), 244 ν(M–S). Conductivity (10^{-3} M, $ohm^{-1}.cm^2.mole^{-1}$): 68.

$[Ni(BNSN)_2]SO_4 \cdot 4H_2O$: Color: pink. Yield = 48%, M.p., 245–246 °C. Anal. Calcd for $C_{32}H_{36}N_8NiO_8S_3$ (%): C, 47.13; H, 4.45; N, 13.74; S, 11.79. Found: C, 47.07; H, 4.17; N, 13.72; S, 11.99. IR (cm^{-1}): 3189 ν(N–H), 1545 ν(C=N), 1064–1090 $\nu_3(SO_4)$, 348 ν(M–N), 250 ν(M–S). Conductivity (10^{-3} M, $ohm^{-1}.cm^2.mole^{-1}$): 71.

$[Cu(BNSN)_2]SO_4 \cdot 4H_2O$: Color: green. Yield = 64%, M.p., 248–249 °C. Anal. Calcd for $C_{32}H_{36}N_8CuO_8S_3$ (%): C, 46.85; H, 4.42; N, 13.66; S, 11.73. Found: C, 46.79; H, 4.17; N, 13.25; S, 11.67. IR (cm^{-1}): 3186 ν(N–H), 1545 ν(C=N), 1060–1088 $\nu_3(SO_4)$, 340 ν(M–N), 243 ν(M–S). Conductivity (10^{-3} M, $ohm^{-1}.cm^2.mole^{-1}$): 74.

$[Zn(BNSN)_2]SO_4 \cdot 2H_2O$: Color: white. Yield = 52%, M.p., 249–252 °C. Anal. Calcd for $C_{32}H_{32}N_8ZnO_6S_3$ (%): C, 48.88; H, 4.10; N, 14.25; S, 12.23. Found: C, 48.98; H, 4.15; N, 14.35; S, 12.27. IR (cm^{-1}): 3187 ν(N–H), 1545 ν(C=N), 1060–1080 $\nu_3(SO_4)$, 338 ν(M–N), 296 ν(M–S). Conductivity (10^{-3} M, $ohm^{-1}.cm^2.mole^{-1}$): 85.

$[Mg(BNSN)_2]SO_4 \cdot 2H_2O$: Color: white. Yield = 54%, M.p., 248–249 °C. Anal. Calcd for $C_{32}H_{32}N_8MgO_6S_3$ (%): C, 51.57; H, 4.34; N, 15.04; S, 12.91. Found: C, 51.60; H, 4.38; N, 15.07; S, 12.88. IR (cm^{-1}): 3186 ν(N–H), 1545 ν(C=N), 1061–1086 $\nu_3(SO_4)$, 306 ν(M–N), 406 ν(M–S). Conductivity (10^{-3} M, $ohm^{-1}.cm^2.mole^{-1}$): 82.

$[Mn(BNSN)_2]SO_4 \cdot 2H_2O$: Color: white. Yield = 58%, M.p., 253–254 °C. Anal. Calcd for $C_{32}H_{32}N_8MnO_6S_3$ (%): C, 49.53; H, 4.17; N, 14.45; S, 12.4. Found: C, 49.87; H, 4.20; N, 14.49; S, 12.42. IR (cm^{-1}): 3180 ν(N–H), 1538 ν(C=N), 1061–1089 $\nu_3(SO_4)$, 323 ν(M–N), 384 ν(M–S). Conductivity (10^{-3} M, $ohm^{-1}.cm^2.mole^{-1}$): 79

4.2.2.1.2. Sulfonate complexes

$[Co(BNSN)_2](RSO_3)_2 \cdot 4H_2O$: Color: orange. Yield = 59%, M.p., 263–264°C. Anal. Calcd for $C_{46}H_{50}N_8CoO_{10}S_4$ (%): C, 52.02; H, 4.74; N, 10.55; S, 12.08. Found: C, 52.09; H, 4.83; N, 10.75; S, 12.11. IR (cm^{-1}): 3410 ν(N–H), 1542 ν(C=N), 1167 $\nu_3(SO_3)$, 399 ν(M–N), 319 ν(M–S). Conductivity (10^{-3} M, $ohm^{-1}.cm^2.mole^{-1}$): 131.

$[Ni(BNSN)_2](RSO_3)_2 2H_2O$: Color: pink. Yield = 48%, M.p., 266–268 °C. Anal. Calcd for $C_{46}H_{46}N_8NiO_8S_4$ (%): C, 53.86; H, 4.52; N, 10.92; S, 12.48. Found: C, 53.98; H, 4.54; N, 10.96; S, 12.11. IR (cm^{-1}): 3412 ν(N–H), 1542 ν(C=N), 1165 $\nu_3(SO_4)$, 396 ν(M–N), 314 ν(M–S). Conductivity (10-3 M, $ohm^{-1}.cm^2.mole^{-1}$): 134.

$[Cu(BNSN)_2](RSO_3)_2 4H_2O$: Color: green. Yield = 43%, M.p., 211–212 °C. Anal. Calcd for $C_{46}H_{50}N_8CuO_{10}S_4$ (%): C, 51.79; H, 4.72; N, 10.50; S, 12.02. Found: C, 51.84; H, 4.96; N,

10.92; S, 12.51. IR (cm^{-1}): 3413 ν(N–H), 1539 ν(C=N), 1161 $\nu_3(SO_4)$, 392 ν(M–N), 336 ν(M–S). Conductivity (10^{-3} M, $ohm^{-1}.cm^2.mole^{-1}$): 138.

$[Zn(BNSN)_2](RSO_3)_2 4H_2O$: Color: white. Yield = 62%, M.p., 213–214 °C. Anal. Calcd for $C_{46}H_{50}N_8ZnO_{10}S_4$ (%): C, 51.70; H, 4.72; N, 10.49; S, 12.00. Found: C, 51.75; H, 4.79; N, 10.54; S, 12.08. IR (cm^{-1}): 3392 ν(N–H), 1535 ν(C=N), 1180 $\nu_3(SO_4)$, 399 ν(M–N), 332 ν(M–S). Conductivity (10^{-3} M, $ohm^{-1}.cm^2.mole^{-1}$): 141.

4.2.2.2. Complexes of bis((1-alkylbenzimidazol-2-yl)methyl)amine (BNNN)

4.2.2.2.1. Sulfate complexes

$[Co(BNNN)_2]SO_4 \cdot 4H_2O$: Color: pink. Yield = 51%, M.p., 252-254ºC. Anal. Calcd. for $C_{32}H_{38}N_{10}CoO_8S$ (%):C, 49.17; H, 4.90; N, 17.92; S, 4.10. Found: C, 49.20; H, 4.46; N, 17.85; S, 4.86. IR (cm^{-1}): 3242 ν(N-H), 1545 ν(C=N), 1037 $\nu_3(SO_4)$, 226 ν(M-N). Conductivity (10^{-3} M, $ohm^{-1}.cm^2.mole^{-1}$): 66.

$[Ni(BNNN)_2]SO_4 \cdot 3H_2O$: Color: mauve. Yield = 57%, M.p., 253-255ºC. Anal. Calcd. for $C_{32}H_{36}N_{10}NiO_7S$ (%): C, 50.34; H, 4.75; N, 18.35; S, 4.20. Found: C, 50.64; H, 4.74; N, 18.28; S, 4.10. IR (cm^{-1}): 3234 ν(N-H), 1538 ν(C=N), 1037 $\nu_3(SO_4)$, 230 ν(M-N). Conductivity (10^{-3} M, $ohm^{-1}.cm^2.mole^{-1}$): 69.

$[Cu(BNNN)_2]SO_4 \cdot 7H_2O$: Color: green. Yield = 65%, M.p., 228-229ºC. Anal. Calcd. for $C_{32}H_{44}N_{10}CuO_{11}S$ (%): C, 45.74; H, 5.28; N, 16.67; S, 3.82. Found: C, 45.81; H, 5.11; N, 16.41;

S, 3.44. IR (cm^{-1}): 3233 ν(N-H), 1565 ν(C=N), 1060-1088 $\nu_3(SO_4)$, 224 ν(M-N). Conductivity (10^{-3} M, $ohm^{-1}.cm^2.mole^{-1}$): 71.

$[Zn(BNNN)_2]SO_4 \cdot 11H_2O$: Color: white. Yield = 64%, M.p., 221-222ºC. Anal.Calcd. for $C_{32}H_{52}N_{10}ZnO_{15}S$ (%): C, 42.04; H, 5.73; N, 15.31; S, 3.51. Found: C, 41.96; H, 5.71; N, 15.00; S, 3.59. IR (cm^{-1}): 3227 ν(N-H), 1548 ν(C=N), 1037 $\nu_3(SO_4)$, 222 ν(M-N). Conductivity (10^{-3} M, $ohm^{-1}.cm^2.mole^{-1}$): 82.

$[Mg(BNNN)_2]SO_4 \cdot 2H_2O$: Color: white. Yield = 58%, m.p., 251–252 °C. Anal. Calcd. For $C_{32}H_{40}N_{10}MgO_{10}S$ (%): C, 50.32; H, 5.28; N, 18.31; S, 4.19. Found: C, 50.46; H, 5.25; N, 18.53; S, 4.21. IR (cm^{-1}): 3285 ν(N–H), 1546 ν(C=N), 1037 $\nu_3(SO_4)$, 228 ν(M–N). Conductivity (10^{-3} M, $ohm^{-1}.cm^2.mole^{-1}$): 74.

$[Mn(BNNN)_2]SO_4 \cdot 5H_2O$: Color: white. Yield = 62%, M.p., 249°C–251°C. Anal. Calcd for $C_{32}H_{40}N_{10}MnO_9S$ (%): C, 48.29; H, 5.08; N, 17.60; S, 4.03. Found: C, 48.42; H, 5.09; N, 17.57; S, 4.01. IR (cm^{-1}): 3251 ν(N–H), 1543 ν(C=N), 1037 $\nu_3(SO_4)$, 228 ν(M–N),. Conductivity (10^{-3} M, $ohm^{-1}.cm^2.mole^{-1}$): 72.

4.2.2.2.2. Sulfonate complexes

$[Co(BNNN)_2](RSO_3)_2 \cdot 4H_2O \cdot 2EtOH$: Color: red. Yield = 71%, M.p., 225–226°C. Anal. Calcd. for $C_{50}H_{64}N_{10}CoO_{12}S_2$ (%): C, 53.66; H, 5.67; N, 12.52; S, 5.73. Found: C, 53.60; H, 5.34; N, 12.67; S, 5.14. IR (cm^{-1}): 3311 ν(N-H), 1551 ν(C=N), 1150-1161$\nu_3(RSO_3)$, 279 ν(M-N). Conductivity (10^{-3} M, $ohm^{-1}.cm^2.mole^{-1}$): 136.

$[Ni(BNNN)_2](RSO_3)_2 \cdot 3H_2O \cdot 2EtOH$: Color: purple. Yield = 58%, M.p., 246–248°C. Anal. Calcd. for $C50H_{62}N_{10}NiO_{11}S_2$ (%): C, 54.50; H, 5.67; N, 12.71; S, 5.82. Found: C, 54.43; H, 5.58; N, 12.47; S, 5.70. IR (cm^{-1}): 3313 ν(N-H), 1550 ν(C=N), 1151-1164 $\nu_3(RSO_3)$, 246 (ν M-N),. Conductivity (10^{-3} M, $ohm^{-1}.cm^2.mole^{-1}$): 139.

$[Cu(BNNN)_2](RSO_3)_2 \cdot 12H_2O$: Color: blue. Yield = 68%, M.p., 201–202°C. Anal. Calc. for $C_{46}H_{68}N_{10}CuO_{18}S_2$ (%): C, 46.95; H, 5.82 N, 11.90; S, 5.45. Found: C, 46.48; H, 5.47; N, 11.76; S, 5.85. IR (cm^{-1}): 3213 ν(N-H), 1550 ν(C=N), 1147-1172 $\nu_3(RSO_3)$, 262 ν(M-N). Conductivity (10^{-3} M, $ohm^{-1}.cm^2.mole^{-1}$): 141

$[Zn(BNNN)_2](RSO_3)_2 \cdot 3H_2O \cdot 2EtOH$: Color: white. Yield = 62%, M.p., 201–202°C. Anal. Calc. for $C_{50}H_{62}N_{10}ZnO_{11}S_2$ (%): C, 54.17; H, 5.64; N, 12.63; S, 5.78. Found: C, 54.50; H, 5.64; N, 12.30; S, 5.53. IR (cm^{-1}): 3304 ν(N-H), 1549 ν(C=N), 1172-1187 $\nu_3(RSO_3)$, 258 ν(M-N). Conductivity (10^{-3} M, $ohm^{-1}.cm^2.mole^{-1}$): 147

4.2.2.3. Complexes of (1*H*- benzimidazol-2-yl)-*N*-methylmethanamine *(BIMA)*

4.2.2.3.1. Sulfate complexes

$[Co(NN)_2]SO_4 \cdot 2H_2O$: Color: Pink. Yield = 52%, M.p. 321–322^oC. Anal. Calc. for $C_{18}H_{24}N_6CoO_5S$ (%): C, 43.64; H, 4.88 N, 16.96; S, 6.47. Found: C, 43.13; H, 4.30; N, 16.67; S, 6.02. IR (cm^{-1}): 3225 ν(imdN-H); 1624 ν(C=N); 1029 $\nu_3(SO_4)$; 387 ν(M-N). Conductivity (10^{-3} M, $ohm^{-1}.cm^2.mole^{-1}$): 71.

$[Ni(NN)_2]SO_4 \cdot 2H_2O$: Color: Green. Yield = 56%, M.p. 324–325^oC. Anal. Calc. for $C_{18}H_{26}N_6NiO_6S$ (%): C, 42.13; H, 5.11; N, 16.38; S, 6.25. Found: C, 42.58; H, 5.15; N, 16.42; S, 6.19. IR (cm^{-1}): 3223 ν(imdN-H); 1624 ν(C=N); 1033 $\nu_3(SO_4)$; 349 ν(M-N);. Conductivity (10^{-3} M, $ohm^{-1}.cm^2.mole^{-1}$): 79.

$[Cu(NN)_2]SO_4 \cdot 3H_2O$: Color: Blue. Yield = 51%, M.p. 241–242^oC. Anal. Calc. for $C_{18}H_{24}N_6CuO_7S$ (%): C, 40.33; H, 5.26; N, 15.68; S, 5.98. Found: C, 40.70; H, 5.17; N, 15.63; S, 5.50. IR (cm^{-1}): 3221 ν(imdN-H); 1623 ν(C=N); 1035 $\nu_3(SO_4)$; 349 ν(M-N). Conductivity (10^{-3} M, $ohm^{-1}.cm^2.mole^{-1}$): 76.

$[Zn(NN)_2]SO_4 \cdot H_2O$: Color: white.Yield = 62%, M.p. 319–320^oC. Anal. Calcd. for $C_{18}H_{24}N_6ZnO_5S$ (%): C, 43.08; H, 4.82 N, 16.75; S, 6.39. Found: C, 43.95; H, 4.80; N, 16.96; S, 6.68. IR (cm^{-1}): 3212 ν(imdN-H); 1625ν(C=N); 1036 $\nu_3(SO_4)$; 349 ν(M-N);. Conductivity (10^{-3} M, $ohm^{-1}.cm^2.mole^{-1}$): 88.

4.2.3. Preparation of single crystals, crystallographic data collection and structure determination

4.2.3.1. Preparation of bis((1H-benzimidazol-2-yl)methyl)amine tetrahydrate (BNNN.4H_2O) crystals

Single crystals for BNNN·4H_2O were obtained by several attempts of re-crystallization of the crude product of BNNN from hot 50-50 (v/v) water-methanol mixture which gave white crystals. The white crystals were further recrystallized with methanol to form white needles.

4.2.3.2. Preparation of the crystals of the complexes

Single crystals of $[Co(BNSN)_2](RSO_3)_2 \cdot 4H_2O$, $[Ni(BNSN)_2](RSO_3)_2 \cdot 2H_2O$ and $[Cu(BNNN)_2](RSO_3)_2 \cdot 12H_2O$ were obtained by slow evaporation of their ethanolic mother liquors at room temperature for about one week. Single crystals of $[Cu(pimH)_2(H_2O)]SO_4$ were obtained by recrystallization of the complex in water/ethanol and then left to evaporate slowly at room temperature for months.

4.2.3.3. X-ray methods and structure determination

X-ray diffraction studies were performed at 200 K using a Bruker Kappa Apex II diffractometer with graphite monochromated Mo Kα radiation (λ = 0.71073 Å). The crystal structures were solved by direct methods using SHELXTL.[124] All non-hydrogen atoms were refined anisotropically. Carbon-bound hydrogens were placed in calculated positions and refined as riding atoms with bond lengths 0.95 (aromatic CH), 0.99 (CH_2), and 0.98 (CH_3) Å and with Uiso(H) = 1.2 (1.5 for methyl) Ueq(C). Hydrogens bonded to nitrogen were located on a Fourier map and allowed to refine freely. Hydrogens on water were restrained to an O–H bond length of 0.84Å and H–O–H angle of 110°. However, for $[Cu(PIMH)_2(H_2O)](SO_4)$ the electron density for the solvents that crystalized with the complex was located in crystallographically special positions and made refinement impossible. It was therefore subjected to a squeeze algorithm and only the connectivity of the ligands to the metal ion was confidently refined. Diagrams and publication material were generated using SHELXTL, PLATON,[125] and ORTEP-3.[126] The crystal data for the ligand ($BNNN \cdot 4H_2O$) and complexes ($[Co(BNSN)_2](RSO_3)_2 \cdot 4H_2O$, $[Ni(NSN)_2](RSO_3)_2 \cdot 2H_2O$, $[Cu(BNNN)_2](RSO_3)_2 \cdot 12H_2O$) and $[Cu(PIMH)_2(H_2O)](SO_4)\cdot$ are given in **Tables 4.1, 4.2** and **4.3**.

Table 4.1: Selected crystallographic data for $[Co(BNSN)_2](RSO_3)_2 \cdot 4H_2O$ and $[Ni(BNSN)_2](RSO_3)_2 \cdot 2H_2O$

Compound	**$[Co(BNSN)_2](RSO_3)_2 \cdot 4H_2O$**	**$[Ni(BNSN)_2](RSO_3)_2 \cdot 2H_2O$**
Chemical Formula	$C_{32}H_{28}CoN_8S_2,2(C_7H_7O_3S),4(H_2O)$	$C_{32}H_{28}N_8NiS_2,2(C_7H_7O_3S),2(H_2O)$
Formulae weight	1062.15	1025.88
Crystal color	Red	Pink
Crystal system	Monoclinic	Triclinic
Space group	P_{21}/c	$P\bar{1}$
Temperature (K)	200	200
a (Å)	10.9513(2)	9.748(5)
b (Å)	9.5582(2)	10.568(5)
c (Å)	23.6177(5)	11.981(5)
α(º)	90	78.130(5)
β(º)	101.726(1)	76.849(5)
γ(º)	90	87.413(5)
V (Å)	2420.58(8)	1176.2(10)
Z	2	1
D_{calc} (g/cm^{-3})	1.457	1.448
μ/mm^{-1}	0.593	0.652
F(000)	1106	534
Wavelength (Å)	0.71073	0.71073
Theta Min-Max [Deg]	2.3, 28.4	1.8,28.5
S	1.03	0.92
Tot., Uniq. Data, R(int)	22584, 6047, 0.019	19058, 5797, 0.469
Observed data [I > 2.0 sigma(I)]	4946	2212
R	0.0476	0.0581
R_w	0.1367	0.1123

Table 4.2: Selected crystallographic data for $[Cu(BNNN)_2](RSO_3)_2 \cdot 12H_2O$

Compound	**$BNNN \cdot 4H_2O$**	**$[Cu(BNNN)_2](RSO_3)_2 \cdot 12H_2O$**
Chemical Formula	$C_{16}H_{23}N_5O_4$	$C_{54}H_{86}CuN_{10}O_{18}S_2$
Formulae weight	349.39	4514.66
Crystal color	white needles	blue
Crystal system	Triclinic	Tetragonal
Space group	$P\bar{1}$	$I4$
Temperature (K)	200	200
Crystal size (mm^3)	0.06 x 0.16 x 0.23	0.05 X 0.11 X 0.50
a (Å)	4.7237(2)	34.4165(11)
b (Å)	12.3565(4)	34.4165(11)
c (Å)	15.4506(6)	9.3238(4)
α(º)	77.550(2)	90
β(º)	83.024(2)	90
γ(º)	85.282(2)	90
V ($Å^3$)	872.64(6)	11044.0(9)
Z	2	2
D_{calc} (g/cm^{-3})	1.330	1.358
μ/mm^{-1}	0.098	0.545
F(000)	372	4696
Wavelength (Å)	0.71073	0.71073
Theta Min-Max (º)	1.9, 28.3	1.9, 28.3
S	0.0477	0.98
Tot., Uniq. Data, R(int)	15068, 4257, 0.037	91906, 13572, 0.095
Observed data [I > 2.0 sigma(I)]	2651	8997
R	0.0477	0.0507
R_w	0.1206	0.1218

Table 4.3: Selected crystallographic data for $[Cu(PIMH)_2 \cdot H_2O](SO_4)$

Compound	$C_{16}H_{16}CuN_6$
Chemical Formula	$C_{16}H_{16}CuN_6O$, O_4S
Formulae weight	467.79
Crystal color	Green
Crystal system	Orthorhombic
Space group	Fd^3
Temperature (K)	200
a (Å)	14.1757(8)
b (Å)	23.9801(8)
c (Å)	25.7056(15)
α(º)	90
β(º)	90
γ(º)	90
V (Å)	8738.2(8)
Z	16
D_{calc} (g/cm^{-3})	1.423
μ/mm^{-1}	1.133
F(000)	3824
Wavelength (Å)	0.71073
Theta Min-Max [Deg]	-18:18, -32:32, -34:34
Tot., Uniq. Data, R(int)	55055, 2741, 0.026
Observed data [I > 2.0 sigma(I)]	2344
R	0.0569
R_w	0.1859

4.3 Results and discussion

4.3.1. The coordination chemistry of bis((1H-benzimidazol-2-yl)methyl)sulfide (BNSN)

4.3.1.1 Preparative aspects

The complexes were prepared by reaction of two-molar equivalents of the ligand with respect to M(II)X·yH_2O, where M= Co(II), Ni(II), Cu(II), Zn(II) and (X = SO_4^{2-}) and (RSO_3^{2-}) (y=2–5), in ethanol under inert conditions. The yields and physical data are presented in **Table 4.4**.

The elemental analyses suggest [M(BNSN)$_2$]X·yH_2O (**Table 4.4**), and the involvement of two ligands in the inner coordination sphere is in agreement with what was observed in extraction studies. The molar conductivity data in DMF showed that the sulfate and sulfonate complexes have molar conductance values of 67–90 and 131–167 M, ohm^{-1}.cm^2.mole^{-1}, respectively, indicating that the sulfate complexes behaved as 1:1 electrolytes while the sulfonate complexes were 1:2 electrolytes.[141] This behavior in solution suggested non-coordinated counter-anions. Both sulfate and sulfonate complexes were prepared to elucidate the nature of these anions with respect to involvement in the inner or outer coordination sphere. This was done for both anions since the extraction studies were carried out in a sulfate medium and a bulky sulfonate was also used to replace the sulfate. This replacement was done owing to the lack of phase transferability of the sulfate complexes due to the high hydration energies of this anion.[133]

Table 4.4: The physical properties of the BNSN complexes

Compounds	Color	Mp.	Yield	Molar Conductance
BNSN	white	210-212	71	
Sulfate complexes				
$[Co(BNSN)_2]SO_4 5H_2O$	mauve	242–243	57	68
$[Ni(BNSN)_2]SO_4 \cdot 4H_2O$	pink	245–246	48	71
$[Cu(BNSN)_2]SO_4 \cdot 4H_2O$	green	248–249	64	74
$[Zn(BNSN)_2]SO_4 \cdot 2H_2O$	white	249–252	52	85
$[Mg(BNSN)_2]SO_4 \cdot 2H_2O$	white	248–249	54	72
$[Mn(BNSN)_2]SO_4 \cdot 5H_2O$	brown	253–254	58	75
Sulfonate complexes				
$[Co(BNSN)_2](RSO_3)_2 \cdot 4H_2O$	orange	263–264	59	131
$[Ni(BNSN)_2](RSO_3)_2 \cdot 2H_2O$	pink	266–262	48	134
$[Cu(BNSN)_2](RSO_3)_2 \cdot 4H_2O$	green	211–212	43	138
$[Zn(BNSN)_2](RSO_3)_2 \cdot 4H_2O$	white	213–214	62	141

Table 4.5: The elemental analysis data of the complexes

Compounds	Elemental analysis Calc. (Found) %			
	C	**H**	**N**	**S**
BNSN	61.52(61.15)	5.16(5.34)	17.93(17.97)	10.26(10.15)
Sulfate complexes				
$[Co(BNSN)_2]SO_4 5H_2O$	46.09(46.13)	4.59(4.68)	13.44 (13.52)	11.54(11.79)
$[Ni(BNSN)_2]SO_4 \cdot 4H_2O$	47.13(47.07)	4.45(4.17)	13.74(13.72)	11.79(11.99)
$[Cu(BNSN)_2]SO_4 \cdot 4H_2O$	46.85(46.79)	4.42(4.17)	13.66(13.25)	11.73(11.67)
$[Zn(BNSN)_2]SO_4 \cdot 2H_2O$	48.88(48.98)	4.10(4.15)	14.25(14.35)	12.23(12.27)
$[Mg(BNSN)_2]SO_4 \cdot 2H_2O$	50.32(50.46)	5.28(5.25)	18.31(18.53)	4.19(4.21)
$[Mn(BNSN)_2]SO_4 \cdot 5H_2O$	48.29(48.42)	5.08(5.09)	17.60(17.57)	4.03(4.01)
Sulfonate complexes				
$[Co(BNSN)_2](RSO_3)_2 \cdot 4H_2O$	52.02(52.09)	4.74(4.83)	10.55(10.75)	12.08(12.11)
$[Ni(BNSN)_2](RSO_3)_2 2H_2O$	53.86(53.98)	4.52(4.54)	10.92(10.96)	12.48(12.11)
$[Cu(BNSN)_2](RSO_3)_2 4H_2O$	51.79(51.84)	4.72(4.96)	10.50(10.92)	12.02(12.51)
$[Zn(BNSN)_2](RSO_3)_2 4H_2O$	51.70(51.75)	4.72(4.79)	10.49(10.54)	12.00(12.08)

4.3.1.2 Spectroscopic studies

In the IR spectrum of the ligand, the absorption band at 3377 cm^{-1} was attributed to the ν(N–H) (**Table 4.6**).[142] The C=N stretch of the benzimidazole ring appeared at 1534 cm^{-1}.[143,144] Upon complex formation, the band shifted to higher frequencies (1535–1550 cm^{-1}), confirming bond formation between the metal ion and nitrogen of benzimidazole. Complexation resulted in an increase in the double-bond character of C=N, perhaps due to the π-acidity of the benzimidazole ring. Far infrared spectra of the sulfate and sulfonate complexes displayed two bands between 240–336 cm^{-1} and 338–406 cm^{-1} which were assigned to ν(M–S) and ν(M–N), respectively.[145,146] A strong and broad peak at 1060–1095 cm^{-1} is present in spectra of complexes, characteristic of un-coordinated sulfate.[144,147] The infrared spectra of these complexes suggest that all three donors of the ligand are involved in coordination and that both sulfate and sulfonate are non-coordinating. The geometry of the complexes was confirmed by UV–Vis solid reflectance electronic studies as well as X-ray crystallography.

Table 4.6: The infrared spectral data for the complexes

Compounds	ν(N-H)	ν(C=N)	$\nu_3(SO_4)$	$\nu_3(SO_3)$	ν(M-N)	ν(M–S)
BNSN	3377	1534				
Sulfate complexes						
$[Co(BNSN)_2]SO_4 5H_2O$:	3191	1547	1068-1095		349	244
$[Ni(BNSN)_2]SO_4 \cdot 4H_2O$	3189	1545	1064-1090		348	250
$[Cu(BNSN)_2]SO_4 \cdot 4H_2O$	3186	1545	1060-1088		340	243
$[Zn(BNSN)_2]SO_4 \cdot 2H_2O$	3187	1545	1060-1080		338	296
$[Mg(BNSN)_2]SO_4 \cdot 2H_2O$	3186	1545	1061-1086		306	406
$[Mn(BNSN)_2]SO_4 \cdot 5H_2O$	3180	1538	1061-1089		323	384
Sulfonate complexes						
$[Co(BNSN)_2](RSO_3)_2 \cdot 4H_2O$	3410	1542		1167	399	319
$[Ni(BNSN)_2](RSO_3)_2 2H_2O$	3412	1542		1165	396	314
$[Cu(BNSN)_2](RSO_3)_2 4H_2O$	3413	1539		1161	392	336
$[Zn(BNSN)_2](RSO_3)_2 4H_2O$	3392	1535		1180	399	332

The crystal field theory predicts three d–d transitions for an octahedral Co(II) complex, $^4T_1g(F) \rightarrow {}^4T_{2g}(F)$ (ν_1), $^4T_{1g}(F) \rightarrow {}^4A_{2g}(F)$ (ν_2), and $^4T_{1g}(F) \rightarrow {}^4T_{1g}(P)$ (ν_3).[148] These absorptions were observed at 1011, 549, and 396 nm, respectively (**Figure 4.1**). For the nickel complexes, bands were observed at 978 and 549 nm which may be ascribed to $^3A_{2g}(F) \rightarrow {}^3T_{2g}(F)$ (ν_1) and $^3A_{1g}(F) \rightarrow {}^3T_{2g}(F)$ (ν_2), respectively, for an octahedral symmetry, assuming that the third transition ($^3A_{2g}(F) \rightarrow {}^3T_{1g}(P)$ (ν_3)) is masked by the intra-ligand transition. Similar complexes of nickel(II), with a distorted octahedral coordination geometry, have been obtained with four nitrogens of benzimidazole and two amine nitrogens from secondary aliphatic amine in place of sulfur.[149,150, 151] The electronic spectrum of the Cu(II) complex showed one band and a shoulder to the charge charge transfer band or intra-ligand transition at 775 and 395 nm, respectively,

which were ascribed to $^2B_{1g} \rightarrow {}^2B_{2g}$ and $^2B_{1g} \rightarrow {}^2A_{1g}$, consistent with distorted octahedral geometry.[148]

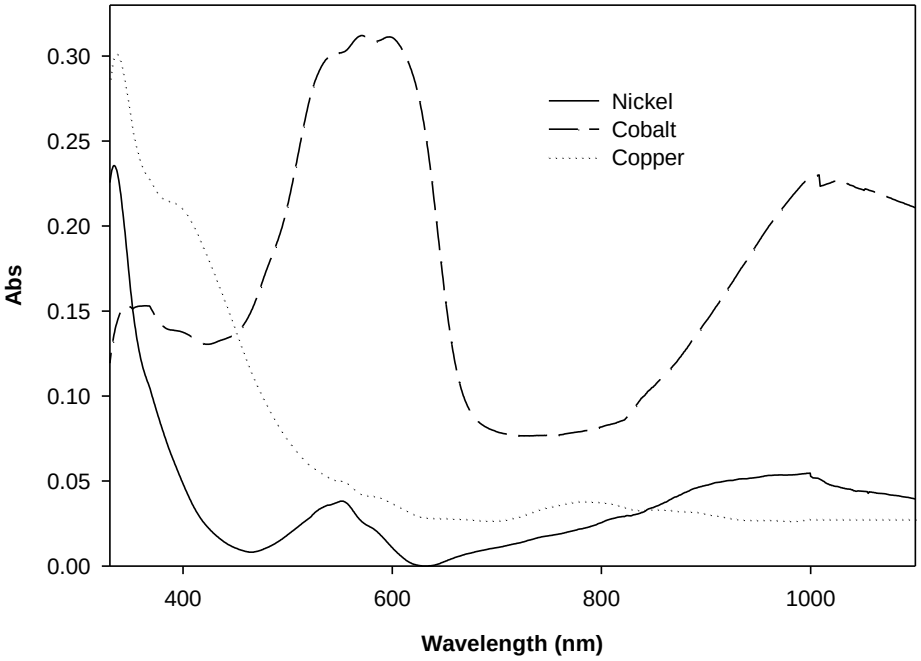

Figure 4.1: The UV-Vis solid reflectance spectra of $[M(BNSN)_2]SO_4 \cdot yH_2O$ (M = Co, Ni, and Cu; y = 2–4)

4.3.1.3.Crystal structures

The ORTEP diagrams of $[Co(BNSN)_2](RSO_3)_2 \cdot 4H_2O$ and $[Ni(BNSN)_2](RSO_3)_2 \cdot 2H_2O$ are illustrated in **Figures 4.2 and 4.3**,and selected bond lengths and angles are given in **Table 4.7**.

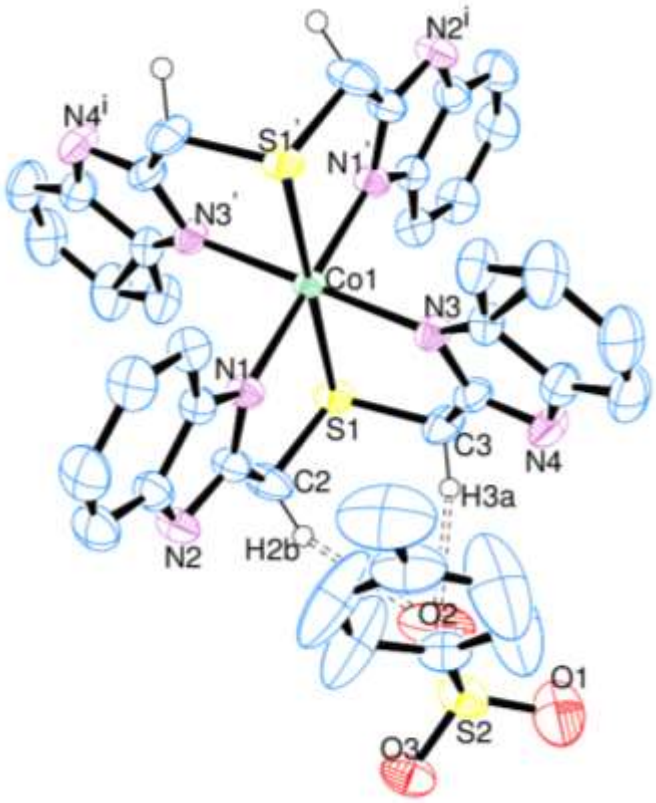

Figure 4.2: ORTEP diagram of the $[Co(BNSN)_2](RSO_3)_2 \cdot 4H_2O$ showing the atom labeling scheme and ellipsoids drawn at 50% probability level

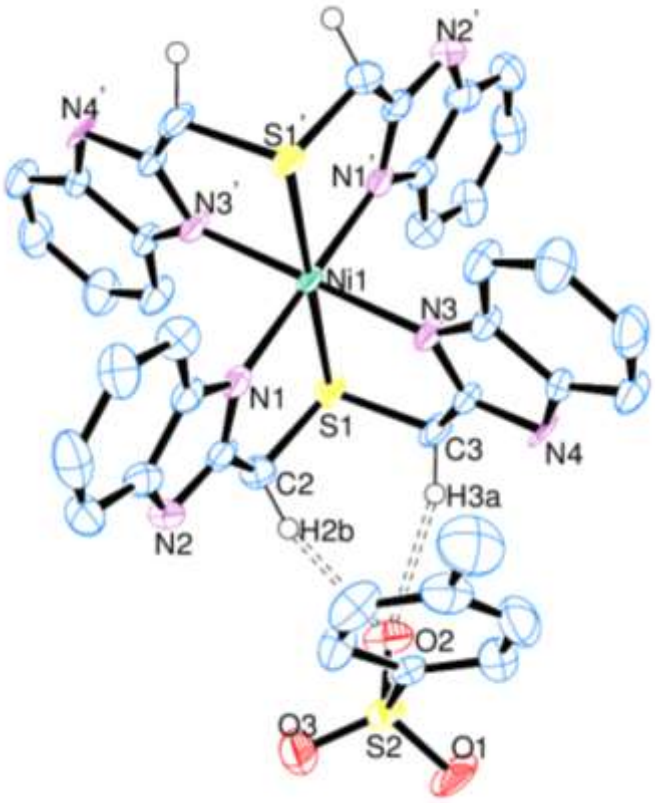

Figure 4.3: ORTEP diagram of the $[Ni(BNSN)_2](RSO_3)_2 \cdot 2H_2O$ showing the atom labeling scheme and ellipsoids drawn at 50% probability level

Table 4.7: Selected bond lengths (Å) and angles (º) for $[Co(BNSN)_2](RSO_3)_2 \cdot 4H_2O$ and $[Ni(BNSN)_2](RSO_3)_2 \cdot 2H_2O$

Bond lengths			
$[Co(BNSN)_2](RSO_3)_2 \cdot 4H_2O$		$[Ni(BNSN)_2](RSO_3)_2 \cdot 2H_2O$	
Co1–S1	2.488(1)	Ni1–S1	2.447(1)
Co1–N1	2.118(2)	Ni1–N1	2.097(3)
Co1–N3	2.119(2)	Ni1–N3	2.104(3)
Co1–S1′	2.488(1)	Ni1–S1′	2.447(1)
Co1–N1′	2.118(2)	Ni1–N1′	2.097(3)
Co1–N3′	2.119(2)	Ni1–N3′	2.104(3)
Bond angles			
S1-Co1-N1	82.38(5)	S1-Ni1-N1	83.30(9)
S1-Co1-N3	82.72(5)	S1-Ni1-N3	83.18(9)
S1-Co1-S1′	180.00	S1-Ni1-S1′	180.00
S1-Co1-N1′	97.62(5)	S1-Ni1-N1′	96.71(9)
S1-Co1-N3′	97.28(5)	S1-Ni1-N3′	96.82(9)
N1-Co1-N3	87.66(7)	N1-Ni1-N3	88.84(12)
S1′-Co1-N1	97.62(5)	S1′-Ni1-N1	96.71(9)
N1-Co1-N1′	180.00	N1-Ni1-N1′	180.00
N1- Co1-N3′	92.34(7)	N1-Ni1-N3′	91.16(12)
S1′- Co1-N3	97.28(5)	S1′-Ni1-N3	96.82(9)
N1′- Co1-N3	92.34(7)	N1′-Ni1-N3	91.16(12)
N3- Co1-N3′	180.00	N3-Ni1-N3′	180.00
S1′- Co1-N1′	82.38(5)	S1′-Ni1-N1′	83.30(9)
S1′- Co1-N3′	82.72(5)	S1′-Ni1-N3′	83.18(9)
N1′- Co1-N3′	87.66(7)	N1′-Ni1-N3′	88.84(12)

The crystal structures of both $[Co(BNSN)_2](RSO_3)_2 \cdot 4H_2O$ and $[Ni(BNSN)_2](RSO_3)_2 \cdot 2H_2O$ consist of discrete cationic complexes and relatively isolated sulfonate anions (**Figures 4.3 and 4.4**). The closest contacts that the sulfonate ions have with the complex molecules are as

follows: H(2)–O(2) = 2.560(1) and H(3)–O(2) = 2.360(1) for the cobalt complex and H(2)–O(2) = 2.300(1) and H(3)–O(2) = 2.340(1) for the nickel complex.

The metal ions, Co(II) and Ni(II), are surrounded by two ligands, each tridentate (two N of benzimidazole and a sulfur). The geometries for both complexes are distorted octahedral with the equatorial plane formed by the four benzimidazole nitrogens while the sulfurs occupy apical positions. These distortions are evidenced by the nonorthogonal angles in the x, y, and z axes intersections around the metal despite linear N–M–N′ and S–M–S′ bonds (**Table 4.7**). The plane that bisects the ligands and parallel to S–M–S presents a vertical plane of symmetry for these molecules as evidenced by the bond lengths and angles. The equatorial distances for cobalt complex are Co–N1 and Co–N1′ = 2.118(2)Å and Co–N3 and Co–N3′ = 2.119(2) Å, while axial Co–S distance is 2.488(6) Å. For the nickel complex, the equatorial distances are Ni–N1 and Ni-N1′ = 2.097(3)Å and Ni–N3 and Ni–N3′ = 2.104(3)Å, while the axial Ni–S distances are 2.488(6)Å. For both complexes, the Co–S, Co–N, Ni–S, and Ni–N bond lengths fall in the range normally observed for octahedral compounds.[152,153,154,155]

This pattern of coordination for BNSN is similar to that of bis((2-benzimidazol-2-yl)ethyl)sulfide in *bis*[*bis*((2-benzimidazol-2-yl)ethyl)sulfide]nickel(II) nitrate (but with a methylene instead of an ethylene spacer between the benzimidazole and sulfur).[156] The X-ray crystal structures of copper complexes similar to $[Cu(BNSN)_2](RSO_3)_2 \cdot 2H_2O$ have been reported.[157,158,159,160,161,162] The isostructural nature of these complexes {$[M(BNSN)_2]SO_4 \cdot yH_2O$ (M = Co, Ni, and Cu; y=2–5)} led us to conclude that the lack of separation between these metal ions with *bis*((1-

octylbenzimidazol-2-yl)methyl)sulfide as extractant (**Section 3.3.21**) is influenced by the lack of stereochemical "tailor making".

4.3.2. The coordination chemistry of BNNN

4.3.2.1. Preparative aspect

The data obtained from elemental analyses suggested the following empirical formulae (**Table 4.9**); $[M(BNNN)_2]X{\cdot}xH_2O{\cdot}y$EtOH (M = Co, Ni, Cu and Zn; X = SO_4^{2-} or $(RSO_3^-)_2$, x = 3-12 y = 0-2).

The involvement of two ligands per metal ion is in agreement with what was observed in the extraction studies. Complexes of Fe(II), Fe(III) and other hard ions could not be isolated with a good level of purity but *bis*-coordination is implied by the slopes of the extraction data. The molar conductivity data in DMF showed that the sulfate and sulfonate complexes have molar conductance values of 66 - 82 and 136 - 147 M, $ohm^{-1}.cm^2.mole^{-1}$, respectively (**Table 4.8**). This indicated that all the sulfate complexes behaved as 1:1 electrolytes while the sulfonate complexes were 1:2 electrolytes.[141] This behavior in solution suggested the non-coordinated nature of the counter-anions.

Table 4.8: The physical properties of BNNN·4H_2O complexes

Compounds	Color	M.p.	Yield	Molar Conductance
BNNN	white needles	268-270	84	
	Sulfate complexes			
[Co(BNNN)$_2$]SO_4·4H_2O	pink	252–254	51	66
[Ni(BNNN)$_2$]SO_4·3H_2O	mauve	253–255	57	69
[Cu(BNNN)$_2$]SO_4·7H_2O	green	228–229	65	71
[Zn(BNNN)$_2$]SO_4·11H_2O	white	221–222	64	82
[Mg(BNNN)$_2$]SO_4·2H_2O:	white	251–252	58	74
[Mn(BNNN)$_2$]SO_4·5H_2O	brown	255–252	62	72
	Sulfonate complexes			
[Co(BNNN)$_2$]$(RSO_3)_2$·4H_2O·2EtOH	red	225–226	71	136
[Ni(BNNN)$_2$]$(RSO_3)_2$·3H_2O·2EtOH	purple	246–248	58	139
[Cu(BNNN)$_2$]$(RSO_3)_2$·12H_2O	blue	201–202	68	141
[Zn(BNNN)$_2$]$(RSO_3)_2$·3H_2O·2EtOH	white	201–202	62	147

Table 4.9: The elemental analysis data of the of the BNNN·$4H_2O$ complexes

Compounds	Elemental analysis Calc.(Found) %			
	C	H	N	S
BNNN	48.72(48.71)	5.89(5.86)	17.76(17.77)	
Sulfate complexes				
$[Co(BNNN)_2]SO_4·4H_2O$	49.17(49.20)	4.90(4.46)	17.92(17.85)	4.10(4.86)
$[Ni(BNNN)_2]SO_4·3H_2O$	50.34(50.64)	4.75(4.74)	18.35(18.28)	4.20(4.10)
$[Cu(BNNN)_2]SO_4·7H_2O$	45.74(45.81)	5.28(5.11)	16.67(16.41)	3.82(3.44)
$[Zn(BNNN)_2]SO_4·11H_2O$	42.04(41.96)	5.73(5.71)	15.31(15.00)	3.51(3.59)
$[Mg(BNNN)_2]SO_4·2H_2O$:	50.32(50.46)	5.28(5.25)	18.31(18.53)	4.19(4.21)
$[Mn(BNNN)_2]SO_4·5H_2O$	48.29(48.42)	5.08(5.09)	17.60(17.57)	4.03(4.01)
Sulfonate complexes				
$[Co(BNNN)_2](RSO_3)_2·4H_2O·2EtOH$	53.66(53.60)	5.67(5.34)	12.52(12.67)	5.73(5.14)
$[Ni(BNNN)_2](RSO_3)_2·3H_2O·2EtOH$	54.50(54.43)	5.57(5.58)	12.71(12.47)	5.82(5.70)
$[Cu(BNNN)_2](RSO_3)_2·12H_2O$	46.95(46.48)	5.82(5.47)	11.90(11.76)	5.45(5.85)
$[Zn(BNNN)_2](RSO_3)_2·3H_2O·2EtOH$	54.17(54.50)	5.64(5.64)	12.63(12.30)	5.78(5.53)

4.3.2.2 Spectroscopic studies

The C=N stretching vibration of the benzimidazole rings of the free ligand (BNNN) appeared at 1592 cm^{-1},[163,164] and coordination-induced frequencies were observed in the range 1548 - 1565 cm^{-1} upon complex formation. The lowering in the double bond character of C=N is perhaps due to the influence of the benzimidazole groups being *trans* to each other. The far infrared spectra of the sulfate and sulfonate complexes displayed bands in the range 222 - 279 cm^{-1} which were assigned to the ν(M-N) .[146] A strong and broad peak in the range 1137 – 1188 cm^{-1} and 1050 - 1090 cm^{-1} was present in the spectra of sulfate and sulfonate complexes respectively, and this is typical of the un-coordinated sulfate and sulfonate ions.[147] The infrared spectra of

these complexes suggested that all the three donor atoms of the ligand are involved in the coordination sphere and that both the sulfate and sulfonate anions are non-coordinating.

Table 4.10: The infrared spectral data for the BNNN·4H_2O complexes

Complexes	ν(N-H)	ν(C=N)	$\nu_3(SO_4)$	$\nu_3(SO_3)$	ν(M-N)
BNNN	3208	1592			
Sulfate complexes					
[Co(BNNN)$_2$]SO_4·4H_2O	3242	1545	1037		226
[Ni(BNNN)$_2$]SO_4·3H_2O	3234	1538	1037		230
[Cu(BNNN)$_2$]SO_4·7H_2O	3233	1565	1060-1088		224
[Zn(BNNN)$_2$]SO_4·11H_2O	3227	1548	1037		222
[Mg(BNNN)$_2$]SO_4·2H_2O:	3285	1546	1037		228
[Mn(BNNN)$_2$]SO_4·5H_2O	3251	1543	1037		228
Sulfonate complexes					
[Co(BNNN)$_2$](RSO_3)$_2$·4H_2O·2EtOH	3311	1551		1150-1161	279
[Ni(BNNN)$_2$](RSO_3)$_2$·3H_2O·2EtOH	3313	1550		1151-1164	246
[Cu(BNNN)$_2$](RSO_3)$_2$·12H_2O	3213	1550		1147-1172	262
[Zn(BNNN)$_2$](RSO_3)$_2$·3H_2O·2EtOH	3304	1549		1172-1187	258

The geometry of the complexes was confirmed by UV-Vis solid reflectance electronic studies as well as by single crystal X-ray crystallography (**Section 4.3.2.3**). Three d-d transitions that are expected in the visible region of the spectrum for an octahedral Co(II) complex are; $^4T_{1g}(F) \rightarrow {}^4T_{2g}(F)$ (ν_1), $^4T_{1g}(F) \rightarrow {}^4A_{2g}(F)$ (ν_2) and $^4T_{1g}(F) \rightarrow {}^4T_{1g}(P)$ (ν_3).[17] These absorption bands were observed at 1095, 544 and 482 nm respectively (**Figure 4.4**). For the nickel complexes the bands were observed at 919, 585 nm which may be assigned to $^3A_{2g}(F) \rightarrow {}^3T_{2g}(F)$ (ν_1), $^3A_{1g}(F) \rightarrow {}^3T_{2g}(F)$ (ν_2) transitions respectively for octahedral and assuming that the third transition ($^3A_{2g}(F) \rightarrow {}^3T_{1g}(P)$ (ν_3)) is masked by the intra-ligand transition.[143] The electronic spectrum of

the Cu(II) complex showed one broad band at 619 nm which was ascribed to the $^2B_{1g} \rightarrow {}^2B_{2g}$ and, assuming that the second transition ($^2B_{1g} \rightarrow {}^2A_{1g}$) is masked by the intraligand transition, this is consistent with a distorted octahedral geometry.[148] The assignment of Cu(II) complexes d-d transitions are known to be more complicated because of the relatively low symmetry environment, in which the Cu(II) ion is characteristically found.

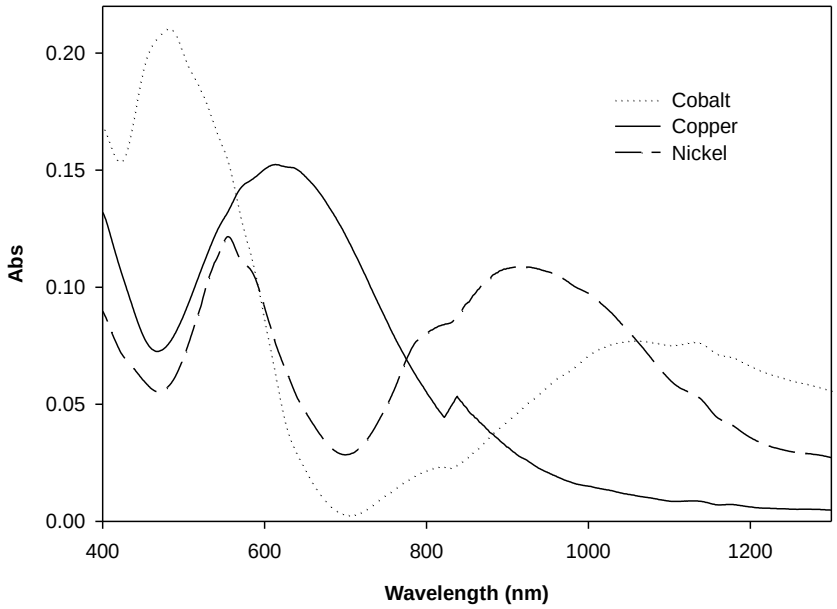

Figure 4.4: The UV-Vis solid reflectance spectra of $[M(BNNN)_2]SO_4 \cdot yH_2O$ (M = Co, Ni and Cu; y = 3 – 12)

4.3.2.3 Crystal structures

4.3.2.3.1 Crystal structure of BNNN·4H$_2$O

An ORTEP diagram of the crystal structure of BNNN·4H_2O is presented in **Figure 4.5**. The selected bond lengths and angles in **Table 4.11**. The average bond length distance and angles for BNNN are in agreement with those of similar *bis*(benzimidazolyl)-substituted compounds, which are 1.30 – 1.40 and 104 – 129.[165,166,167]

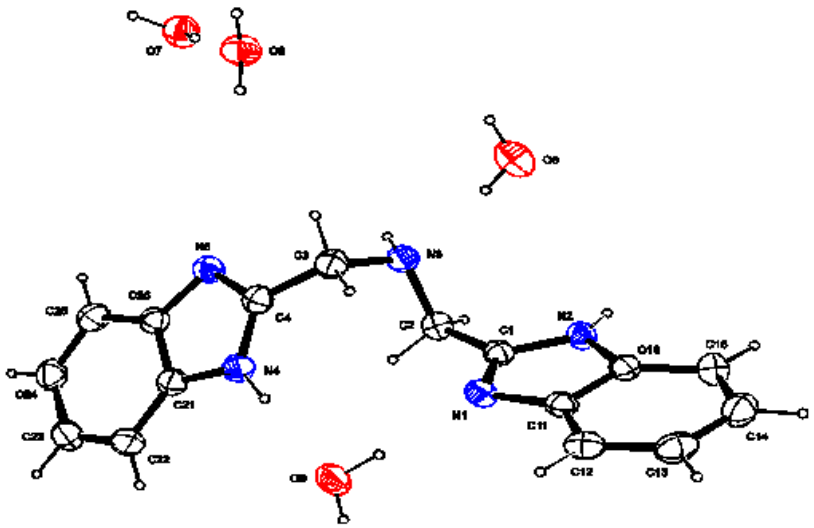

Figure 4.5: ORTEP diagram of BNNN·4H_2O showing the atom labeling scheme and ellipsoids drawn at 50% probability level.

Table 4.11: Selected bond lengths (Å) and angles (º) for BNNN·4H_2O

Bond lengths			
N1–C1	1.321(2)	N3–C3	1.470(2)
N2–C1	1.360(2)	N4-C4	1.354(2)
N3-C2	1.472(2)	N5-C4	1.319(2)
Bond angles			
C1–N1–C11	105.06(14)	N1–C1–C2	125.29(15)
C1–N2–C16	107.41(14)	N2–C1–C2	121.95(15)
C2–N3–C3	114.36(14)	N1–C1–N2	112.66(15)
C4–N4–C21	107.42(14)	N3–C2–C1	110.61(15)
C4–N5–C26	104.87(14)	N2–C3–C4	113.79(15)
C1–N2–H2	128.70(15)	N4–C4–N5	112.77(15)
C3–N3–H3	110.00(13)	N4–C4–C3	112.82(15)
C2–N3–H3	108.60(13)	N5-C4-C3	124.34(15)
C4–N4–H4	126.30(15)		

The C–N bond lengths in the imidazole ring are in the range 1.35(1)–1.36(1) Å; these are shorter than the single bond length of 1.480 Å and longer than the typical C=N distance of 1.280 Å, indicating partial double-bond character.[168]

The benzimidazole moieties of the molecule are planar; the displacements of all nine atoms contained in the rings are less than 0.0065(1) Å from the least-squares plane. Planarity of the benzimidazole ring system is usually observed. In the ORTEP diagram, the conformations of the –CH2– groups are *anti* to each other owing to the *anti*-conformational structure.[168]

4.3.2.3.2. Crystal structure of $[Cu(BNNN)_2](RSO_3)_2 \cdot 12H_2O$

An ORTEP diagram of the crystal structure of $[Cu(BNNN)_2](RSO_3)_2 \cdot 12H_2O$ is presented in **Figure 4.6**. The selected bond lengths and angles in **Table 4.12**.

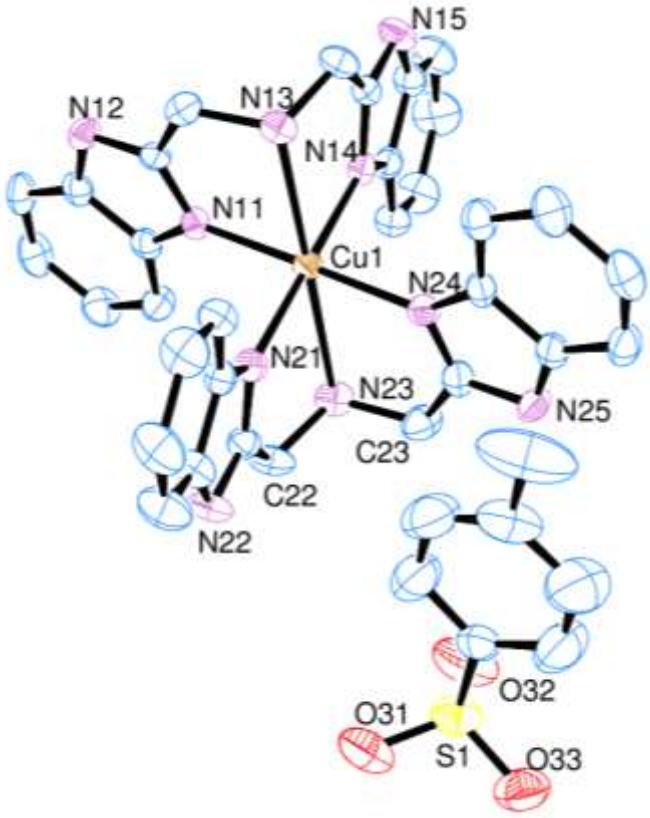

Figure 4.6: ORTEP diagram of $[Cu(BNNN)_2](RSO_3)_2 \cdot 12H_2O$ showing the atom labeling scheme and ellipsoids drawn at 50% probability level. One toluene-4-sulfonate anion and twelve water molecules have been omitted for clarity

Table 4.12: Selected bond lengths (Å) and angles (º) for **$[Cu(BNNN)_2](RSO_3)_2 \cdot 12H_2O$**

Bond lengths			
Cu1–N11	1.998(14)	Cu1–N21	2.045(14)
Cu1–N13	2.509(14)	Cu1–N23	2.547(14)
Cu1–N14	2.040(14)	Cu1–N24	2.012(15)
Bond angles			
N11–Cu1–N13	77.0(5)	N13–Cu1–N24	104.0(5)
N11–Cu1–N14	86.5(6)	N14–Cu1–N21	179.9(8)
N11–Cu1–N21	93.6(6)	N14–Cu1–N23	105.3(5)
N11–Cu1–N23	103.1(5)	N14–Cu1–N24	93.9(6)
N11–Cu1–N24	179.0(6)	N21–Cu1–N23	74.8(5)
N13–Cu1–N14	75.9(5)	N21–Cu1–N24	86.0(6)
N13–Cu1–N21	104.0(5)	N23–Cu1–N24	75.9(5)
N13–Cu1–N23	178.9(4)	C22–N23–C23	114.2(14)

The crystal structure of $[Cu(BNNN)_2](RSO_3)_2 \cdot 12H_2O$ conclusively depicted that the complex is cationic with relatively isolated sulfonate anions (**Figure 4.5**). The closest contact that the sulfonate ion has with the cationic molecule is H(23)-O(31) = 2.560(1). The two ligands are tridentately coordinated to the copper(II) ion in the formation of a tetragonally distorted Oh geometry with the four benzimidazoles in the square plane while the two aliphatic amines occupy the apical positions. The five membered chelate rings have bite angles in the range 74.8° - 77.0°. The aliphatic amines are bonded *trans* to each other and the Cu-N lengths of 2.509 and 2.547 Å are rather long possibly due to Jahn-Teller distortion. However, the Cu-N (benzimidazole) lengths are rather short (average of 2.014 Å) due to the π-acidity character of the benzimidazole group. An X-ray crystal structure of the copper complex similar to $[Cu(BNNN)_2](RSO_3)_2 \cdot 12H_2O$ was presented by Berends and Stephan [160] but no crystallographic parameters were reported because the complete refinement of the model was unsuccessful, and

the ORTEP diagram presented was based on parameters obtained in "best" model. A similar nickel complex crystal structure has also been reported [169, 170] but had a different arrangement of the donor groups, for example the aliphatic amine groups from each ligand were bonded *trans* to the benzimidazole group of another ligand. The similarity in the geometry of these base metal complexes afforded us to conclude that the lack of pH-metric separation with the use of *bis*((1-decylbenzimidazol-2-yl)methyl)amine as extractant (Section 3.3.4.2) is influenced by the lack of stereochemical "tailor-making".

4.3.3. The coordination chemistry of BIMA

4.3.3.1. *Preparative aspect*

The physical properties of the metal complexes are given in **Table 4.13**. This high conductivity values indicate or suggest a cationic character to these complexes which again agrees with non-coordinated nature of the sulfate ion. The microanalysis data (**Table 4.14**) suggested a 1:2 metal-to-ligand ratio for all the complexes.

Table 4.13: The physical properties of BIMA complexes

Compounds	Color	M.p.	Yield	Molar Conductance
BIMA	white	126-128	71	
$[Co(BIMA)_2]SO_4 \cdot H_2O$	pink	321–322	52	71
$[Ni(BIMA)_2]SO_4 \cdot 2H_2O$	purple	324–325	56	79
$[Cu(BIMA)_2]SO_4 \cdot 3H_2O$	blue	241–242	51	76
$[Zn(BIMA)_2]SO_4 \cdot H_2O$	white	319–320	62	88

Table 4.14: The elemental analysis data of the BIMA complexes

Complexes	Elemental analysis Calc. (Found) %			
	C	H	N	S
BIMA	67.06(67.13)	6.88(6.03)	26.07(26.13)	
Sulfate complexes				
$[Co(BIMA)_2]SO_4 \cdot H_2O$	43.64(43.13)	4.88(4.30)	16.96(16.67)	6.47(6.02)
$[Ni(BIMA)_2]SO_4 \cdot 2H_2O$	42.13(42.58)	5.11(5.15)	16.38(16.42)	6.25(6.19)
$[Cu(BIMA)_2]SO_4 \cdot 3H_2O$	40.33(40.70)	5.26(5.17)	15.68(15.63)	5.98(5.50)
$[Zn(BIMA)_2]SO_4 \cdot H_2O$	43.08(43.95)	4.82(4.80)	16.75(16.96)	6.39(6.68)

4.3.3.2.Spectroscopic studies

The important infrared frequencies exhibited by the ligand and sulfate complexes are listed in **Table 4.14**. The spectrum of the free ligand show bands at 3318 and 1622 cm^{-1} which are due to ν(imdN-H) and ν(C=N) respectively.[163,164,171] The C=N stretching vibrational band of the ligand were observed in the range of 1623-1625 upon complex formation. The shift of this band towards higher frequencies suggest that the coordination of the ligand to metal ion involves the

N atom of benzimidazole, and it also confirms the strong pi bonding between the metal ions and benzimidazole. The appearance of the strong band of the complexes in the range 1029- 1036 cm^{-1} (**Table 4.14**) suggested the non-coordinated nature of the sulfate ion.[147] The far infrared spectra complexes displayed bands in the range 349-387 cm^{-1} which were assigned to the ν(M-N).[146]

Table 4.15: The infrared data for the BIMA complexes

Compounds	ν(imdN-H)	ν(C=N)	$\nu_3(SO_4)$	ν(M-N)
BIMA	3318	1622		
Sulfate complexes				
$[Co(BIMA)_2]SO_4 \cdot H_2O$	3225	1624	1029	387
$[Ni(BIMA)_2]SO_4 \cdot 2H_2O$	3223	1624	1033	349
$[Cu(BIMA)_2]SO_4 \cdot 3H_2O$	3221	1623	1035	349
$[Zn(BIMA)_2]SO_4 \cdot H_2O$	3212	1625	1036	349

The steochemistry of the metal complexes derived from BIMA was confirmed by UV-Vis solid reflectance studies. The electronic absorption spectroscopy provides insight to the possible stereochemistry of the metal complexes. The reflectance spectrum of the cobalt(II) complex (**Figure 4.7**) showed two bands at 1186 and 523 nm, and were ascribed to the $^4T_{1g}(F) \rightarrow {}^4A_{2g}(F)$ and $^4T_{1g}(F) \rightarrow {}^4T_{2g}(F)$ transitions.[73,74,148] The small peak around 800 nm is due to the known spin-forbidden band in octahedral Co(II) complexes. The pink colour of the complex is also characteristic of octahedral Co(II) complexes. The octahedral Co(II) complex suggests that there is two coordinated water molecules in this complex since the microanalysis showed only a possibility of two ligands coordinated to Co(II) (**Table 4.14**).

The majority of Cu(II) complexes which are blue or green and are usually distorted octahedral or tetrahedral.[73,74,148] These complexes exhibit one absorption band. However, two bands were observed in the spectrum of Cu(II)-BIMA and this suggested that the complex is not octahedral nor tetrahedral. Crystals that were suitable for XRD were not obtained for the complexes involving BIMA in order to elucidate the structure of these complexes. However, the complex formed by 2,2'-pyridylimidazole (PIMH) with Cu(II) shows a similar electronic spectrum and the crystal structure showed evidence of a coordinated water molecule in the fifth position resulting in a trigonal bipyramidal geometry (see **Figure 4.9**). Therefore, the Cu(II)-BIMA complex could be confidently assigned to be a trigonal bipyramidal structure based on the two peaks observed by UV-Vis ($^2E \rightarrow {}^2A$ and $^2E \rightarrow {}^2E$) (**Figure 4.7**).[148] The extraction patterns of BIMA and PIMH towards base metal ions (**Figures 3.25** and **3.26**) were similar, and the copper(II) anomaly can now be explained due to the formation of the less extractible aquated species.

Six- coordinated Ni(II) complexes have the spin allowed transitions from the ground $^3A_{2g}$ term to $^3T_{2g}$ (F) , $^3T_{1g}$ (F) and $^3T_{1g}$ (P) which will generally fall within 770-1430 nm, 500-910 nm and 370-530 nm, respectively, depending on the ligand field strength.[148] The colour of such complexes is usually green but the complex obtained by a reaction of Ni(II) with BIMA was purple. The electronic spectrum of the Ni(II)-BIMA chelate exhibited bands around 1000, 800 and 600 nm with some shoulders (**Figure 4.7**), and it is unlikely that these represent an octahedral geometry due to their positions considering the high ligand field strength of BIMA. The high % extraction of Ni^{2+} at low pH (**Figures 3.25** and **3.26**) seems to suggest a stable square planar geometry since T_d d^8 complexes are usually unstable.[101] However, the

spectroscopic evidence does not rule out the T_d geometry beyond reasonable doubt but this can only be solved by single crystal X-ray analysis. According to Lever[148], however, the square planar geometry should show three absorption bands at 1000 nm, 555-400 nm and 435–333 nm which are attributed to $^1A_{1g} \rightarrow {}^1A_{2g}$ and $^1A_{1g} \rightarrow {}^1B_{2g}$ and charge transfer transitions, and these are somewhat consistent with the observations in the electronic spectrum of the Ni(II)-BIMA complex.

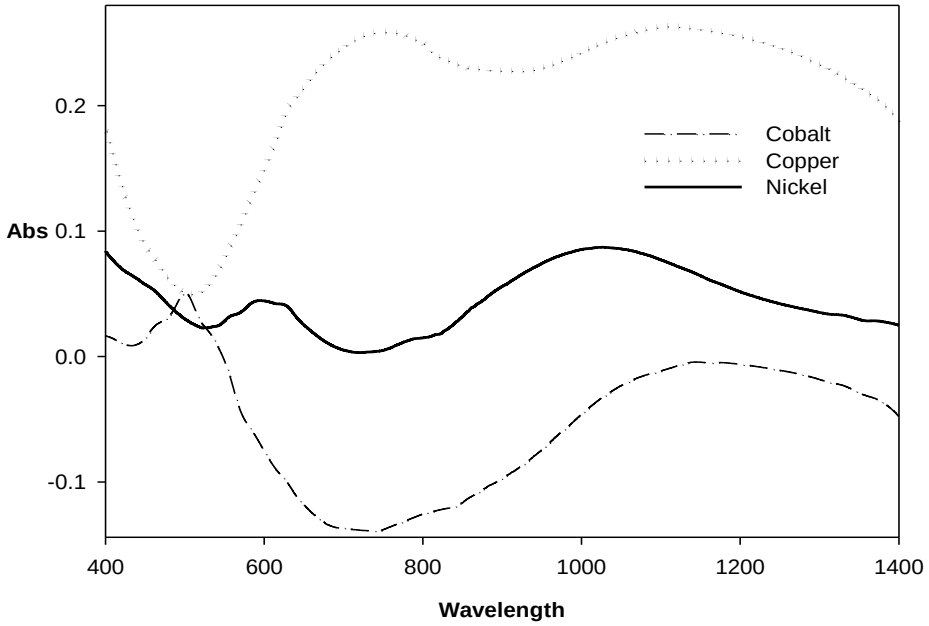

Figure 4.7: The UV-Vis solid reflectance spectra of $[M(BIMA)_2]SO_4 \cdot yH_2O$ (M = Co, Ni and Cu; $y = 1 – 2$

The coordination chemistry discussed above seems to corroborate well with the extraction data (**Figure 3.25**) obtained for the use of BIMA as an extractant (as OBIMA). The coordination of the water molecules onto Co(II) and Cu(II) ions resulted in the formation of less extractable

complexes, and the complexes that are proposed to form are presented in **Figure 4.8** and are also presented in the extraction order of the metal ions. This effect can be inferred to what was described as the Hofmeister bias for anions, from those that can be strongly hydrated to the ones that can be weakly hydrated, and wherein the strongly hydrated anions could not be readily phase transferred to the organic phase.[172]

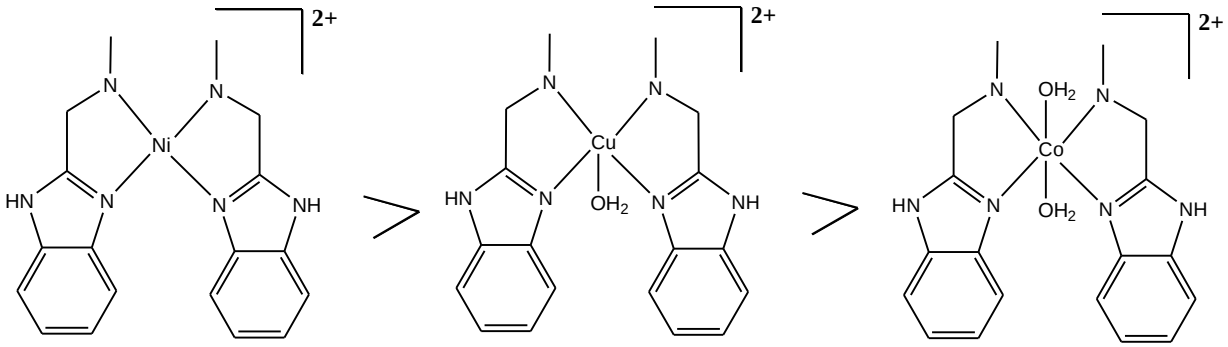

Figure 4.8: The proposed structures of the extractible complex species presented in their extraction order.

4.3.3.3.Crystal structure of [Cu(PIMH)$_2$·H$_2$O](SO$_4$)·H$_2$O

Since the coordination behavior of BIMA is similar to that of PIMH, we were able to obtain a crystal structure of [Cu(PIMH)$_2$·H$_2$O](SO$_4$)·H$_2$O. The ORTEP diagram of the crystal structure of [Cu(PIMH)$_2$·H$_2$O](SO$_4$)·H$_2$O is presented in **Figure 4.9**. The selected bond lengths and angles in **Table 4.16**

The crystal structures of [Cu(PIMH)$_2$(H$_2$O)](SO$_4$)·H$_2$O consist of discrete cationic complex and relatively isolated sulfate anion (**Figure 4.9**). The sulfate ion is disordered. The closest contacts that the sulfate ion have with the complex molecule are as follow: H"(1)–O(2) = 2.73(8) and

H”(15)–O(2) = 2.77. The two ligands are bidentately coordinated to the copper(II) ion in the formation of a trigonal bipyramidal geometry with N atom of the pyridine and one N atom of the imidazole group (in each ligand) in the trigonal plane. The trigonal plane is defined by the two pyridine nitrogens and a water oxygen.

The N atoms of the imidazole are bonded *cis* to each other and the Cu-N lengths of 1.963 and 1.963 Å are rather short, forming a stronger bond because imidazole has a stronger σ donor and π acceptor as compared to pyridine. The N atoms of pyridine are also bonded *cis* to each other, the Cu-N bond length of 2.089 and 2.089 Å are rather longer than that of imidazole possibly due to Jahn-Teller distortion. The coordination of the water to the copper(II)-PIMH complex resulted in a species that is not readily extractible into the organic phase hence the variation is in the series observed in Section 3.3.4.2.

Table 4.16: Selected bond lengths (Å) and angles (º) for $[Cu(PIMH)_2 \cdot H_2O](SO_4) \cdot H_2O$

Bond lengths			
Cu1–N1”	2.089(2)	Cu1–N1	2.089(2)
Cu1–N2”	1.963(2)	Cu1–N2	1.963(2)
Bond angles			
O1–Cu1–N1	111.33(6)	N1”–Cu1–N2”	97.06(9)
O1–Cu1–N2	92.67(6)	N2–Cu1–N2”	174.67(9)
O1–Cu1–N1”	111.33(6)	N1”-Cu1-N2”	80.98(9)
O1–Cu1–N2”	92.67(6)	C11-N1-C12	117.9(2)
N1–Cu1–N2	80.98(9)	C1-N2-C2	106.2(2)
N1–Cu1–N1”	137.35(8)	C1-N3-C3	107.9(2)
N1–Cu1–N2”	97.06(9)		

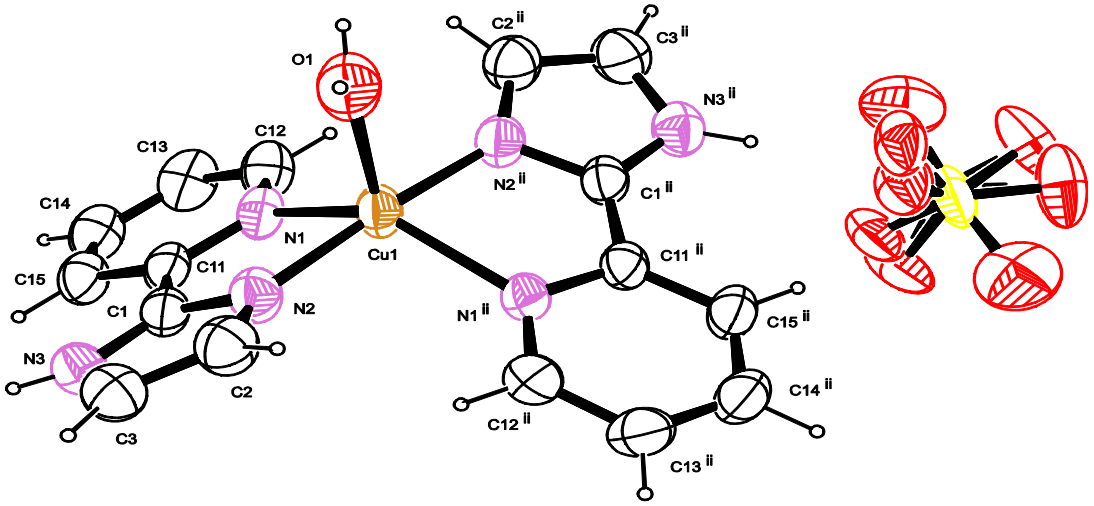

Figure 4.9: ORTEP diagram of $[Cu(PIMH)_2 \cdot H_2O](SO_4) \cdot H_2O$ showing the atom labeling scheme and ellipsoids drawn at 50% probability level. The sulfate ion is disordered.

4.4. Conclusions

For the tridentate systems, BNSN and BNNN, the spectral and X-ray characterization studies have shown that both systems form stable octahedral complexes with all the divalent later 3d metal ion transitions. This was unexpected since nickel is known to form octahedral while cobalt can stabilize in both tetrahedral and octahedral environments. It had been envisaged that separation could be achieved through formation of different geometries of the metal ion complexes since different metals show relative stabilization in different stereochemical environments. The coordination chemistry studies and extraction data indicated that all the metal ions exhibit similar geometry and the metal ions coordinate to two ligands to form stable octahedral complexes. This lack of stereochemical tailoring, with the use of tridentate ligands, is proposed to have resulted in lack of pH-metric separation of the base metals. The bidentate system (BIMA) showed nickel(II) separation and this may be influenced by stereochemical aspects and the Hofmeister bias since some complexes formed have coordinated water molecules.

The coordination chemistry studies obtained from the three ligand systems, BNSN, BNNN and BIMA, confirmed the findings observed in **Chapter 3**, which indicated that the separation of nickel(II) from other base metals was not possible for tridentate ligands due to the lack of stereochemical tailoring while it was possible with a bidentate ligand. It is therefore desirable to understand driving force for the *bis*-tridentate coordination for all the metal ion complexes hence **Chapter 5** reports on the thermodynamic aspects of this coordination chemistry.

CHAPTER 5

5. STABILITY CONSTANTS OF THE BENZIMIDAZOLE-BASED LIGANDS AND LATER DIVALENT 3d METALS

5.1 Overview

The solvent extraction experiments carried out in this study involve complexation in solution. Therefore, the nature, equilibria and stability of complexes in solution are very important in developing successful methods for metal ions separation. In **Chapter 4**, the stereochemistry of the coordination compounds isolated from a reaction mixture of the respective metal ions and the ligands was described. This provided valuable information on the complexes formed by the metal ions and the ligands under investigation, and the extraction isotherms could be described from a coordination chemistry point of view. However, the factors that drive towards the coordination patterns observed have not been deconvoluted. In this chapter, the results of the study into the energetics of the complexation reactions will be reported and discussed.

The stabilities of the metal complexes formed between the ligands and each of the metal ions in solution is a very important factor in the separation of the metal ions *via* solvent extraction. This has been demonstrated in **Equations 34 and 35**, where the distribution ratio (D) has been correlated with formation constants (K_f). Stability constants measure the strength of the interaction between the reagents that come together to form the complex. The studies conducted by Irving and Williams on the stability of the high-spin octahedral complexes of bivalent ions of the first row transition metals indicated the following sequence: Mn < Fe < Co < Ni < Cu < Zn.[101] The sequence of these stabilities was found to be applicable to all the complexes known then and it is based on the reciprocal of the ionic radii and the second ionisation potentials of the

metal as well as the crystal field stabilization energy (CFSE). The Irving and Williams order is also known to be influenced by variations of the coordination number and stereochemical considerations, and the entropy factor may affect this stability order.

In the formation of a metal complex, denoted by ML_n, from a metal (M) and a ligand (L) in a stepwise process the equilibria of the successive complexation stages is denoted by **Equations 4-6**. The equilibrium constant, also termed as formation constant, is given by **Equation 7**. The logarithm value of either β_n or K_n are often used to denote the extent of the stability of the metal complex or the protonated ligand as the case may be. In practice, factors contributing to the stability of a given metal complex are; the chelate effect, the geometrical effect, ionic radius of the metal and the classification of the metal ions. The chelate effect is known to be predominantly depends on the entropy change[103] while other factors such as solvation changes and ring formation also play a very crucial role. 5-Membered and 6-membered chelate rings are known to give the most stable complexes.

In general, since two or more different metals will form complexes of unequal stability with one and the same ligand, possibilities of analytical separations is dependent on the formation of a strong chelate complex with few metal ions or at best with only one of the metal ions by the ligand. This makes the application of a given extractant as a selective or "singular" reagent or better put a truly specific reagent realisable.

It is also possible to delve into the thermodynamics of the complexation process since geometric effect (sterecochemical "tailor making") was not favoured with tridentate ligands while it was

realized for a bidentate ligand. The equations used to calculate the thermodynamic parameters are given below.[173]

$$\Delta G = -RT\ln\beta_n \quad (39)$$

$$\Delta G = \Delta H - T\Delta S \quad (40)$$

$$-RT\ln\beta_n = \Delta H - T\Delta S \quad (41)$$

$$\ln\beta_n = -\Delta H/RT + \Delta S/R \quad (42)$$

The equation shows that enthalpy (ΔH) and entropy (ΔS) changes of a reaction are the two contributions to the Gibbs free energy and they can be obtained from the slope and the y-intercept of a plot of 1/T vs $\ln\beta_n$ (van't Hoff Plot).[172]

It would therefore be expected that in a given metal ion extraction system, to achieve a metal ion specificity, the stability constant ($\log\beta$) of the complex formed between the extractant and the metal ion of interest must not only be higher than the protonated species but must also be significantly higher than that of the other metal ions present. Thus, the position of the extraction curves relative to each other in an extraction isotherm would be in order with the relative formation constants. The thermodynamics (ΔH and ΔS values) of the complexation would also provide invaluable information with regards factors that drive the coordination patterns observed.

5.2. Potentiometric determination of formation constants

5.2.1. Instrumentation

The protonation and formation constants were determined by potentiometric acid-base titrations using the Metrohm 888 Titrando equipped with a Metrohm LL Ecotrode. The titration vessel was conditioned for constant temperature using a Grant Water Circulation System. A Varian SpectrAA 110 Atomic Absortion Spectrometer was used for standardization of metal ions solutions using the following wavelength: Co^{2+} =240.7 nm, Cu^{2+} = 324.7 nm, Ni^{2+} = 232.0 nm and Zn^{2+} = 213.9 nm.

5.2.2. Preparation of solutions

5.2.2.1. Perchloric acid solution

A 0.1 M solution of $HClO_4$ was standardized using 0.1 M sodium hydroxide solution with the dynamic endpoint detection using the Titrando 888. All solutions were prepared using freshly boiled and degassed deionized milli-Q water to ensure the removal of dissolved oxygen and carbon dioxide.

5.2.2.2. Preparation of metal ion solutions

The metal ion solutions were prepared from metal ion perchlorate salts ($M(ClO_4)_2$) and perchloric acid using using Millipore Milli-Q water that had been boiled, and degassed under high vacuum to remove oxygen and carbon dioxide. The amount of perchloric acid (mmol) in the metal solution volumes used in the titrations is accounted for when calculating the total moles of the hydrogen ion.

5.2.3 Experimental procedure for protonation/stability constants determination

The protonation and stability constants for the ligands and divalent complexes (Ni^{2+}, Co^{2+}, Cu^{2+} and Zn^{2+}) were determined by potentiometric titration of approximately 25 mL solutions (10% ethanol in water). The ligand concentration was 1.5 mM (and it was introduced as a solid in the titration vessel before addition of other reagents), and metal-to-ligand ratios of 1:2, 1:3 and 1:4 were used. Titrations were performed over the pH range of 2-11 under a continuous flow of purified nitrogen using $HClO_4$ and sodium hydroxide (NaOH). The ionic strength of the titration solutions was kept constant at 0.10 M sodium perchlorate ($NaClO_4$). Titrations were controlled using Tiamo 2.0 software. The glass electrode was calibrated for a strong acid-base reaction by the Gran-method[128] using GLEE,[174] which allows one to determine the standard potential $E°$. The ionic product of water (pKw) of 13.77(1) at 25.0±0.1 °C in 0.10 M $NaClO_4$ was used in all calculations.[175] The concentration stability constants, $\beta_{pqr} = [M_pL_qH_r]/[M]_p[L]_q[H]_r$ (**Equation 10**), were calculated by using the computer program HYPERQUAD.[127] The final values of the constants were obtained from an average of six independent titrations using an average of 400 data points in total for each refinement.

5.2.4. Electrode calibration

The electrode system used in the potentiometric titrations was calibrated before each titration, and it was performed in the same medium as the titration of the ligand and/or metal. This was done by titrating a mixture of perchloric acid (~1 mL of 0.1 M solution), sodium perchlorate (~ 21.5 mL of 0.1 M solution) and ethanol (~2.5 mL) with sodium hydroxide (0.1 M). The data obtained was then processed using a program called GLEE to obtain E°.[174]

5.2.5. Processing of data

All the potentiometric titration data collected from the titration studies were processed by a program called HYPERQUAD.[127] The data was transferred from titroprocessor to Microsoft-Excel and saved in a notepad format. The data was then uploaded from notepad to HYPERQUAD for the determination of protonation and formation constants.

5.5. Results and discussion

The protonation equilibrium constant for BNSN, BNNN and BIMA were determined at 25ºC. The totally protonated forms of the two benzimidazole-based tridenate ligands, *bis*((1*H*-benzimidazol-2-yl)methyl)sulfide (BNSN) and *bis*((1*H*-benzimidazol-2-yl)methyl)amine (BNNN) involve three dissociable protons for each ligand and their general formulae is H_3L^{3+} in their fully protonated form. For the benzimidazole-based bidentate ligand, (1*H*-benzimidazol-2-yl)-*N*-methylmethanamine (BIMA), a two-stage protonation process is exhibited and its general formula is H_2L^{2+} (for the fully protonated form). The protonation constants of the three ligands are reported in **Table 5.1** and their protonation equilibria are presented in **Schemes 5.1, 5.2 and 5.3.**

The complex formation studies of the three ligands, BNSN, BNNN and BIMA, with the divalent metal ions (Ni^{2+}, Co^{2+}, Cu^{2+} and Zn^{2+}) were also conducted at 25ºC. The complex formation constants of the three ligands with the divalent metal ions are reported in **Tables 5.2, 5.3 and 5.4,** and their stepwise formation processes are illustrated in **Schemes 5.4, 5.5 and 5.6**.

5.5.1. Protonation-dissociation equilibria of the ligands (BNSN, BNNN and BIMA)

The protonation-dissociation equilibria studies of the investigated imidazole-based ligands (BNSN, BNNN and BIMA) are given in **Table 5.1** (logβ not log$K$ values). The logβ values can readily be converted to pK values by considering the steps not the overall cumulative constants. The data obtained provided invaluable information on the basicity of the ligands.

Table 5.1: The protonation constants for the three benzimidazole-based ligands (BNSN, BNNN and BIMA). The constants were determined at 25ºC and at I = 0.1 M $NaClO_4$.

Ligand (L)	**logβ_1**	**logβ_2**	**logβ_3**
BNSN	6.10(2)	11.00(5)	12.30(5)
BNNN	8.31(4)	14.70(1)	17.60(1)
BIMA	7.73(6)	11.32(8)	-

5.5.1.1. The protonation equilibria of bis((1H-benzimidazol-2-yl)methyl)sulfide (BNSN)

The titration and fitted curve for the ligand BNSN is shown in **Figure 5.1**. The protonation constant data (**Table 5.1)** indicated pK values of 6.10 and 4.90 for the successive loss of the protons at the benzimidazole groups while pK value of 1.3 was obtained for loss of the proton on the sulfur group. These values are typical for the basicity of the benzimidazole and sulfur groups, respectively.

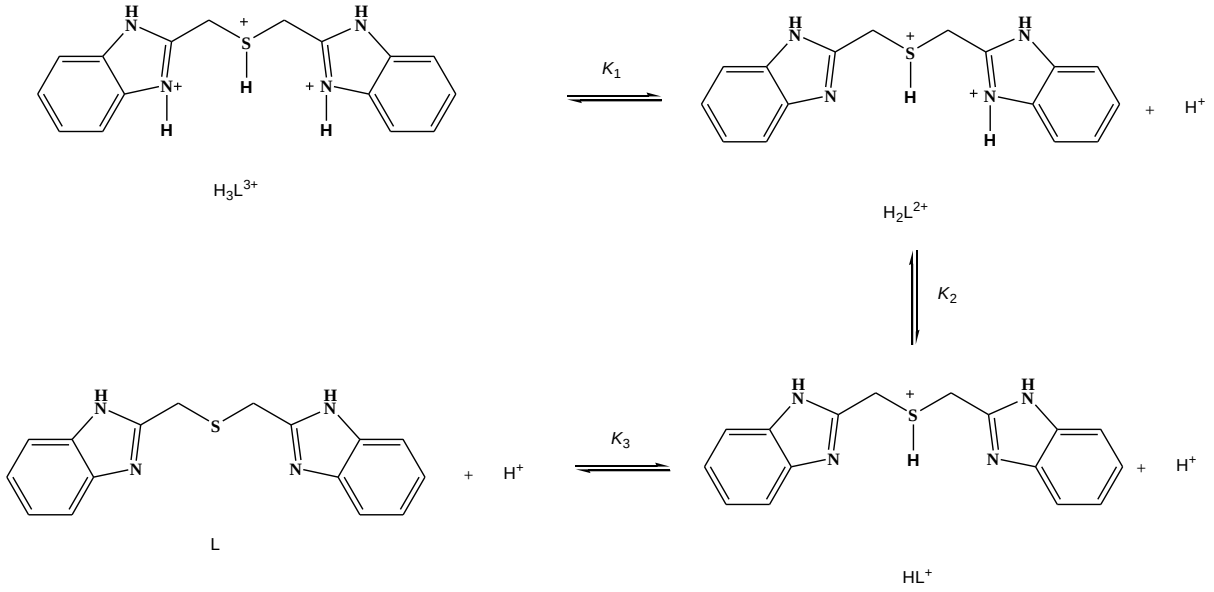

Scheme 5.1: Deprotonation steps for the *bis*((1*H*-benzimidazol-2-yl)methyl)sulfide (BNSN, L)

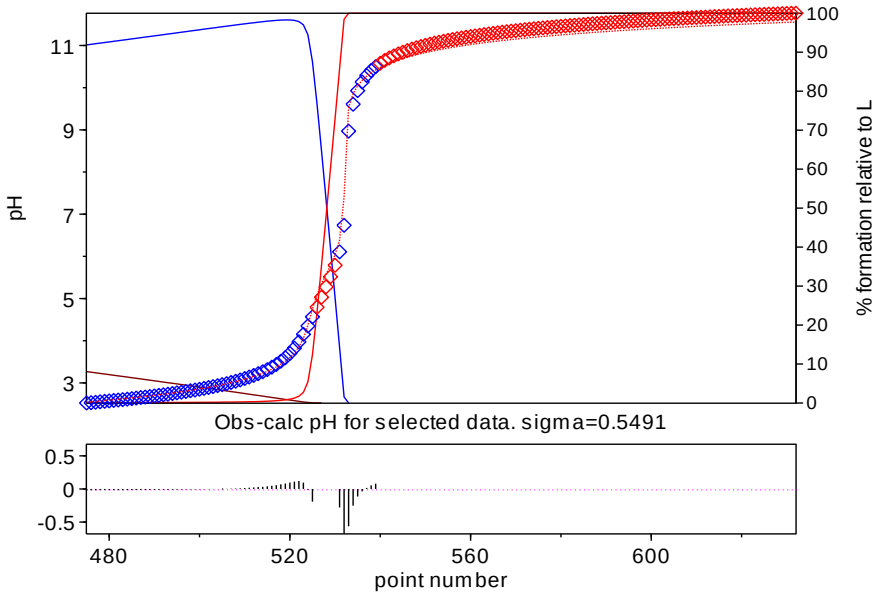

Figure 5.1: Titration and fitted curves BNSN protonation studies. Experimental points are represented by blue squares and the red dotted continuous line is the calculated line based on the fitted protonation constants. The red squares represent the experimental points that have been ignored in the refinement process. The other solid lines represent the species (not specified here).

5.5.1.2. The protonation equilibria of bis((1H-benzimidazol-2-yl)methyl)amine (BNNN)

The titration and fitted curve for the ligand BNNN is shown in **Figure 5.2**. The ligand exhibited a three-stage protonation process (**Scheme 5.2**) with a p*K* value of 8.31 for the amine nitrogen followed by the two benzimidazole nitrogen atoms at 6.39 and 2.90, respectively (**Table 5.1**). This suggested that the third site does not have a high proton affinity perhaps because the electron density may have already been shared with the proton on the aliphatic amine. The basicity of this ligand is shown to be higher than that of BNSN which is expected due to the presence of the aliphatic amine in place of sulfur.

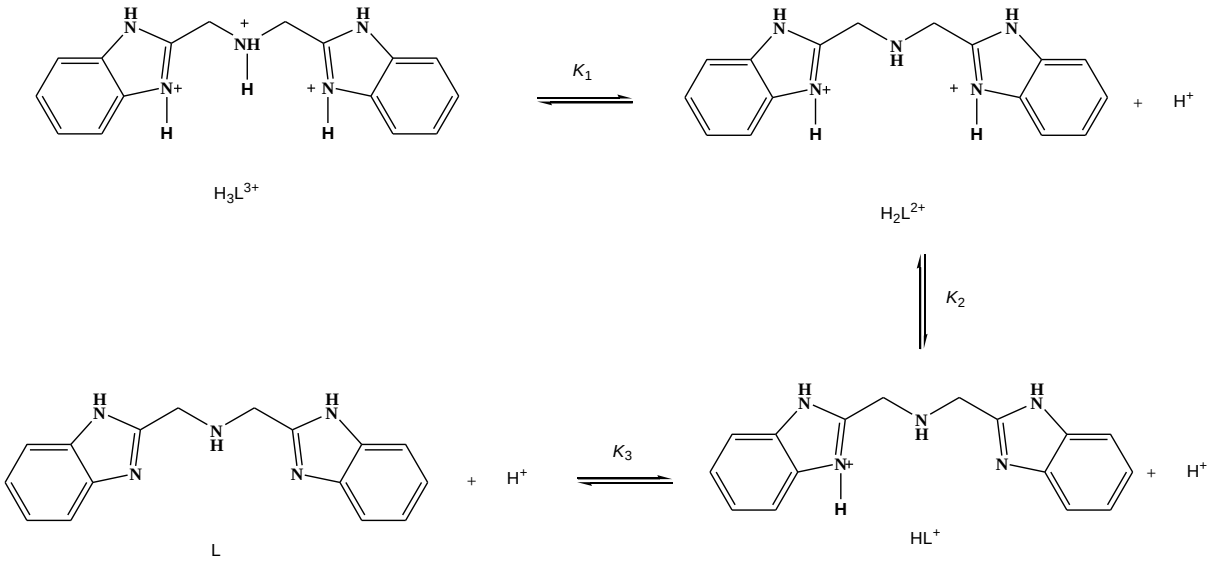

Scheme 5.2: Deprotonation steps for the *bis*((1*H*-benzimidazol-2-yl)methyl)amine (BNNN, L).

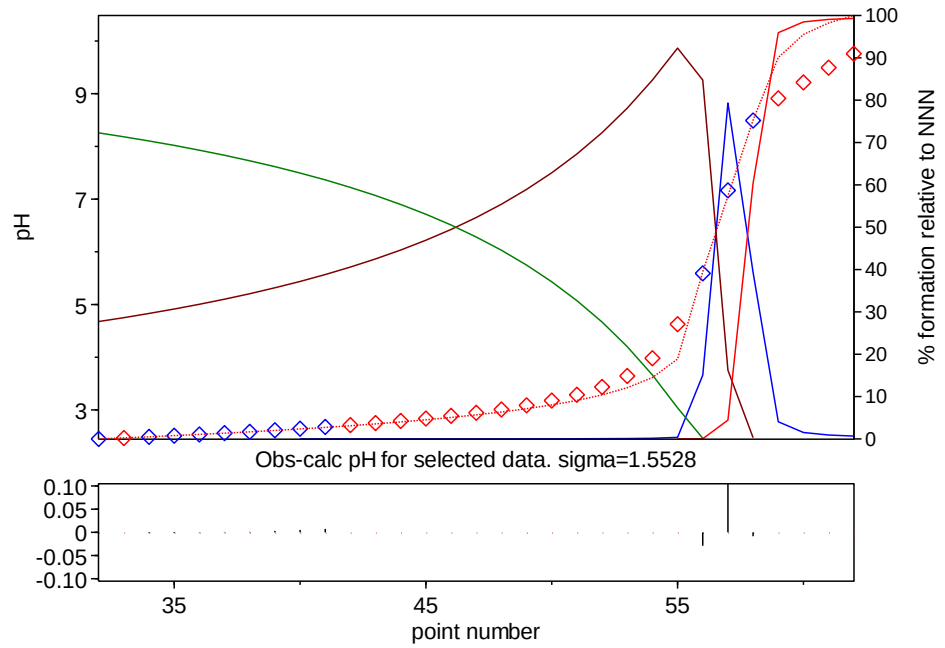

Figure 5.2: Titration and fitted curves BNNN protonation studies. Experimental points are represented by blue squares and the red dotted continuous line is the calculated line based on the fitted protonation constants. The red squares represent the experimental points that have been ignored in the refinement process. The other lines represent the species (not specified).

5.5.1.3. The protonation equilibria of (1H-benzimidazol-2-yl)-N-methylmethanamine (BIMA)

The protonation dissociation constants of the ligand BIMA are reported in **Table 5.1** and the titration and fitted curves are shown in **Figure 5.3**. The analysis of the potentiometric data of BIMA in the deprotonated form yields two p*K* values corresponding to the protonated benzimidazole nitrogen and the aliphatic amine group. The highest p*K* value is due to the amino group (7.73) and the lowest one is due to the benzimidazole nitrogen (3.59) as shown in **Scheme 5.3**. It is interesting to note how the presence of another group can influence another in terms of basicity since the electron density on the nitrogen atoms can be shared by the protons. It seems that the basicity of the amine group has been lowered by the presence of the aromatic nitrogen of

benzimidazole because a proton on the amine also interacts weakly with the benzimidazole nitrogen.

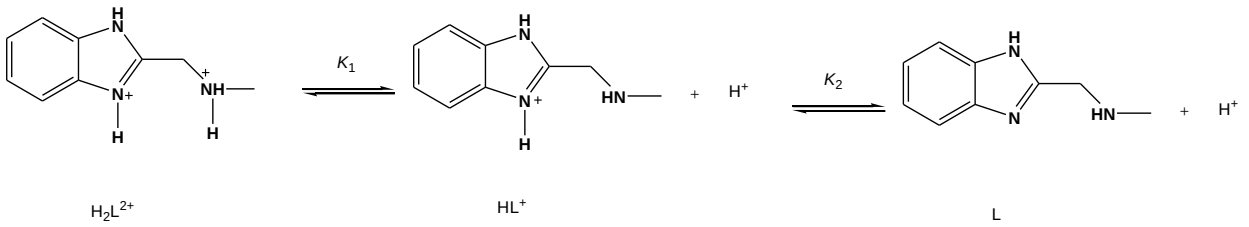

Scheme 5.3: Deprotonation steps for the *(1H-benzimidazol-2-yl)-N-methylmethanamine* (BIMA, L)

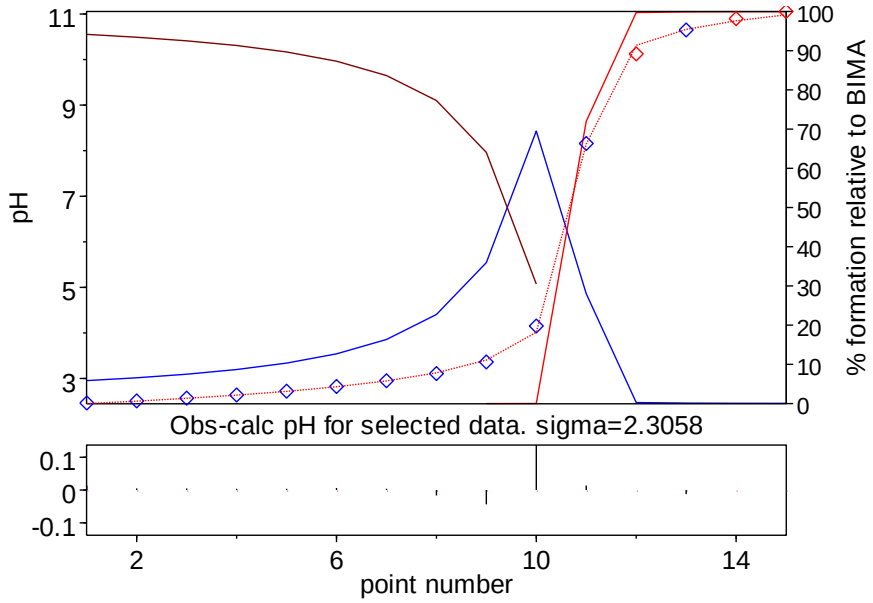

Figure 5.3: Titration and fitted curves BIMA protonation studies. Experimental points are represented by blue squares and the red dotted continuous line is the calculated line based on the fitted protonation constants. The red squares represent the experimental points that have been ignored in the refinement process. The other lines represent the species (not specified).

5.5.1.4. Comparison and the chemical behaviour of the BNSN, BNNN and BIMA ligands

The protonation-dissociation equilibria data, collected for the ligands (BNSN, BNNN and BIMA) provided important information on the base character of these ligands. The data showed that BNNN is more basic than BNSN which is to be expected. The data also indicated that BNNN and BIMA have similar basicity with BNNN having slightly higher constants. However, BNNN has an additional benzimidazole nitrogen which can present a different dimension with respect to coordination and result in much more stable complexes due to the chelate effect. It is expected that the interaction of BNNN with base metal will give slightly higher complex formation constants than BNSN, and much higher constants than BIMA.

5.5.2. Complexation formation equilibria of the three ligands (BNSN, BNNN and BIMA) with the divalent metal ions (Ni^{2+}, Co^{2+}, Cu^{2+} and Zn^{2+})

The stability constants obtained between the three ligands (BNSN, BNNN and BIMA) and divalent metal ions (Ni^{2+}, Co^{2+}, Cu^{2+} and Zn^{2+}) are presented in **Tables 5.2, 5.3 and 5.4**. The reaction equilibria involved can be seen in **Schemes 5.4, 5.5 and 5.6**.

5.5.2.1. Stability constants of BNSN with the divalent metal ions (Ni^{2+}, Co^{2+}, Cu^{2+} and Zn^{2+})

The titration and fitted curves for the reaction of nickel(II) with BNSN is given in **Figure 5.4**. The complex formation constants for the interaction of the benzimidazole-based tridentate ligand (BNSN) with the divalent metal ions is given in **Table 5.2**. The tridentate coordination of the ligand was evidenced by the high formation constants (**Table 5.2**). The overall second stability constants are of this order Ni^{2+} (20.26) > Cu^{2+} (19.78) > Co^{2+} (18.02). This is the same order that is observed in the extraction pattern (see **Chapter 3, Section 3.3.2.1.4**). The second stability

constant could not be determined for Zn^{2+}-BNSN complexation. This result shows that the extraction pattern is driven by the thermodynamics of the complexation since the compounds are isostructural. It will, however, be necessary to determine the constants at different temperatures and evaluate the enthalpy (ΔH) and entropy (ΔS) values for this reaction. The entropy effect is proposed to be the major driver for the six-coordination in these tridentate systems.

Table 5.2: The formation constants of M^{2+}-BNSN complexes (M^{2+} = Ni^{2+}, Co^{2+}, Cu^{2+} and Zn^{2+})

Complex	**logβ_1**	**logβ_2**
Ni-BNSN	11.51(2)	20.26(2)
Cu-BNSN	9.81(2)	19.78(1)
Co-BNSN	-	18.02(4)
Zn-BNSN	7.53	-

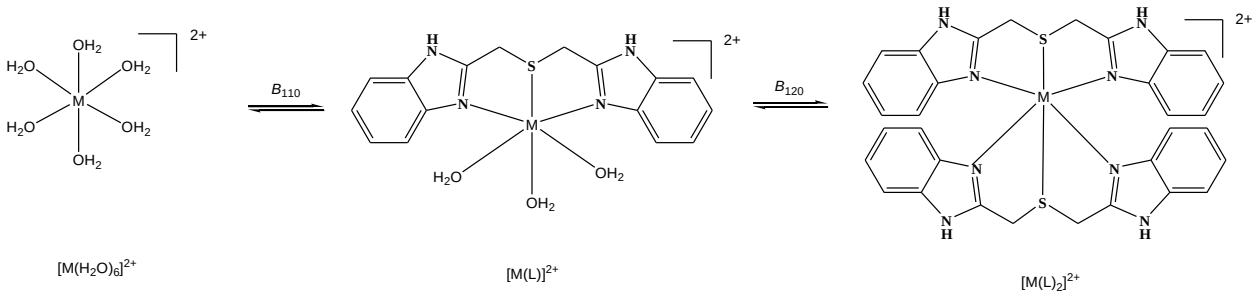

Scheme 5.4: The stepwise formation of base metal ion complexes with *bis*((1*H*-benzimidazol-2-yl)methyl)sulfide (BNSN).

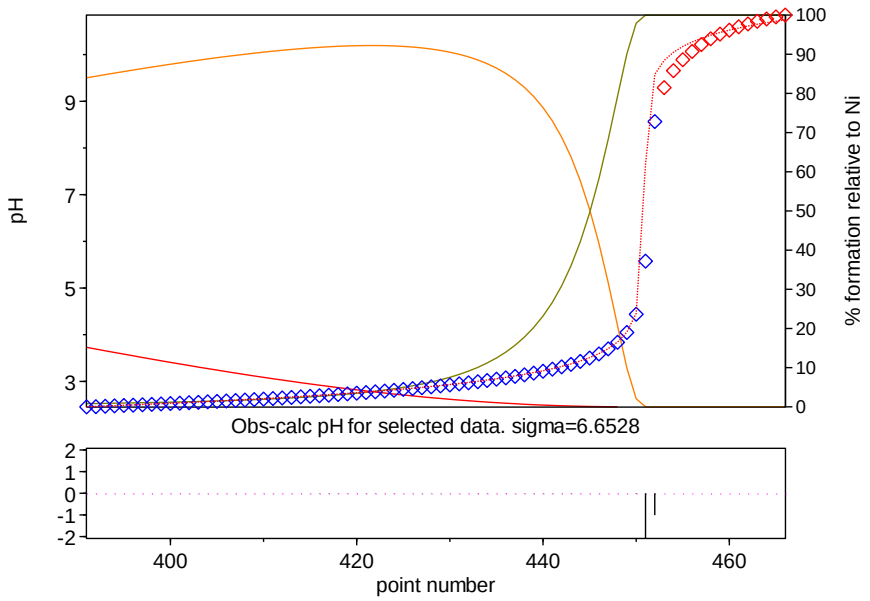

Figure 5.4: Titration and fitted curves of Ni-BNSN system. Experimental points are represented by blue squares and the red dotted continuous line is the calculated line based on the fitted protonation constants. The red squares represent the experimental points that have been ignored in the refinement process. The other lines represent the species (not specified).

5.5.2.2. Stability constants of BNNN with the divalent metal ions (Ni^{2+}, Co^{2+}, Cu^{2+} and Zn^{2+})

The potentiometric data of the BNNN –M^{2+} system (M^{2+} = Ni^{2+}, Co^{2+}, Cu^{2+} and Zn^{2+}) provided a good fit assuming the formation of the species $[M(BNNN)]^{2+}$ and $[M(BNNN)_2]^{2+}$. The experimental and theoretical curves (**Figure 5.5**) support the complex formation model given in **Scheme 5.6**. The formation constant ($\log\beta_2$) of BNNN-complexes of the divalent metal ions are given in **Table 5.3**, and are in the order of Ni^{2+} (21.29) > Zn^{2+} (20.14) > Co^{2+} (20.14). The results are in accordance with the extraction pattern observed with this ligand as an extractant (**Chapter 3, Section 3.3.2.2.5**). The copper(II)-BNNN complexation constants could not be determined confidently. As expected, the constants for the M-BNNN system are slightly higher than for the M-BNSN system due to the higher basicity of BNNN.

Table 5.3: The formation constants of M^{2+}-BNNN complexes (M^{2+} = Ni^{2+}, Co^{2+}, Cu^{2+} and Zn^{2+})

Complex	**logβ_1**	**logβ_2**
Ni-BNNN	11.08(2)	21.29(2)
Cu-BNNN	11.83(5)	-
Co-BNNN	10.28(3)	20.14(3)
Zn-BNNN	11.62(7)	20.47(1)

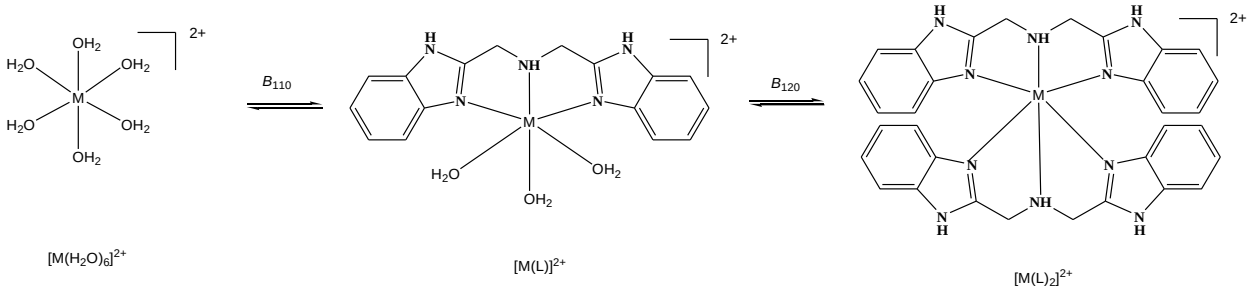

Scheme 5.5: The stepwise formation of base metal ion complexes with *bis*((1*H*-benzimidazol-2-yl)methyl)amine (BNNN).

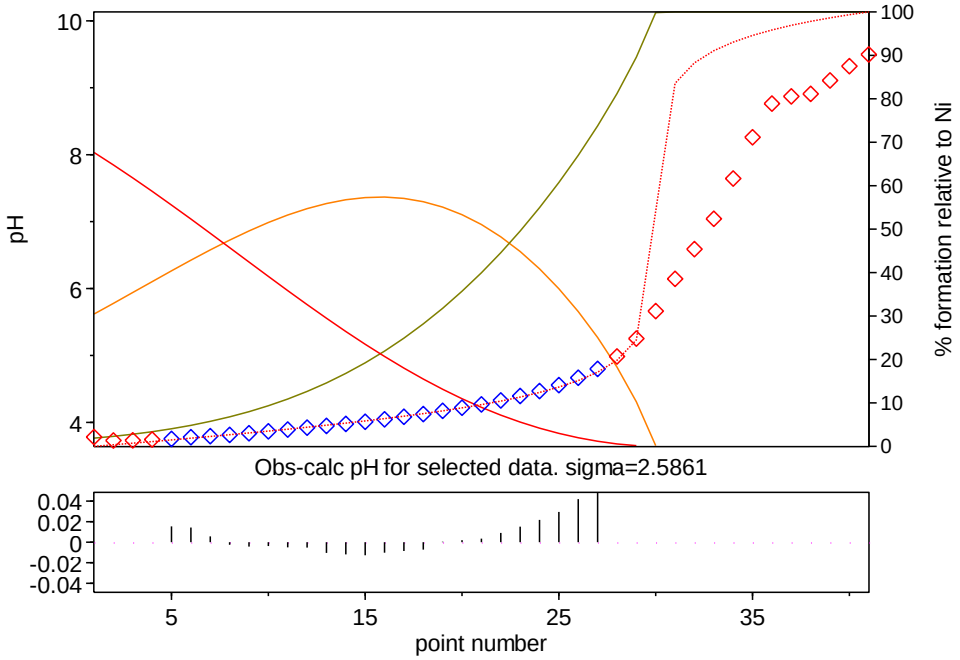

Figure 5.5: Titration and fitted curves of Ni-BNNN system. Experimental points are represented by blue squares and the red dotted continuous line is the calculated line based on the fitted protonation constants. The red squares represent the experimental points that have been ignored in the refinement process. The other lines represent the species (not specified).

5.5.2.3. Stability constants of BIMA with the divalent metal ions (Ni^{2+}, Co^{2+}, Cu^{2+} and Zn^{2+})

The titration and fitted curves for the reaction of cobalt(II) with BIMA is given in **Figure 5.6**, and the stability constants data is tabulated in **Table 5.4**. From the data it can be seen that the order of binding strength ($\log\beta_2$) is Ni^{2+} (13.97) > Cu^{2+} (13.94) > Co^{2+} (13.90) > Zn^{2+} (12.74) and this is accordance with the extraction pattern obtained with OBIMA as an extractant (**Chapter 3, Section 3.3.2.3**).

Table 5.4: The formation constants of M^{2+}-BIMA complexes (M^{2+} = Ni^{2+}, Co^{2+}, Cu^{2+} and Zn^{2+})

Complex	**logβ_1**	**logβ_2**
Ni BIMA	7.12(1)	13.97(4)
Cu BIMA	8.96(1)	13.94(2)
Co BIMA	8.98(1)	13.90(2)
Zn BIMA	7.40(1)	12.74(2)

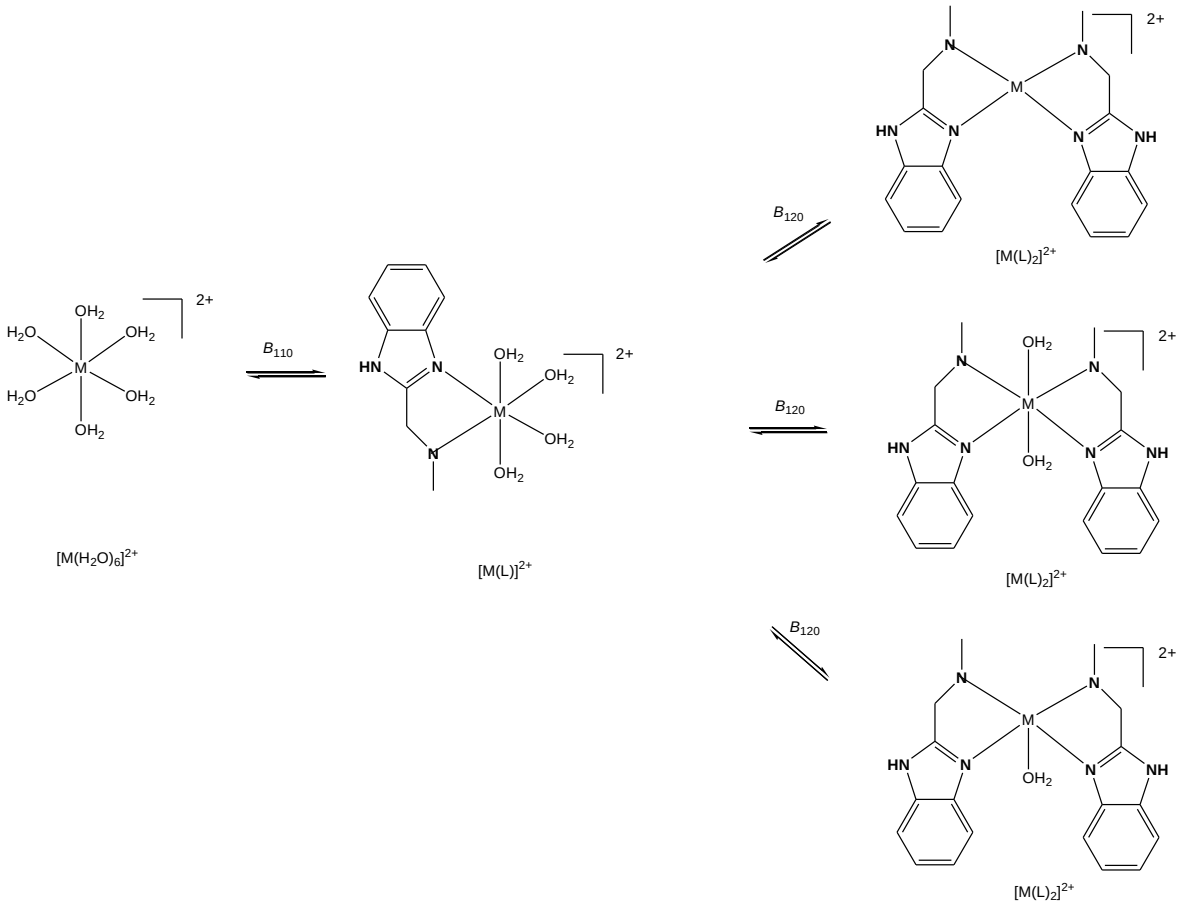

Scheme 5.6: The stepwise formation of base metal ion complexes with (*1H*-benzimidazol-2-yl)-*N*-methylmethanamine (BIMA). A square planar complex is formed with nickel(II), an octahedral complex is formed with Co(II) (with *bis*coordination of the BIMA ligand), a trigonal bipyrimidal complex is formed with Cu(II) while a tetrahedral complex is formed with Zn(II).

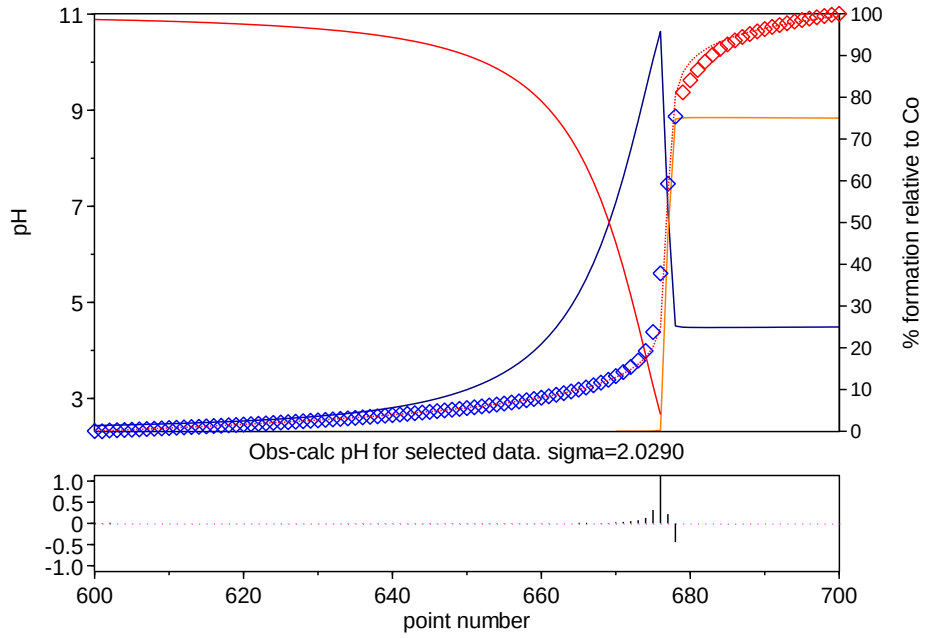

Figure 5.6: Titration and fitted curves of Co-BIMA system. Experimental points are represented by blue squares and the red dotted continuous line is the calculated line based on the fitted protonation constants. The red squares represent the experimental points that have been ignored in the refinement process. The other lines represent the species (not specified).

5.5.2.4 Comparison of the complexation between BNSN, BNNN and BIMA ligands and divalent metal ions (Ni^{2+}, Co^{2+}, Cu^{2+} and Zn^{2+})

The formation constants of $[ML_2]^{2+}$ complex, formed by a reaction of the two respective tridentate ligands (BNSN and BNNN) and divalent metal ions (Ni^{2+}, Co^{2+}, Cu^{2+} and Zn^{2+}), are much higher than for the bidentate ligand (BIMA). This is indicative of a very strong chelate effect for the benzimidazole-based tridentate ligands (BNSN and BNNN) as compared to the benzimidazole-based bidentate system. The constant formation obtained with the tridentate systems were observed to be quite similar to each other and slightly higher for BNNN indicating

the greater basic character of this ligand. The high formation constant values of the tridentate systems which are also quite similar between the metal ions seems to support the lack of selectivity of these ligands towards the divalent metal ions (**Chapter 3, Section 3.3.2.14 and 3.3.2.2.5**). However, the bidentate system showed selectivity for nickel(II) but the constants do not present such a huge difference in stabilization between Ni(II), Cu(II) and Co(II). This seems to suggest that the study of the solvation effects might provide better insight to the separations observed since they are possibly based on the Hofmeister bias[172] between $Ni(BIMA)_2]^{2+}$, $Cu(BIMA)_2(H_2O)]^{2+}$ and $Cu(BIMA)_2(H_2O)_2]^{2+}$. This bias resulted in the aquated complexes being less extractable; hence study of the interaction of the complexes with water (solvation effects) may provide a clear answer to the pattern observed.

5.6. Conclusions

Protonation studies of the tridentate ligands, *bis*((1*H*-benzimidazol-2-yl)methyl)sulfide (BNSN) and *bis*((1*H*-benzimidazol-2-yl)methyl)amine (BNNN) indicated that BNNN is more basic than BNSN which resulted in slightly higher formation constants for M-BNNN. The stability constants for the tridentate systems (BNNN and BNSN) were much higher than those of the bidentate system. The order of the stability constants was in agreement with the order of extraction of the metal ions in the solvent extraction studies. The relative magnitude of the constants for the tridentate systems was in agreement with the lack of pH-metric separation of the base metals with tridentate ligands (as observed in the solvent extraction studies). The constants derived from the bidentate ligand also followed the extraction pattern but the nickel(II)-BIMA constants were not much higher, suggesting that other factors may influence the separation observed.

However more studies on thermodynamic parameters (ΔH and ΔS) of the complexation of these ligands (BNSN, BNNN and BIMA) with base metals still need to be investigated. These will allow one to explain the drive towards *bis*-tridentate coordination of the tridentate ligands with base metals which results in lack of sterecochemical "tailor-making", and which in turn results in lack of pH-metric separation of base metal ions.

CHAPTER 6

6. CONCLUSIONS-RESULTS IN PERSPECTIVE

6.1 Introduction

At the end of this extensive investigation in a quest to develop amine ligands that can act as Ni^{2+} specific separating agents in a sulfate medium, it will be advantageous to summarize the different parameters revealed in this study. This may provide a clearer perspective of the problem in its totality and perhaps assist in future developments in this field.

Detailed conclusive remarks were already made at the end of each of the chapters in this work, and therefore it will not be repeated here.

6.2. Conclusions

The benzimidazole-based tridentate ligands were exploited in an investigation of nickel(II)-selective extractants from base metals in a highly acidic sulfate medium. The study was undertaken with the extractant (ligand) alone and in the presence of DNNSA as a synergist. The presence of highly hydrated sulfate ions prevented a meaningful extraction of the cationic complexes formed with the extractant in the former case while in the latter the desired separation was not obtained. This scenario of non-selective extraction was attributed to the non-specificity of DNNSA as an ion-pairing agent for all the cations studied. However, the use of the extractant (ligand) and DNNSA, results in a different extraction pattern where there begins to be a shift in the extraction curves than when DNNSA alone is used. From the results obtained in this study, it could be inferred that benzimidazole-based tridentate ligands are not relevant reagents for the

separation of nickel(II) from other base metals at the low pH since there was no meaningful pH-metric separation extraction curves.

The bidentate *N*,*N*′-donor benzimidazole-based extractant has been synthesized (a derivative of the BNNN tridentate ligand, with one benzimidazole group removed), characterized and applied as an extractant for the separation of nickel from other base metal ions in an acidic sulfate medium in the presence of hard ions such as Fe(III) and Mn(II). It was observed that the bidentate ligand has a number of advantages over the tridentate ligands, namely:

- Firstly, the exploitation of the subtle stereochemical aspects of coordination for the extraction of base metals was observed to be lacking with tridentate system, whereas for the bidentate ligand an efficient separation of nickel(II) was observed.
- Secondly, tridentate ligands can more readily achieve six-coordination for all of the base metal ions, making it less Ni^{2+}-specific but the bidentate system showed nickel(II) separation, and it was proven that this may be influenced by stereochemical aspects as well as Hofmeister bias.
- Thirdly, the formation constants for the tridentate system were observed to be much higher than those of the bidentate system. The fact that formation constants of the benzimidazole-based extractants are larger, play a more dominant role in the extraction system. The fact that the constants are similar for the different metal ions is in agreement with the lack of separation observed in the extraction system.

Another parameter that should be considered in the development of these extractants is the fact that with increasing dentate character, and thus increasing entropy contribution, tridentate

extractants can form such stable complexes that stripping (reversibility) may not be readily achieved in such cases. It will be advisable to use tridentate extractant of which the enthalpy contribution is smaller, which will make it possible to still enjoy the advantages (positive factors) of the tridentate extractants.

It can be stated that the combination of the bidentate extractant (BIMA) developed in this study, with the bulky sulfonic acid (DNNSA), proved to be a very promising Ni^{2+}-specific extraction system in a sulfuric acid medium.

6.3. Suggestions for the future work

Thermodynamic parameters for the complexation of the ligands (BNSN, BNNN and BIMA) still need to be investigated by determining stability constants at different temperatures and extrapolating the ΔH and ΔS from the van′t Hoff plot. Alternatively, these can be determined from isothermal calorimetric measurements, and this method will be more accurate than the former. This data will provide more insight into the chemistry observed, especially on the nature of the driving force for the complexes formed during extraction. Complex formation is said to be favoured by a negative enthalpy change and a positive entropy change,[176] and there has been speculations as to whether the entropy change or enthalpy changes are the main driving forces behind complex formation with multidentate ligands. In this present study, the denticity and the basicity of the ligands differ and so meaningful thermodynamic information will be obtained.[176]

7. REFERENCES

1. R.G. Cawthorn, *S. Afr. J. Sci*., 95 (1999) 481-489.

2. A.B. Alafara, I.A. Kuranga, A.A. Folahan, K.G. Malay, S.A. Olushola, *Int. J. Min. Eng. Miner. Process.* 1 (2012) 1-16.

3. D. Dreisinger, *J. S. Afr. Inst. Min. Metall*., 109 (2009) 253-271.

4. L. Gotfryd, *Physicochem. Probl. Miner. Process*, 39 (2005), 117-128.

5. A. Feather, W. Bouwer, A. Swarts, V. Vagel, *J. S. Afr. Inst. Min. Metall*. (2002) 457-462.

6. B.R. Reddy, S.V. Rao, K.H Park, *Miner. Eng.* 22 (2009) 500-505.

7. J. Pearsall, *Base metal definition, New Oxford Dictionary of English*, Oxford University Press 1998, 876.

8. J.O. Nriagu, *Copper in the Environment Part I: Ecological Cycling*; John Wiley and Sons Inc.: New York, NY, 1979.

9. K. L. Barry, J. A. Grout, C. D. Levings, B. H. Nidle, G. E. Piercey, *Can. J. Fish. Aquat. Sci.*, 57 (2000) 2032-2043.

10. G.C. Bortleson, S.E. Cox, M.D. Munn, R.J. Schumaker, E.K. *Block, U.S. Geological Survey Water-Supply Paper*, (2001) 1-120.

11. W.D. Nesse, *Introduction to Mineralogy*, Oxford University Press, Oxford, 2000, 1-10.

12. P. W. Jolly, The Organic Chemistry of Nickel: Organonickel Complexes, Vol 1, Academic Press, 1974, 206.

13. J.R. Davis, *Copper and Copper Alloys, Davis & Associates Chagrin Falls*, Ohio, 2001, 3.

14. A.J. Monhemius, *Bull. Chem. Technol. Macedonia*, 13(2) (1994) 7-12.

15. G.A. Kordosky, *J. S. Afr. Inst. Min. Metall*., (2002) 445-450.

16. J. Szymanowski, Hydroxyoximes and copper Hydrometallurgy, CRC Press, 1993, 14-15.

17. J. Szymanowski, K. Prochaska, *J. Radioanal. Nucl. Chem, Articles*, 129 (1989) 251-263.

18. J. Szymanowski, *Polyhedron.* 4 (1985) 269-278.

19. P.R. Danesi, R. Chiarizia, *Crit. Rev. Anal Chem*., 10 (1980) 1-26.

20. R.S. Forgan, B.D. Roach, P.A. Wood, F.J. White, J. Campbell, D.K. Henderson, E. Kamenetzky, F.E. McAllister, S. Parsons, E. Pidcock, P. Richardson, R.M. Swart, P.A. Tasker, *Inorg. Chem*., 50 (2011) 4515–4522.

21. M. Cempel, G. Nikel, *Polish J. Environ. Stud*., 15(3) (2006), 375-382.

22. G. M. Mudd, *Nickel Sulfide Versus Laterite: The Hard Sustainability Challenge Remains. Proc., "48th Annual Conference of Metallurgists", Canadian Metallurgical Society*, Sudbury, Ontario, Canada, August 2009.

23. R.T. Jones, *S. Afr. J. Sci*., 95 (1999) 525-534.

24. J.T. Bruce, *Platinum Met. Rev*., 40 (1996) 2-7.

25. K.C. Sole, A.M. Feather, P.M. Cole, *Hydrometallurgy*, 78 (2005) 52-78.

26. B. Dlovu, T. Mahlangu, *J. S. Afr. Inst. Min. Metall*., 108 (2008) 223-228.

27. L. Aspola, R. Matusewicz, K. Haavanlammi, S. Hughes. *J. S. Afr. Inst. Min. Metall. Platinum* (2012) 235-245.

28. J. Kyle, Nickel laterite processing technologies – where to next? In: ALTA 2010 Nickel/Cobalt/Copper Conference, Perth, Western Australia, 24 -27 May 2010.

29. C.Y. Cheng, *Hydrometallurgy*, 84 (2006) 109–117.

30. D.S. Flett, M. Cox, J.D. Heels, Extraction of nickel by α-hydroxyoxime/lauric acid mixtures. Proceedings of ISEC '74, vol. 3. Society of Chemical Industry, London, 1974, pp. 2560–2575.

31. K.M. Mackay, R.A. Mackay, *Modern Inorganic Chemistry*, 3rd Ed. 1972, 220-223.

32. K. Burger, I Ruff, F. Ruff, *J. Inorg. Nucl. Chem*. 27 (1965) 179-190.

33. T. Osawa, M. Abe, A. Morigami, Y. Nozaka, *J. Electron Microsc*., 47 (1998) 273-276.

34. M.E. Weeks, *J. Chem. Educ*., 9(1) (1932) 22-29.

35.D.D.J. Clemente, B.I. Dewar, J. Hill, Canadian Inst. of Metal. 10th Annual Hydrometallurgical Meeting, Paper No. 7 Edmonton, Alberta, Canada, 1980.

36. F.W. Clarke, *Bulletin No 770*, U. S. Geological Survey 1925.

37. F.W. Clarke, H.S. Washington, *U. S. Geological Survey, Professional Paper* 127 (1924).

38. T.L. Phipson, *Chem. News,* 6 (1862) 47-49.

39. M. Neira, T.J.O'Keefe, J.L. *Watson*, *Miner. Eng*., 5 (1992) 521-534.

40. J. Monhemius, *Chem. Ind*., 12 (1981) 410-420.

41. R.G. Pearson, *J. Am. Chem. Soc*., 85 (1963) 3533-3543.

42. S.G. Galbraith, P.A. Tasker, *Supramol. Chem.,* 17 (2005) 191-207.

43. D.S. Flett, *Cobalt-Nickel Separation in Hydrometallurgy: A Review," Chemistry for Sustainable Development*, 12 (2004) 81-91.

44. M. Cox, D.S. *Fleet, Proceedings of ISEC '71. Society of Chemical Industry, London*. 34 (1971) 204-213.

45. D.S. Flett, S. Titmuss, *J. Inorg. Nucl. Chem*., 31 (1968) 2162-2163.

46. R. R. Grinstead, A.L. Tsang*in: Int. Solvent Extraction Conf*. Denver, Colorado, American Ins. Of Chem. Engnrs. New York, 1983 230.

47. A. R. Burkin, "Extractive Metallurgy of Nickel" in *Critical Reports on Applied Chemistry*, Vol. 17, John Wiley & Sons, New York, 1987 98.

48. K.C. Jones and R.M. Wheaton, *U.S. Patent* 3998 (1976) 924.

49. D.T. Thomson, *Insight into Specialty Inorganic Chemicals*, RSC, United Kingdom 1995 17-20.

50 . R.R. Grinstead, *Hydrometallurgy* 12 (1984) 387-400.

51. C. Xiong, C. Yao, *Indian J. Technol.*, 18 (2011) 13-20

52. C. Kumar, S.K. Sahu, B.D. Pandey, *Hydrometallurgy*, 103 (2010) 45–53

53. A.I. Okewole, N.P. Magwa and Z.R. Tshentu, *Hydrometallurgy*, 121–124 (2012) 81–89.

54. R.G. Bautista, *The solvent extraction of nickel, cobalt and their associated metals, Extractive Metallurgy of Copper, Nickel and Cobalt*, Vol. 1 : Fundamental Aspects (1993).

55. P.M. Cole, *Review of advances in solvent extraction, Hyrdometallurgy School, South Africa Institution of Mining and Metallurgy*, Johannesburg (1994).

56. M. Cox, *Solvent extraction in hydrometallurgy, in Solvent Extraction Principles and Practice*, 2nd New York (2004) 455-506.

57. E. Wigstol, K. Froyland, *Het. Ingenieursblad*, 41 (1972) 476-486.

58. A. Suetsuna, N. Ono, K. Yamada, *Metallurgical Society of the AIME, TMS Paper Selection* A80-2

59. W. A. Ricckelton, D. Nucciarone, *The treatment of cobalt/nickel solutions using Cyanex extractants, in Hydrometallurgy and Refining of Nickel and Cobalt* (1997).

60. J.S. Preston, *Hydrometallurgy* 9 (1982) 115-133.

61. F.A. Cotton and G. Wilkinson, *Advance Inorganic Chemistr*y, 4th Ed., 1980 590, 757

62. J.J. Smith, *Extraction of nickel with the use of supported liquid membranes*, Potchefstroom University, Report No. 617/1/97, 19.

63. H.J. Schalekamp, *MSc Dissertation*, UPE, 1995.

64. J.M. Postma, *MSc Dissertation*, UPE, 1995

65. Q. Xu, D. Shen, Y. Jiang and C. Yuan, *Solv. Ext. Ion Exch*., 4 (1986) 927-930.

66. W.A. Rickelton, D.S. Flett, D.W. West. *Solv. Extr. Ion Exch*., 2 (1984) 815-816.

67. D.S. Flett. *J. Organomet. Chem*., 690 (2005) 2426-2438.

68. A.K. De, S.M. Khopkar, R.A. Chalmers. *Solvent Extraction of Metals,*Van Nostrand Reinhold, New York, 1970.

69. J.G.H. du Preez, J. Postma, S. Ravindran, B.J.A.M. van Brecht. *Solv. Extr. Ion Exch.*, 15(1) (1997) 79-96.

70. R.G Pearson. *J. Am. Chem. Soc*., 85 (1963) 581-583.

71. J.G.H. du Preez, *Solv. Extr. Ion Exch*., 18(4) (2000) 679–701.

72. J. G. H. du Preez, T. I. A. Gerber, W. Edge, V. L. V. Mtotywa and B. J. A. M. van Brecht, *Solv. Extr. Ion Exch.*, 19(1) (2001) 143-154.

73. G. Wilkinson, R.D. Gillard, J.A. McCleverty, *Comprehensive Coordination Chemistry, Later Transition Elements*, Pergamon Press, Vol. 5 (1987) 596, 681.

74. G. Wilkinson, R.D. Gillard, J.A. McCleverty, *Comprehensive Coordination Chemistry, Later Transition Elements*, Vol. 4. 222.

75. M.N. Gandhi, N.V. Deorkar, S.M. Khopkar, *Talanta* 40 (1993)1535–1539.

76. P.K. Parhi, E. Padhan, A. K Palai, K. Sarangi, K. C. Nathsarma, K. H. Park, *Desalination* 267 (2011) 201–208.

77. C. Parija, P.V.R. Bhaskara Sarma, *Hydrometallurgy* 54 (2000) 195–204.

78. K.H. Park, D. Mohapatra, *Met. Mater. Int*., 12 (2006) 441–446.

79. W.A. Rickelton, D. Nucciarone, In: Mihaylov, W.C. (Ed.), *The Metallurgical Society of CIM, Nickel–Cobalt 97 Int.* Symposium, Canada, 1, 1997 275–292.

80. K. Sole, *Baker lecture at Rhodes University*, 1995.

81. R.D. Hancock, A. E. Martell, *Chem. Rev*., 89 (1989) 1875-1886.

82. L.G. Sillen, *Quart. Rev. London* 13 (1959) 146-164.

83. S. Dobson, A.J. van der Zeeuw, *Chem. Ind*. (1976) 175-181.

84. K.T. Brian, *Hydrometallurgy*, 10 (1983) 187-202.

85. Y. Marcus, A.S. Kertes, *Ion Exchange and Solvent Extraction of Metal Complexes*, Wiley Interscience, New York, 1969.

86. J.G.H. du Preez, D.P. Shillington, E. Herselman, H.E. Rohwer, B.J.A.M. van Brecht, H. Wilke, *Solv. Extr. Ion Exch*., 13 (1995) 189-214.

87. J.G.H. du Preez, C. Mattteus, N. Sumter, S. Ravindra, C. Pogieter, B.J.A.M. van Brecht, *Solv. Extr. Ion Exch*., 16 (1998) 565-586.

88. J.G.H. du Preez, S.B. Schanknecht, D.P. Shillington, *Solv. Extr. Ion Exch*., 5 (1987) 789-809.

89. J.J.R. Frausto da Silva, *J. Chem. Educ*., 60 (1983) 39.

90. J. McMurry, *Organic Chemistry*, *Cornell University*, Brookes Cole publishing Co, 4th Ed. 1996 56-59.

91. G.D. Christian, "*Analytical Chemistry*", 6th Ed, John Wiley and Sons Inc, United States of America, 2003 444–445.

92. R.W. Hay, T.C. Clifford, P. Lightfoot, *Polyhedron*, 17 (1998) 3575–3581.

93. B. Kurzak, D. Kroczewska and J. Jezierska, *Polyhedron*, 17(11) (1998) 1831–1841

94 S.O. Bondareva, Y.I. Murinov, V.V. Lisitskii, *Russ. J. Inorg. Chem*., 52(5) (2007) 796–799.

95. L. Rosato, G.B. Harris, R.W. Stanley. *Hydrometallurgy*, 13 (1984) 33-44.

96. R. Katritzky, J.M. Lagowski, *Comprehensive Heterocyclic Chemis*try, Oxford Press, 1984 469-498.

97. E.G. Brown, Ring Nitrogen and Key Biomolecules. Kluwer Academic Press, 1998.

98. Haranda, S. Takahashi, *J. Chem. Soc., Chem. Commun*., (1986) 1229-1243.

99. R.M. Smith, A.E. Martell, *Critical Stability Constants.* Plenum Press, New York. 4, 144 (1976) 207-247.

100. L.D. Pettit, K. J. Powell, Stability Constants Database-IUPAC and Academic Software, UK, 2007.

101. H.M. Irving, R.J.P. Williams, *J. Chem. Soc*., (1953) 3192-3210.

102. J.S. Preston, A.C. du Preez, *Hydrometallurgy*, 58 (2000) 239-250.

103. G. Gran, *Analyst* 77 (1952) 813-825.

104. A.P. Gray, T.B. O'dell, *Nature*, 181 (1958) 634-637.

105. F. Vidal, *J. Org. Chem*., 24 (1959) 681-683.

106. A.S. Kertes, *J. Inorg. Nucl. Chem*., 26 (1964) 1764-1766.

107. A.S. Kertes, Y.E. Habousha, *J. Inorg. Nucl. Chem*., 25 (1963) 1531-1533.

108. K.H. Soldenhoff, *Solv. Extr. Ion Exch.,* 5 (1987) 833-837.

109. B.Lenarcik, A. Kierzkowska, *Solv. Extr. Ion Exch.,* 24 (2006) 433-445.

110. E. Radzyminska-Lenarcik, B. Lenarcik , XXI ARS SEPARATORIA – Torun, Poland 2006.

111. B. Lenarcik, K. Kurdziel, *Pol. J. Chem*., 55 (1981) 737-374.

112. B. Lenarcik, K. Kurdziel, *Pol. J. Chem*., 56 (1982) 3-5.

113. B. Lenarcik, A. Adach, E. Radzymińska-Lenarcik, *Pol. J. Chem*., 73 (1999) 1273-1275.

114. E. Radzyminska-Lenarcik *Sep. Sci. Technol*., *42* (2007) 2661-2664.

115. J.G.H. du Preez, C. Mattteus, N. Sumter, S. Ravindra, C. Pogieter, B.J.A.M. van Brecht, *Solv. Extr. Ion Exch*., 16 (1998) 1033-1035.

116. P.S.K. Chia, S.E. Livingstone, T.N. Lockyer, *Helv. Chim. Acta* 47 (1964) 1745-1746.

117. M. Enamullah, *J. Coord. Chem*., 45(1-4) (1998).

118. J.G.H. du Preez, C. Mattteus, N. Sumter, S. Ravindra, C. Pogieter, B.J.A.M. van Brecht, *Solv. Extr. Ion Exch*., 15(6) (1997) 1007-1021.

119. Elementar Analysensysteme GmbH, CHNOS Elemental Analyzer Vario Micro operating instruction (2005).

120. Elementar.de, Technologia Aplicada Internacionan, San Jose, Costa Rica, America Central, (2000).

121. U.S. Environmental protection agency, method 200.7 Trace elements in water, solids, and biosolids by ICP-OES, Revision (2001).

122. H.J. Van de wiel, *Horizontal* 19 (2004) 1- 46.

123. SII Nanotechnology Inc, Product Brochure 2012.

124. Bruker. SHELXTL-5.1. (includes XS, XL, XP, XSHELL), Bruker AXS Inc., Madison, Wiskonsin, USA (1999).

125. A.L. Spek, *J. Appl. Crystallogr.*, 36 (2003). 7-13.

126. L.J. Farrugia, *J. Appl. Crystallogr*., 30 (1997) 565-566.

127. P. Gans, A. Sabatini, A. Vacca, *Talanta* 43(10) (1996) 1739 -1745.

128. G. Gran, *Analyst*, 77 (1952) 661-678.

129. J.V. Dagdigian, C.A. Reed, *Inorg. Chem*., 18 (1979) 2623-2626.

130. M. Haring. *Helv. Chim. Acta*, 42, (1959) 1845-1846.

131. H. Adams, N.A. Bailey, J.D. Crane, D.E. Fenton, *J. Chem. Soc., Dalton Trans*. (1990) 1727-1735.

132. T.M. Aminabhavi, N.S. Biradar, S.B. Patil, *Inorg. Chim. Acta*,. 125 (1986) 125-128.

133. K.A. Allen, *J. Phys. Chem*., 60(7) (1956) 943–946.

134. A.I. Okewole, R.S. Walmsley, B. Valtancoli, A. Bianchi, Z. R. Tshentu, *Solv. Extr. Ion*

Exch., 31(1) (2013) 61-78.

135. J.M. Schaekers, J.G.H. du Preez, Patent No.: US 2004/0208808 A1, 2004.

136. J.S. Preston, A.C. du Preez, *J. Chem. Technol. Biotechnol*., 71(1) (1998) 43-50.

137. L. Alderighi, P. Gans, A. Ienco, D. Peters, A. Sabatini, A. Vacca, *Coord*. *Chem*. *Rev*., 184(1) (1999) 311-318.

138. M.F. Perutz, *Philos*. *Trans*.: *Phys*. *Sci*. *Eng*., 345(1674) (1993) 105-112.

139. G. Wilkison, R.D. Gillard, J.A. McCleverty, Comprehensive Coordination Chemistry Later Transition Elements, Pergamo Press, Vol. 5 (1987) pp. 596–681.

140. D.P. Mellor, L.E. Maley, *Nature*, 159 (1947) 370-371.

141. W.J. Geary, *Coord. Chem. Rev*., 7(1) (1971) 81-122.

142. N.L. Alpert, W.E. Keiser, H.A. Symanski, Theory and Practice of Infrared Spectroscopy, 2nd Edn, Heyden & Sons Ltd, New York (1970) pp. 280.

143. C.N.R. Rao, Chemical Applications of Infrared Spectroscopy, Academic Press, New York (1963).

144. L.J. Bellamy, Advances in Infrared Group Frequencies, pp. 49–224, Barnes & Noble, Inc., New York (1968) pp. 265–266.

145. J.V. Hodgson, G. Percy, D.A. Thornton, *J. Mol. Struct*., 66 (1980) 81-90.

146. E.S. Raper, J.L. Brooks, *J. Inorg. Nucl. Chem*., 39(12) (1977) 2163-2166.

147. Z. Nakamoto, Infrared and Raman Spectra of Inorganic and Coordination Compounds, 3rd Edn, John Wiley and Sons, New York (1978) pp. 239.

148. A.B.P. Lever, Inorganic Electronic Spectroscopy, 2nd Edn, Elsevier (1984) pp. 554–557.

149. M. Hvastijova, J. Kohout, M. Okruhlica, *Transition Met. Chem*., 18 (1993) 579-582.

150. P.D. Bauer, M.S. Mashuta, R.J. O'Brein, J.F. Richardson, R.M. Buchanan, *J. Coord.*

Chem., 57 (2004) 361-372.

151. R. Carballo, A. Castineiras, *Polyhedron*, 12(9) (1993) 1083-1092.

152. T. Pandiyan, J.G. Hernandez, N.T. Medina, S. Bernes, *Inorg. Chim. Acta*, 357 (2004) 2570-2578.

153. K. Takahashi, Y. Nishidas, S. Kida, *Bull. Chem. Soc. Jpn*., 57 (1984) 2628-2633.

154. M.S. Lah, M. Moon, *Bull. Korean Chem. Soc*., 18(4) (1997) 406-409

155. E. Kwaskowska-Chec, M. Kubiak, T. Glowiak, J.J. Zoilkowski, *J. Chem. Crystallogr*., 25(12) (1995) 837-840.

156. T. Pandiyan, K. Panneerselvam, M. Soriano-Garcia, C. Duran de Bazua, E.M. Holt, *Acta Crystallogr., Sect.C*, 52(5) (1996) 1137-1139.

157. F.J. Rietmeijer, P.J.M.W.L. Birker, S. Gorter, J. Reedijk, *J. Chem. Soc., Dalton Trans*., (1982) 1191-1198.

158. J.C. Lockhart, W. Clegg, M.N.S. Hill, D.J. Rushton, *J. Chem. Soc., Dalton Trans*., (1990). 3541-3548.

159. J.V. Dagdigian, V. Mckee, C.A. Reed, *Inorg. Chem*., 21(4) (1982) 1332-1342.

160. H.P. Berends, D.W. Stephan, *Inorg. Chim. Acta*, 93 (1984). 173-178.

161. A.W. Addison, P.J. Burke, K. Henrick, T.N. Rao, *Inorg. Chem*., 22 (24) (1983) 3645-3653.

162. R. Balamurugan, M. Palaniandavar, R.S. Gopalan, G.U. Kulkarni, *Inorg. Chim. Acta*, 357 (4) (2004) 919-930.

163. T.J. Lane, I. Nakagawa, J.L. Walker and A.J. Kandathil, *Inorg. Chem.*, 1(2) (1962) 267-276.

164. J. Reedijk, *J. Inorg. Nucl. Chem.*, 33(1) (1971) 179-188.

165. W. Clegg, M. R. J. Elsegood, et al., *J. Chem. Soc., Dalton Trans*., (1996) 1531–1538.

166. S. Ozbey, S. Ide, and E. Kendi, *J. Mol. Struct*., 442 (1998) 23–30.

167. S. Pinar, M. Akkurt, H. Kücükbay, N. Sireci, and O. Büyükgüngör, *Acta Crystallogr.* E, 62 (2006) o2223–o2225.

168. L. Dobrzanska, G. O. Lloyd, *Acta Crystallogr. E*, 62 (2006) o1205–o1207.

169. J.-Y. Xu, W. Gu, L. Li, S.-P. Yan, P. Cheng, D.-Z. Liao and Z.-H. Jiang, *J. Mol. Struct.*, 644(1-3) (2003) 23-27.

170. P. Thangarasu, S. Bernès and C. Durán de Bazúa, *Acta Crystallogr Section C-Crystal Str Commun.*, 53(11) (1997) 1607-1609.

171. C. Gyanakumari, M. Lakshmi, *Eur. J. Chem*., 8 (2011) 1662-1669.

172. F. Hofmeister, *Arch. Exp. Pathol. Pharmokol*., 24 (1888) 247 -260.

173. S.J. Ashcroft, G. Beech, An introduction to the thermodynamics of inorganic and organometallic compounds. New York, 1973.

174. P.Gans, B. O'Sullivan, *Talanta* 51 (2000) 33-36.

175. M.L. Turonek, G.T. Hefter, P.M. May, *Talanta* 45 (1998) 931–934.

176. T. Singh, MSc. Thesis, University of Natal, 1995.